AD-A175 522

DNA-TR-86-158

PROPAGATION OF RF SIGNALS THROUGH STRUCTURED IONIZATION
Theory and Antenna Aperture Effect Applications

Roger A. Dana
Mission Research Corporation
P. O. Drawer 719
Santa Barbara, CA 93102-0719

15 May 1986

Technical Report

DTIC
ELECTE
DEC 1 2 1986
S   D
B

DTIC FILE COPY

Prepared for
    Director
    DEFENSE NUCLEAR AGENCY
    Washington, DC 20305-1000

86 12 12 100

DISTRIBUTION LIST UPDATE

This mailer is provided to enable DNA to maintain current distribution lists for reports. We would appreciate your providing the requested information.

☐ Add the individual listed to your distribution list.

☐ Delete the cited organization/individual.

☐ Change of address.

NAME: _____

ORGANIZATION: _____

OLD ADDRESS	CURRENT ADDRESS
_____	_____
_____	_____
_____	_____

TELEPHONE NUMBER: (___) _____

SUBJECT AREA(s) OF INTEREST:

_____	_____
_____	_____
_____	_____

DNA OR OTHER GOVERNMENT CONTRACT NUMBER: _____

CERTIFICATION OF NEED-TO-KNOW BY GOVERNMENT SPONSOR (if other than DNA):

SPONSORING ORGANIZATION: _____

CONTRACTING OFFICER OR REPRESENTATIVE: _____

SIGNATURE: _____

SECURITY CLASSIFICATION OF THIS PAGE

HD-A175522

REPORT DOCUMENTATION PAGE

1a. REPORT SECURITY CLASSIFICATION	1b. RESTRICTIVE MARKINGS
UNCLASSIFIED	
2a. SECURITY CLASSIFICATION AUTHORITY	3. DISTRIBUTION / AVAILABILITY OF REPORT
N/A since UNCLASSIFIED	Approved for public release; distribution
2b. DECLASSIFICATION / DOWNGRADING SCHEDULE	is unlimited.
N/A since UNCLASSIFIED	
4. PERFORMING ORGANIZATION REPORT NUMBER(S)	5. MONITORING ORGANIZATION REPORT NUMBER(S)
MRC-R-976	DNA-TR-86-158

6a. NAME OF PERFORMING ORGANIZATION	6b. OFFICE SYMBOL (If applicable)	7a. NAME OF MONITORING ORGANIZATION
Mission Research Corporation		Director Defense Nuclear Agency
6c. ADDRESS (City, State, and ZIP Code)		7b. ADDRESS (City, State, and ZIP Code)
P.O. Drawer 719 Santa Barbara, CA 93102-0719		Washington, DC 20305-1000

8a. NAME OF FUNDING / SPONSORING ORGANIZATION	8b. OFFICE SYMBOL (If applicable)	9. PROCUREMENT INSTRUMENT IDENTIFICATION NUMBER
		DNA 001-85-C-0067

8c. ADDRESS (City, State, and ZIP Code)	10. SOURCE OF FUNDING NUMBERS			
	PROGRAM ELEMENT NO.	PROJECT NO	TASK NO.	WORK UNIT ACCESSION NO
	62715H	S99QMXB	B	DH008719

11. TITLE (Include Security Classification)
PROPAGATION OF RF SIGNALS THROUGH STRUCTURED IONIZATION
Theory and Antenna Aperture Effect Applications

12. PERSONAL AUTHOR(S)
Dana, R. A.

13a. TYPE OF REPORT	13b. TIME COVERED	14. DATE OF REPORT (Year, Month, Day)	15. PAGE COUNT
Technical	FROM 850301 TO 860501	860515	140

17	COSATI CODES		18. SUBJECT TERMS (Continue on reverse if necessary and identify by block number)
FIELD	GROUP	SUB-GROUP	Signal Scintillations Channel Simulation
17	2		Ionospheric Propagations Transponders
22	2		Antennas

19. ABSTRACT (Continue on reverse if necessary and identify by block number)

This report presents a review of the theory of propagation of RF signals through random ionospheric disturbances that would result from high altitude chemical releases or nuclear detonations. Starting with Maxwell's equations, an analytic expression for the two-position, two-time, two-frequency mutual coherence function is derived for strong, anisotropic scattering conditions. The physics that are contained in this important function and the approximations that are made in its derivation are explained. Two models for the temporal variations of the signal are used. The first is the usual frozen-in approximation which models the ionosphere as a rigid structure that drifts across the line-of-sight. The second, called the turbulent model, is developed in this report which decouples the spatial and temporal fluctuations in the ionosphere. This model may be more accurate at times before striations have formed in the ionosphere or when multiple layers of striations with different velocities are drifting across the line-of-sight.

20. DISTRIBUTION / AVAILABILITY OF ABSTRACT	21. ABSTRACT SECURITY CLASSIFICATION
☐ UNCLASSIFIED/UNLIMITED ☒ SAME AS RPT ☐ DTIC USERS	UNCLASSIFIED
22a. NAME OF RESPONSIBLE INDIVIDUAL	22b. TELEPHONE (Include Area Code)	22c. OFFICE SYMBOL
Betty L. Fox	(202) 325-7042	STTI

DD FORM 1473, 84 MAR   83 APR edition may be used until exhausted.   SECURITY CLASSIFICATION OF THIS PAGE
All other editions are obsolete.

i

19. ABSTRACT (Continued)

The second part of this report presents several new results and applications of the theory. The generalized power spectral density (GPSD), which is the Fourier transform of the mutual coherence function, is used to compute the second order statistics of the signal at the output of an anisotropic aperture antenna. Analytic results are presented for antennas with Gaussian beam profiles and numerical results are presented for uniformly weighted apertures. These results are then generalized to transponder communication link geometries with two independent propagation paths and four antennas.

The last application section presents new analytical/numerical techniques for generating and validating realizations of the impulse response function at the outputs of multiple antennas using either the frozen-in or the turbulent approximations. Several examples are presented which illustrate the effects of frequency selective and spatially selective scintillation.

PREFACE

Accession For

NTIS

DTI

U

J

D

A-1

iii

TABLE OF CONTENTS

iv

TABLE OF CONTENTS (Continued)

TABLE OF CONTENTS (Concluded)

LIST OF ILLUSTRATIONS

LIST OF ILLUSTRATIONS (Concluded)

ix

SECTION 1
INTRODUCTION

Satellite communications systems that utilize transionospheric propagation links may be subject to severe performance degradation when the ionosphere is highly disturbed by high altitude nuclear explosions (Arendt and Soicher 1964; King and Fleming 1980) or by chemical releases (Davis et al. 1974; Wolcott et al. 1978). During these events, the increased electron concentrations and the irregular structure of the ionization can lead to intense Rayleigh signal scintillation at the RF carrier frequencies used for communication links.

Under severe scintillation conditions, the signal incident at the receiver can vary randomly in amplitude, phase, time-of-arrival, and angle-of-arrival. If all frequency components of the signal vary essentially identically with time, the propagation channel is referred to as nonselective or flat fading. When the scintillations exhibit statistical decorrelation at different frequencies within the signal bandwidth, the channel is referred to as frequency selective. Frequency selective scintillations are therefore encountered when the communication link bandwidth exceeds the frequency selective or coherence bandwidth of the channel. When the scintillations exhibit statistical decorrelation across the face of an aperture antenna, the channel may also be referred to as spatially selective. Spatially selective scintillations are therefore encountered when the antenna aperture size exceeds the decorrelation distance of the incident signal.

Under conditions where the signal is spatially selective, the antenna beamwidth is smaller than the angle-of-arrival fluctuations and the effect of the antenna is to attenuate the incident signal that is arriving at off-boresight angles. In the spatial domain, the incident electric field is somewhat decorrelated across the face of the antenna. The induced voltages in the antenna then do not add coherently as they would for an incident plane wave with a loss in the gain of the antenna as a result. Because of this angular filtering or spatial selectivity, the second order statistics of the signal at the output of the antenna will be different than those of the incident signal.

The effects of antennas on signals that have propagated through randomly ionized media have been reported by Wittwer (1982, 1986) and Knepp (1983a, 1985). The purpose of this report is to review the basic theory, starting with Maxwell's equations, of radio frequency (RF) signal propagation through random media. Then several new applications of antenna filtering effects are presented. These include the filtering of anisotropic signals with anisotropic antennas; generation of realizations of the impulse response function at the output of multiple antennas; and transponder communication links with two independent propagation paths and four antennas.

1.1   THEORY.

The starting point for antenna aperture effects calculations is the generalized power spectal density (GPSD). The first part of this report is a review of the derivation of the GPSD. The intent of this review is to give the reader an understanding of the underlying physics that are contained in the GPSD and an understanding of the assumptions used to calculate the GPSD. The first part of this review follows Tatarskii (1971, §64-65) and the second part follows Knepp (1983a).

2

The derivation of the GPSD starts with Maxwell's equations from which the parabolic wave equation is derived. The parabolic wave equation can be solved to give the received electric field for a specific electron density distribution in the ionosphere. However, the electron density distribution is a random process so the received electric field is also a random process. The parabolic wave equation is therefore used to derive an equation for the two-position, two-frequency, two-time mutual coherence function of the electric field, $\Gamma(\Delta\vec{r}, \Delta\omega, \Delta t)$. The solution of the differential equation for Γ, which is a solution of Maxwell's equations, then provides a description of the second order statistics of the received electric field. The Fourier transform of Γ is the GPSD of the received signal.

1.2   APPLICATIONS.

The second part of this report presents several new results. The GPSD for anisotropic scattering is used to compute the mean power, decorrelation distance, and frequency selective bandwith of the signal out of an anisotropic antenna. These results allow an arbitrary rotation about the line-of-sight between the antenna axis and the natural axis of the scattering. Analytic results are presented for antennas with Gaussian beam profiles and numerical results are given for uniformly weighted circular apertures.

These results are then generalized to transponder communication link geometries where there are two independent propagation paths through disturbed regions of the ionosphere and four antennas. It is assumed for simplicity in these calculations that all of the antennas have circularly symmetric antenna beam profiles.

3

In the last application section analytical/numerical techniques
are described to generate realizations of the impulse response function of
the signal after propagation through randomly ionized media and reception
by multiple antennas. These statistical realizations of the signal out of
. multiple antennas have Rayleigh amplitude statistics and spatial and fre-
quency correlation properties given by the mutual coherence function.
These realizations of the impulse response function are then used to con-
struct the received signal which may be used to exercise simulations of
transionospheric communications links.

SECTION 2
THEORY

The starting point for antenna aperture effects calculations is the generalized power spectral density (GPSD). This section presents a review of the derivation of the GPSD and discusses the physics that are contained in this important function.

In deriving the GPSD, two key approximations are made about the spatial and temporal electron density fluctuations that cause the scattering in the ionosphere. The first of these is the delta layer approximation which says that the scattering occurs in an infinitesimally thin layer normal to the line-of-sight. This approximation has been relaxed in the calculations of Wittwer (1982) and Knepp (1983b) and has been found to result in small errors in the GPSD provided that the propagation parameters (frequency selective bandwidth, decorrelation time and decorrelation distance) that characterize the channel are properly specified. The delta layer approximation is not, in general, adequate to calculate the propagation parameters (Wittwer 1982).

The second approximation is for the temporal variation model of the electron density fluctuations. The usual approximation is Taylor's frozen-in hypothesis which treats the ionization fluctuations or striations as rigid "frozen-in" structures that drift across the line-of-sight. Under this approximation there is strong coupling between the spatial and temporal variations of the random electric field that is incident at the plane of the receiver. A second approximation proposed by Wittwer (1985), called the turbulent approximation, is developed in this section which decouples the spatial and temporal variations of the random electric

5

fields. This approximation may be more accurate at times before the striations have formed in the ionosphere or when multiple layers of striations with different drift velocities are in the line-of-sight. The GPSD under both of these approximations is derived in this section.

An analytic solution is obtained in this section for the two-position, two-frequency, two-time mutual coherence function $\Gamma(\Delta\vec{r},\Delta\omega,\Delta t)$ of the complex electric field incident on the plane of the receiving antenna. This solution is valid for arbitrary line-of-sight geometries relative to the ionization structures in the ionosphere that cause the scattering of the RF wave. The mutual coherence function then provides the basis for the antenna aperture effect calculations and for the statistical signal generation techniques discussed in Sections 3 and 5 of this report. The Fourier transform of Γ is the GPSD of the received signal.

2.1   PARABOLIC WAVE EQUATION.

Consider a monochromatic spherical wave with an electric field $\vec{\mathscr{E}}(\vec{r},\omega,t)$ which is a function of position $\vec{r}$, carrier radian frequency ω, and time t. The wave originates from a transmitter located at $\vec{r} = (0,0,-z_t)$ and propagates in free space in the positive z direction until it is incident on an irregularly ionized layer which extends from $0 < z < L$ and is infinite in the x-y plane. After emerging from the layer at $z = L$, the wave propagates in free space to a receiver located at $\vec{r} = (0,0,z_r)$. This geometry is shown in Figure 2-1.

The propagation of the wave is governed by Maxwell's equations:

$$\vec{\nabla}\times\vec{\mathscr{E}} + (1/c)\,\partial\vec{\mathscr{H}}/\partial t = 0 \qquad \vec{\nabla}\cdot\epsilon\vec{\mathscr{E}} = 0$$

$$\vec{\nabla}\times\vec{\mathscr{H}} - (\epsilon/c)\,\partial\vec{\mathscr{E}}/\partial t = 0 \qquad \nabla\cdot\vec{\mathscr{H}} = 0$$

(2-1)

where c is the speed of light in vacuum, $\vec{\mathscr{H}}$ is the magnetic field, and ϵ is the dielectric constant.

6
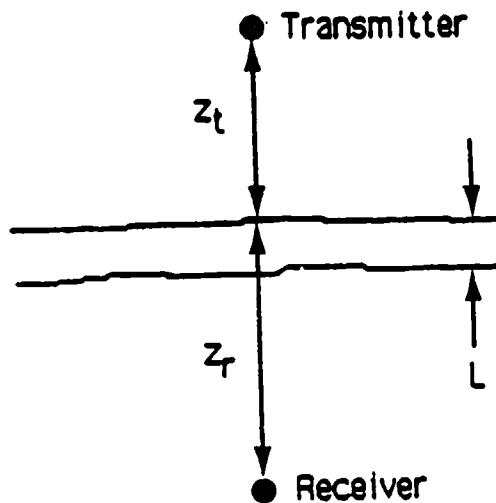
Figure 2-1. Propagation geometry.

The dielectric constant of the propagation medium undergoes random fluctuations with a characteristic frequency which is assumed to be small when compared to the carrier frequency of the wave. With this assumption, the electric and magnetic fields may be written as the product of slowly varying complex envelopes, denoted $\tilde{E}$ and $\vec{H}$, times $\exp(i\omega t)$:

$$\vec{\mathcal{E}}(\vec{r},\omega,t) = \tilde{E}(\vec{r},\omega,t)e^{i\omega t}$$

$$\vec{\mathcal{H}}(\vec{r},\omega,t) = \vec{H}(\vec{r},\omega,t)e^{i\omega t}$$

(2-2)

Inserting these into Maxwell's equations gives

$$\vec{\nabla}\times\vec{E} + ik\vec{H} = 0 \qquad\qquad (2\text{-}3a)$$

$$\vec{\nabla}\times\vec{H} - i\epsilon k\vec{E} = 0 \qquad\qquad (2\text{-}3b)$$

7

where $k = \omega/c$ is the wave number of the carrier. After applying the curl operator to Equation 2-3a and substituting Equation 2-3b for the $\vec{\nabla}\times\vec{H}$ term, the equation for $\vec{E}$ becomes

$$\vec{\nabla}\times\vec{\nabla}\times\vec{E} - \varepsilon k^2\vec{E} = 0 \quad . \tag{2-4}$$

The vector identity $\vec{\nabla}\times\vec{\nabla}\times\vec{E} = \vec{\nabla}(\vec{\nabla}\cdot\vec{E}) - \nabla^2\vec{E}$ reduces the curl curl term in Equation 2-4 with the result

$$\vec{\nabla}(\vec{\nabla}\cdot\vec{E}) - \nabla^2\vec{E} - \varepsilon k^2\vec{E} = 0 \quad . \tag{2-5}$$

The $\vec{\nabla}\cdot\vec{E}$ term is reduced by expanding the divergence equation for $\vec{E}$:

$$\vec{\nabla}\cdot\varepsilon\vec{E} = \varepsilon\vec{\nabla}\cdot\vec{E} + \vec{E}\cdot\vec{\nabla}\varepsilon = 0 \tag{2-6}$$

or

$$\vec{\nabla}\cdot\vec{E} = - \vec{E}\cdot\vec{\nabla}(\ln\varepsilon) \quad . \tag{2-7}$$

The wave equation for the complex envelope of the electric field then becomes

$$\nabla^2\vec{E} + \varepsilon k^2\vec{E} + \vec{\nabla}[\vec{E}\cdot\vec{\nabla}(\ln\varepsilon)] = 0 \quad . \tag{2-8}$$

The dielectric constant ε in a plasma at radio frequencies is given approximately by

$$\varepsilon = 1 - \omega_p^2/\omega^2 \tag{2-9}$$

where the plasma frequency is

$$\omega_p^2 = 4\pi\, r_e c^2 n_e(\vec{r},t) \quad . \tag{2-10}$$

8

The quantity r_e is the classical electron radius ($r_e = 2.8179 \times 10^{-15}$ m) and $n_e(\vec{r}, t)$ is the free electron density as a function of position and time. Equation 2-9 is valid when the carrier frequency is large compared to the plasma frequency. The free electron density is a random variable that will be represented as a mean value plus a random variation:

$$n_e(\vec{r}, t) = \langle n_e \rangle + \Delta n_e(\vec{r}, t) \quad . \tag{2-11}$$

The electron density fluctuation $\Delta n_e(\vec{r}, t)$ is assumed to be a zero mean random process with a standard deviation that is small compared to the mean electron density. The term ϵk^2 in the wave equation may now be rewritten as

$$\epsilon k^2 = \overline{k}^2 (1 - \epsilon_1) \tag{2-12}$$

where

$$\overline{k}^2 = (\omega/c)^2 [1 - 4\pi r_e c^2 \langle n_e \rangle / \omega^2] \tag{2-13}$$

and

$$\epsilon_1 = [\Delta n_e(\vec{r}, t) / \langle n_e \rangle][\overline{\omega}_p^2 / (\omega^2 - \overline{\omega}_p^2)] \quad . \tag{2-14}$$

The quantity $\overline{\omega}_p$ is the plasma frequency evaluated at the mean electron density. The magnitude of the gradient term $\vec{\nabla}(\ln \epsilon)$ in the wave equation may be estimated as follows:

$$\left| \vec{\nabla}(\ln \epsilon) \right| = \left| \vec{\nabla}[\ln(1 - \omega_p^2/\omega^2)] \right|$$

$$\approx -(4\pi r_e \langle n_e \rangle c^2/\omega^2) \left| \vec{\nabla}(\Delta n_e / \langle n_e \rangle) \right|$$

$$\approx -(\overline{\omega}_p^2/\omega^2)/L_o$$

9

where L_0 is the scale size of the electron density fluctuations. As long as $L_0 \gg \lambda$, where λ is the RF wavelength, the term $\vec{\nabla}[\vec{E} \cdot \vec{\nabla}(\ln \epsilon)]$ is small compared to $\epsilon k^2 \vec{E}$ and may be ignored. The steps that follow are therefore only valid when the scale size of the electron density fluctuations is large compared to the carrier wavelength. With this restriction, the wave equation becomes

$$\nabla^2 \vec{E} + \overline{k}^2 (1-\epsilon_1) \vec{E} = 0 \quad . \tag{2-15}$$

Now consider the complex components of the electric field and let

$$E(\vec{r},\omega,t) = U(\vec{r},\omega,t) \exp \left(-i \int \overline{k}(z')dz'\right) \quad . \tag{2-16}$$

This scalar equation for $\vec{E}$ may be used because it is usual for trans-ionospheric RF links to be circularly polarized. It is therefore not necessary to carry out separate calculations for each polarization state. The exponential term in Equation 2-16 represents the dispersive effects of the smooth plasma and will be considered in Section 2.9. The voltage U contains the diffractive effects that are of interest under strong scattering conditions. Substituting Equation 2-16 for $E(\vec{r},\omega,t)$ in the wave equation gives the following differential equation for U:

$$\nabla_{\perp}^2 U + \partial^2 U/\partial z^2 - 2i\overline{k}\partial U/\partial z - \overline{k}^2 \epsilon_1 U = 0 \tag{2-17}$$

where

$$\nabla_{\perp}^2 \equiv \partial^2/\partial x^2 + \partial^2/\partial y^2 \quad . \tag{2-18}$$

The complex amplitude U varies as the electron density fluctuations. The second derivative $\partial^2 U/\partial z^2$ is then the order of U/L_0^2. On the other hand, the term $\overline{k}\partial U/\partial z$ varies as $U/\lambda L_0$. As long as $\lambda \ll L_0$, the second derivative is small compared to the first derivative and may be ignored. This is equivalent to neglecting reflected rays and is called the "parabolic" approximation. The parabolic wave equation is then

10

$$\nabla_{\perp}^2 U - 2i\bar{k}\partial U/\partial z - \bar{k}^2\epsilon_1 U = 0 \quad . \qquad (2\text{-}19)$$

It will be seen that this parabolic or small angle scattering approxima-tion is very robust in that it degrades gracefully as the scattering angles get large. The source term $\epsilon_1 U$ in the parabolic wave equation is a function of the electron density fluctuations and of frequency. Different frequencies within a signal bandwidth may therefore propagate along dif-ferent paths through the same ionization structure. When this happens, the propagation channel is said to be frequency selective.

2.2   TRANSPORT EQUATION.

A partial differential equation for the two-position, two-fre-quency, two-time mutual coherence function Γ is derived from the parabolic wave equation in this section and is solved in Section 2.5. This trans-port equation is derived using the Novikov theorem which requires that the electron density fluctuations be normally distributed. However, Lee and Jokipii (1975a) give an alternative derivation that relaxes this assump-tion.

2.2.1   First Form of the Transport Equation.

The two-position, two frequency, two-time mutual coherence function is defined in a plane normal to the line-of-sight as

$$\Gamma = \langle U(\vec{\rho}_1,z,\omega_1,t_1)U^*(\vec{\rho}_2,z,\omega_2,t_2)\rangle \qquad (2\text{-}20)$$

where $\vec{\rho}$ is a two-dimensional position vector in the normal plane.

In order to obtain an equation for Γ, the parabolic wave equa-tion for $U(\vec{\rho}_1,z,\omega_1,t_1)$ is multiplied by $U^*(\vec{\rho}_2,z,\omega_2,t_2)$. This results in the following equation:

11

$$(1/k_1)\nabla_{\perp_1}^2 U(\vec{\rho}_1,z,\omega_1,t_1)U^*(\vec{\rho}_2,z,\omega_2,t_2) \; -$$

$$2i[\partial U(\vec{\rho}_1,z,\omega_1,t_1)/\partial z]U^*(\vec{\rho}_2,z,\omega_2,t_2) \; -$$

$$k_1\epsilon_1(\vec{\rho}_1,z,\omega_1,t_1)U(\vec{\rho}_1,z,\omega_1,t_1)U^*(\vec{\rho}_2,z,\omega_2,t_2) = 0 \qquad (2\text{-}21)$$

where k_j is given by Equation 2-13 evaluated at ω_j, $\epsilon(\vec{\rho}_j,z,\omega_j,t_j)$ is given by Equation 2-14, and $\nabla_{\perp_j}^2$ is given by Equation 2-18 evaluated at $\vec{\rho}_j$. A similar equation can be written down by interchanging the subscripts 1 and 2 and by taking the complex conjugate with the result:

$$(1/k_2)\nabla_{\perp_2}^2 U^*(\vec{\rho}_2,z,\omega_2,t_2)U(\vec{\rho}_1,z,\omega_1,t_1) \; +$$

$$2i[\partial U^*(\vec{\rho}_2,z,\omega_2,t_2)/\partial z]U(\vec{\rho}_1,z,\omega_1,t_1) \; -$$

$$k_2\epsilon_1(\vec{\rho}_2,z,\omega_2,t_2)U^*(\vec{\rho}_2,z,\omega_2,t_2)U(\vec{\rho}_1,z,\omega_1,t_1) = 0 \quad . \quad (2\text{-}22)$$

Upon subtracting Equation 2-22 from Equation 2-21 and taking the expectation value, the equation for Γ is

$$(1/k_1)\nabla_{\perp_1}^2\Gamma - (1/k_2)\nabla_{\perp_2}^2\Gamma - 2i\partial\Gamma/\partial z \; -$$

$$k_1\langle\epsilon_1(\vec{\rho}_1,z,\omega_1,t_1)U(\vec{\rho}_1,z,\omega_1,t_1)U^*(\vec{\rho}_2,z,\omega_2,t_2)\rangle \; +$$

$$k_2\langle\epsilon_1(\vec{\rho}_2,z,\omega_2,t_2)U(\vec{\rho}_1,z,\omega_1,t_1)U^*(\vec{\rho}_2,z,\omega_2,t_2)\rangle = 0 \quad . \quad (2\text{-}23)$$

The expectation of the two source terms in this equation must be carefully evaluated. They involve the product of UU^* and ϵ_1 where ϵ_1 is proportional to the fluctuations in the electron density. However, the electric field complex envelope U is a function of the electron density fluctuations that are encountered along the propagation path. Therefore U and ϵ_1 are correlated.

2.2.2 Novikov Theorem.

The Novikov theorem is used to evaluate the source terms in Equation 2-23. This theorem is proved in Tatarskii (1971, §65) and Ishimaru (1978, pp. 457-458). The theorem states that

$$\langle f(\vec{R})\phi[f]\rangle = \int \langle f(\vec{R})f(\vec{R}')\rangle\langle\delta\phi[f]/\delta f(\vec{R}')\rangle \, d^n \vec{R}' \qquad (2\text{-}24)$$

where $f(\vec{R})$ is a zero-mean, normally distributed random function of the n dimensional vector $\vec{R}$ and $\delta\phi/\delta f$ is a functional derivative. In applying this theorem, $f = \epsilon_1$ and $\phi = UU^*$. The theorem is proved by expanding $\phi(f)$ in a Taylor series.

2.2.3 Source Terms.

Before proceeding with evaluating the source terms, it will be convenient to write ϵ_1 as the product of a frequency term and a term that varies only with space and time:

$$\epsilon_1(\vec{\rho},z,\omega,t) = \xi(\vec{\rho},z,t)\beta(\omega) \qquad (2\text{-}25)$$

where

$$\xi(\vec{\rho},z,t) = \Delta n_e(\vec{\rho},z,t)/\langle n_e\rangle \qquad (2\text{-}26)$$

is a random function of the electron density fluctuations and

$$\beta(\omega) = \bar{\omega}_p^{-2}/(\omega^2-\bar{\omega}_p^{-2}) \qquad (2\text{-}27)$$

is a deterministic function of frequency and the mean free electron density.

A straightforward application of the Novikov theorem gives for the first source term in Equation 2-23

13

$$S_1 = k_1\beta(\omega_1)\langle\xi(\vec{\rho}_1,z,t_1)U(\vec{\rho}_1,z,\omega_1,t_1)U^*(\vec{\rho}_2,z,\omega_2,t_2)\rangle$$

$$= k_1\beta(\omega_1)\int_{-\infty}^{\infty}dz'\iint_{-\infty}^{\infty}d^2\vec{\rho}'\int_{-\infty}^{\infty}dt'\,\langle\xi(\vec{\rho}_1,z,t_1)\xi(\vec{\rho}',z',t')\rangle\times$$

$$\langle[\delta U(\vec{\rho}_1,z,\omega_1,t_1)/\delta\xi(\vec{\rho}',z',t')]U^*(\vec{\rho}_2,z,\omega_2,t_2)\,+$$

$$U(\vec{\rho}_1,z,\omega_1,t_1)[\delta U^*(\vec{\rho}_2,z,\omega_2,t_2)\delta\xi(\vec{\rho}',z',t')]\rangle\quad.\qquad(2\text{-}28)$$

At this point, the electron density fluctuations are assumed to be stationary and delta-correlated along the z axis. This Markov assumption has the mathematical form

$$\langle\xi(\vec{\rho},z,t)\xi(\vec{\rho}',z',t')\rangle = \delta_F(z-z')A(\vec{\rho}-\vec{\rho}',t-t')\quad.\qquad(2\text{-}29)$$

The notation $\delta_F(x)$ is used throughout this report for the Dirac delta function to distinguish $\delta_F(x)$ from the functional differential $\delta\phi/\delta f$ and from the parameter δ defined in Section 2.6. The Markov assumption is discussed in some detail by Tatarskii (1971, §64) and is based on the fact that fluctuations in the dielectric constant in the direction of propagation have little effect on the transverse fluctuation characteristics of the electric field. It is the fluctuations of the dielectric constant transverse to the direction of propagation that dominate the scattering and the transverse fluctuations of the electric field.

Under the assumption of small angle scattering for which the parabolic wave equation is valid, the component of the electric field traveling in the backward direction will be negligible compared to the component of the electric field traveling in the forward direction. The electric field $U(\vec{\rho},z,\omega,t)$ may then be assumed to depend on $\xi(\vec{\rho}',z',t')$ only for $z' < z$ (i.e. the electric field does not depend on electron density irregularities that have not yet been encountered along the forward

14

propagation path). Also, $U(\vec{\rho}, z, \omega, t)$ depends on $\xi(\rho', z', t')$ only for $t' < t$ (i.e. the electric field does not depend on irregularities that have not yet occurred). Thus $\delta U(\vec{\rho}, z, \omega, t) / \delta \xi(\vec{\rho}', z', t') = 0$ for $z' > z$ and for $t' > t$.

The source function S_1 may now be rewritten as

$$S_1 = k_1 \beta_1 \int\limits_{-\infty}^{z} dz' \; \delta_F(z-z') \iint\limits_{-\infty}^{\infty} d^2\vec{\rho}' \int\limits_{-\infty}^{t} dt' \; A(\vec{\rho}_1 - \vec{\rho}', t_1 - t') \times$$

$$<[\delta U(\vec{\rho}_1, z, \omega_1, t_1) / \delta \xi(\vec{\rho}', z', t')] U^*(\vec{\rho}_2, z, \omega_2, t_2) +$$

$$U(\vec{\rho}_1, z, \omega_1, t_1)[\delta U^*(\vec{\rho}_2, z, \omega_2, t_2) / \delta \xi(\vec{\rho}', z', t')]> \quad (2\text{-}30)$$

where β_j is given by Equation 2-27 evaluated at ω_j. Recalling that

$$\int\limits_{-\infty}^{a} \delta_F(x-a) dx = 1/2 \qquad (2\text{-}31)$$

further reduces the source term S_1 to

$$S_1 = (k_1 \beta_1 / 2) \iint\limits_{-\infty}^{\infty} d^2\vec{\rho}' \int\limits_{-\infty}^{t} dt' \; A(\vec{\rho}_1 - \vec{\rho}', t_1 - t') \times$$

$$<[\delta U(\vec{\rho}_1, z, \omega_1, t_1) / \delta \xi(\vec{\rho}', z, t')] U^*(\vec{\rho}_2, z, \omega_2, t_2) +$$

$$U(\vec{\rho}_1, z, \omega_1, t_1)[\delta U^*(\vec{\rho}_2, z, \omega_2, t_2) / \delta \xi(\vec{\rho}', z, t')]> . \quad (2\text{-}32)$$

The $\delta U / \delta \xi$ terms in this expression will be evaluated next.

The parabolic wave equation is used to evaluate the functional derivatives $\delta U / \delta \xi$. Integrating this equation from $-\infty$ to z results in

15

$$\int_{-\infty}^{z} \nabla_{\perp}^2 U(\vec{\rho},\zeta,\omega,t)d\zeta - 2i\overline{k}[U(\vec{\rho},z,\omega,t) - U_0(\vec{\rho},\omega)] -$$

$$\overline{k}^2 B(\omega) \int_{-\infty}^{z} \xi(\vec{\rho},z,t)U(\vec{\rho},z,\omega,t)d\zeta = 0 \qquad (2\text{-}33)$$

where $U_0(\vec{\rho},\omega)$ is the transmitted signal. After applying the operator $\delta/\delta\xi(\vec{\rho}',z',t')$, where $-\infty < z' < z$ and $-\infty < t' < t$, and noting that

$$\delta\xi(\vec{\rho},z,t)/\delta\xi(\vec{\rho}',z',t') = \delta_F(z-z')\delta_F(\vec{\rho}-\vec{\rho}')\delta_F(t-t') \quad , \qquad (2\text{-}34)$$

Equation 2-33 becomes

$$2i\overline{k} \, \delta U(\vec{\rho},z,\omega,t)/\delta\xi(\vec{\rho}',z',t') + \overline{k}^2 B(\omega)\delta_F(\vec{\rho}-\vec{\rho}')\delta_F(t-t')U(\vec{\rho},z',\omega,t) +$$

$$\int_{z'}^{z} [\overline{k}^2 B(\omega)\xi(\vec{\rho},\zeta,t) - \nabla_{\perp}^2][\delta U(\vec{\rho},\zeta,\omega,t)/\delta\xi(\vec{\rho}',z',t')]d\zeta = 0 \quad . \qquad (2\text{-}35)$$

The lower limit of the integral in this equation is z' because $\delta U(\vec{\rho},z,\omega,t)/\delta\xi(\vec{\rho}',z',t')$ is zero for $z < z'$. Because the source term S_1 contains factors of the form $\delta U(\vec{\rho},z,\omega,t)/\delta\xi(\vec{\rho}',z,t')$, z' is set equal to z in Equation 2-35 with the result

$$\delta U(\vec{\rho},z,\omega,t)/\delta\xi(\vec{\rho}',z,t') = (i\overline{k}B(\omega)/2)\delta_F(\vec{\rho}-\vec{\rho}')\delta_F(t-t')U(\vec{\rho},z,\omega,t) \qquad (2\text{-}36)$$

After substituting this into Equation 2-32, the source term becomes

$$S_1 = \iint_{-\infty}^{\infty} d^2\vec{\rho}' \int_{-\infty}^{t} dt' \, A(\vec{\rho}_1-\vec{\rho}',t_1-t') \, \Gamma \times$$

$$[(ik_1 B_1{}^2/4)\delta_F(\vec{\rho}_1-\vec{\rho}')\delta_F(t_1-t') - (ik_2 B_1 B_2/4)\delta_F(\vec{\rho}_2-\vec{\rho}')\delta_F(t_2-t')]$$

$$= (ik_1 B_1{}^2/4)A(\vec{0},0) \, \Gamma - (ik_2 B_1 B_2/4)A(\vec{\rho}_1-\vec{\rho}_2,t_1-t_2) \, \Gamma \quad . \qquad (2\text{-}37)$$

16

A similar expression may be written down for the second source term in Equation 2-23:

$$S_2 = k_2\beta(\omega_2)\langle\xi(\vec{\rho}_2,z,t_2)U(\vec{\rho}_1,z,\omega_1,t_1)U^*(\vec{\rho}_2,z,\omega_2,t_2)\rangle$$

$$= (ik_1\beta_1\beta_2/4)A(\vec{\rho}_1-\vec{\rho}_2,t_1-t_2)\ \Gamma - (ik_2\beta_2{}^2/4)A(\vec{0},0)\ \Gamma\quad . \qquad (2\text{-}38)$$

2.2.4 Second Form of Transport Equation.

The transport equation for the mutual coherence function is now given by combining Equations 2-37 and 2-38 with 2-23 with the result

$$\partial\Gamma/\partial z + (i/2)[(1/k_1)\nabla_{\perp 1}{}^2 - (1/k_2)\nabla_{\perp 2}{}^2]\ \Gamma -$$

$$(1/8)[2k_1k_2\beta_1\beta_2A(\vec{\rho}_1-\vec{\rho}_2,t_1-t_2) - (k_1{}^2\beta_1{}^2+k_2{}^2\beta_2{}^2)A_0]\ \Gamma \qquad (2\text{-}39)$$

where $A_0 = A(\vec{0},0)$.

The differential equation for Γ will be solved by first letting $\Gamma = \Gamma_0\Gamma_1$ where Γ_0 is the free space solution. The well known solution of the wave equation for the electric field in free space (Equation 2-15 with $\epsilon_1 = 0$) may be written down directly. The Fresnel approximation that $z \gg |\vec{\rho}|$ is then used to expand the electric field and the free space solution Γ_0 is computed. The quantity Γ_0 contains the $1/z^2$ term that partly determines the mean power at the receiver. The next step is to derive a differential equation for Γ_1 from Equation 2-39 and the free space solution. It is the mutual coherence function Γ_1 that determines the second order statistics of the received signal.

2.2.4.1 <u>Free Space Solution Γ_0</u>. In free space and for spherical geometry, the complex envelope of the electric field is

$$\vec{E} = \vec{E}_0\ \exp\ (-ik|\vec{r}|)/|\vec{r}|\quad . \qquad (2\text{-}40)$$

It is easy to verify that this is a solution of the wave equation with ε_1 set to zero. Under the assumption of small angle scattering, $z^2 \gg x^2 + y^2$ in the region of interest and $|\vec{r}|$ may be expanded as

$$|\vec{r}| = (x^2+y^2+z^2)^{1/2} \approx z + (x^2+y^2)/2z \quad . \qquad (2\text{-}41)$$

With this Fresnel approximation,

$$\vec{E} = (\vec{E}_0/z) \exp\left[-ikz-ik(x^2+y^2)/2z\right] \quad . \qquad (2\text{-}42)$$

After recalling that $U = \exp(ikz)\vec{E}$, the free space mutual coherence function is

$$\Gamma_0 = \langle U(\vec{\rho}_1,z,\omega_1)U^*(\vec{\rho}_2,z,\omega_2)\rangle$$

$$= z^{-2} \exp\left[ik_1(x_1^2+y_1^2)/2z + ik_2(x_2^2+y_2^2)/2z\right] \quad . \qquad (2\text{-}43)$$

2.2.4.2 <u>Differential Equation for Γ_1</u>. After substituting $\Gamma = \Gamma_0\Gamma_1$ into Equation 2-39 and using Equation 2-43, the equation for Γ_1 becomes

$$\partial\Gamma_1/\partial z = (i/2k_1)\nabla_{\perp 1}^2\Gamma_1 - (i/2k_2)\nabla_{\perp 2}^2\Gamma_1 +$$

$$(x_1/z)\partial\Gamma_1/\partial x_1 + (y_1/z)\partial\Gamma_1/\partial y_1 + (x_2/z)\partial\Gamma_1/\partial x_2 + (y_2/z)\partial\Gamma_1/\partial y_2$$

$$- S\,\Gamma_1 = 0 \qquad (2\text{-}44)$$

where the source term is

$$S = \left[2k_1k_2\beta_1\beta_2 A(\vec{\rho}_1-\vec{\rho}_2,t_1-t_2) - (k_1^2\beta_1^2+k_2^2\beta_2^2)A_0\right]/8 \quad . \qquad (2\text{-}45)$$

In order for Γ_1 to represent a statistically stationary random process in space, frequency, and time, Γ_1 must be a function only of the differences $\vec{\rho}_1 - \vec{\rho}_2$, $\omega_1 - \omega_2$, and $t_1 - t_2$. It is therefore useful to transform Equation 2-44 to sum and difference spatial and frequency coordinates

18

$$X = (x_1 + x_2)/2$$

$$Y = (y_1 + y_2)/2$$

$$\zeta = x_1 - x_2$$

$$\eta = y_1 - y_2$$

$$\nabla_s^2 = \partial^2/\partial x^2 + \partial^2/\partial y^2 \tag{2-46}$$

$$\nabla_d^2 = \partial^2/\partial \zeta^2 + \partial^2/\partial \eta^2$$

$$\vec{\nabla}_s \cdot \vec{\nabla}_d = \partial^2/\partial X \partial \zeta + \partial^2/\partial Y \partial \eta$$

$$k_s = (k_1 + k_2)/2$$

$$k_d = k_1 - k_2 \quad .$$

After some manipulations, the equation for Γ_1 reduces to

$$\partial \Gamma_1/\partial z - (i/2)(k_s^2 - k_d^2/4)^{-1} \left[k_d \nabla_d^2 + (k_d/4)\nabla_s^2 - k_s \vec{\nabla}_s \cdot \vec{\nabla}_d \right] \Gamma_1 +$$

$$z^{-1} \left[X \, \partial/\partial X + Y \, \partial/\partial Y + \zeta \, \partial/\partial \zeta + \eta \, \partial/\partial \eta \right] \Gamma_1 - S\Gamma_1 = 0 \quad . \tag{2-47}$$

The boundary condition on Γ_1 is that $\Gamma_1(z=-z_t) \equiv 1$ independent
of the other spatial coordinates. Also, the source term S under most con-
ditions is a function only of the difference coordinates. It will there-
fore be assumed that Γ_1 is independent of X and Y. However, the source
term will be a function of X and Y if the spatial extent of the scattering
region is small as, for example, in a barium cloud. The assumption that
Γ_1 is independent of X and Y then requires that the disturbed region in
the ionosphere be large compared to the region from which scattered signal
energy is received.

19

The transport equation may be further reduced by noting that the $1/z$ term, when z is large, will be small compared to the other terms and this term may be neglected. The differential equation for Γ_1 then becomes

$$\partial\Gamma_1/\partial z - (ik_d/2)(k_s^2-k_d^2/4)^{-1}\nabla_d^2\Gamma_1 - S\Gamma_1 = 0 \quad . \qquad (2\text{-}48)$$

2.3   DELTA LAYER APPROXIMATION.

As an RF wave propagates through a thick, irregularly structured ionization layer, the wave first suffers random phase perturbations due to random variations in the index of refraction. As the wave propagates farther, diffractive effects introduce fluctuations in amplitude as well as phase. If the standard deviation σ_ϕ of the phase fluctuations that are suffered by the wave is large, then the amplitude fluctuations are characterized by a Rayleigh probability distribution when the wave emerges from the layer. The delta layer approximation assumes that the phase and amplitude fluctuations are imparted on the wave in an infinitesimally thin layer. This assumption is consistent with the Markov assumption made in deriving the differential equation for the mutual coherence function.

An analytic solution for the two-position, two-frequency mutual coherence function has been obtained by Wittwer (1979) and Knepp (1983b) for a thick ionization layer. The analytic form of this solution is sufficiently complex, however, that the necessary Fourier transforms required to compute the GPSD cannot be performed in closed form. The complex analytic form is simplified by the use of the delta layer approximation to obtain tractable expressions for the mutual coherence function and the GPSD. Wittwer and Knepp have evaluated the accuracy of the delta layer approximation in detail as it affects the delay distribution of the received signal and have found that the maximum error is small for transionospheric satellite communication link geometries as long as the parameters of the GPSD are properly selected. Wittwer (1979) has derived expressions for the signal parameters of the GPSD that include the effects of a thick scattering layer.

Now a relationship between the electron density fluctuations and the phase variations imposed on the wave may be calculated. The differential phase change of the wave along the propagation path ℓ is

$$d\phi/d\ell = r_e \lambda \Delta n_e(\vec{\rho}, z, t) \quad . \tag{2-49}$$

Under the assumption of small angle scattering used to derive the differential equation for Γ, $d/d\ell \approx d/dz$ and the total phase change of the wave is

$$\phi = r_e \lambda \int \Delta n_e(\vec{\rho}, z, t) dz = r_e \lambda \langle n_e \rangle \int \xi(\vec{\rho}, z, t) dz \quad , \tag{2-50}$$

integrated through the ionization layer. The autocorrelation function of the phase ϕ is

$$\langle \phi(\vec{\rho}, t) \phi(\vec{\rho}', t') \rangle = (r_e \lambda \langle n_e \rangle)^2 \int dz \int dz' \langle \xi(\vec{\rho}, z, t) \xi(\vec{\rho}', z', t') \rangle$$

$$= (r_e \lambda \langle n_e \rangle)^2 \int dz \, A(\vec{\rho} - \vec{\rho}', t - t')$$

$$= (r_e \lambda \langle n_e \rangle)^2 L_\delta A(\vec{\rho} - \vec{\rho}', t - t') \tag{2-51}$$

where L_δ is the delta layer thickness. The Markov approximation (Equation 2-29) has been used in evaluating the autocorrelation of ξ. However, it is shown in Appendix A that Equation 2-51 is valid as long as the scattering layer thickness is large compared to the parallel decorrelation distance of the electron density fluctuations. Finally, the phase variance imparted on the wave is

$$\sigma_\phi^2 = (r_e \lambda \langle n_e \rangle)^2 L_\delta A_0 \quad . \tag{2-52}$$

The quantity A_0 depends on the power spectrum of the electron density fluctuations in the ionosphere. The value of A_0 for a three-dimensional k^{-4} in situ power spectrum and for the delta layer approximation is given in Appendix B.

21

In general, only part of the total phase variance results in the Rayleigh amplitude fluctuations that are of described by the GPSD. Wittwer (1979, 1980) calls this part the Rayleigh phase variance. The rest of the total phase variance is associated with the mean dispersive effects described by the exponential term of Equation 2-16. Physically, it is the smaller sized electron density fluctuations that result in diffractive effects and the larger sized fluctuations that result in dispersive effects. Both Wittwer and Knepp (1982) describe how the Rayleigh phase variance may be separated from the total phase variance. In the developments that follow, the phase variance in Equation 2-52 will be assumed to be the Rayleigh phase variance associated with amplitude fluctuations.

2.4   FROZEN-IN APPROXIMATION.

Under the frozen-in approximation, the temporal variation of the electron density fluctuations is given by

$$n_e(\vec{\rho},z,t) = n_e(\vec{\rho}-\vec{v}t,z,0) \quad . \tag{2-53}$$

This equation is valid if the electron density fluctuations with a scale size L_0 do not appreciably change their shape within the time required for the structures to drift a distance L_0. This is called Taylor's frozen-in approximation. With this approximation, the function A becomes

$$A(\vec{\rho},t) = A(\vec{\rho}-\vec{v}t,0) \quad . \tag{2-54}$$

This approximation is accurate for ionospheric conditions where the ionization has broken up into a single layer of striations aligned with the earth's magnetic field lines. The frozen-in approximation may not be valid before striations have formed or when there are multiple scattering layers in the line-of-sight. Alternative forms for the coherence functionand the generalized power spectral density for this latter situation are considered in Section 2.9.

22

2.5   SOLUTION OF THE TRANSPORT EQUATION.

Before proceeding with the solution of the transport equation, it is convenient to expand the source term S by making two non-restrictive assumptions. First, it will be assumed that the RF frequencies of interest are large compared to the plasma frequency. Second, it will be assumed that k_d is much smaller than k_s. The solution obtained will then be valid for a small range of frequencies around k_s and for frequencies large compared to typical peak ionospheric plasma frequencies of a few hundred MHz. With these assumptions, the source term becomes

$$S = (k_p^4/4k_s^2)[A(\vec{\rho}_d,t_d) - A_o] - (k_d^2 k_p^4/8k_s^4)A_o \qquad (2\text{-}55)$$

where $\vec{\rho}_d$ is a two dimensional position vector in the ζ-n plane, t_d is the time difference, and $k_p = \overline{\omega}_p/c$.

The last term in Equation 2-55 is a function of frequency and z but is independent of ζ and n. This suggests that another useful factorization is $\Gamma_1 = \Gamma_2\Gamma_3$ where Γ_3 is independent of ζ and n. After substituting $\Gamma_2\Gamma_3$ for Γ_1 in Equation 2-48 and separating variables, the result is

$$(1/\Gamma_2)\partial\Gamma_2/\partial z - (ik_d/2k_s^2\Gamma_2)\nabla_d^2\Gamma_2 - (k_p^4/4k_s^2)[A(\vec{\rho}_d,t_d) - A_o] +$$

$$(1/\Gamma_3)\partial\Gamma_3/\partial z + (k_d^2 k_p^4/8k_s^4)\,A_o = 0 \quad . \qquad (2\text{-}56)$$

The last two terms of this equation are spatial functions only of z and therefore must be separately equal to zero for arbitrary values of ζ and n.

The source term in the Γ_3 equation is only non-zero within the delta layer. Thus from the transmitter to the delta layer, Γ_3 is unity. With this boundary condition, the solution of the Γ_3 equation is

23

$$\Gamma_3 = \exp\left[-(k_p^4 k_d^2/8k_s^4)A_0(z-z_t)\right] \quad , \quad z > z_t \quad . \qquad (2\text{-}57)$$

This term gives the effect of the different transit times of the different frequencies due to the frequency dependence of the index of refraction.

Now the equation for Γ_2 may be solved using the delta layer approximation. The equation for Γ_2 is

$$(1/\Gamma_2)\partial\Gamma_2/\partial z - (ik_d/2k_s^2\Gamma_2)\nabla_d^2\Gamma_2 - (k_p^4/4k_s^2)[A(\vec{\rho}_d,t_d) - A_0] = 0 \quad . \quad (2\text{-}58)$$

Within the delta layer, the k_d term is small compared to the source term and may be ignored. This is equivalent to saying that diffractive effects are not important within the delta layer (Lee and Jokipii 1975b). Integrating Equation 2-58 through the delta layer gives the value of Γ_2 at the point where the wave emerges from the delta layer:

$$\Gamma_2 = \exp\left\{(k_p^4 L_\delta/4k_s^2)[A(\vec{\rho}_d,t_d) - A_0]\right\} \quad . \qquad (2\text{-}59)$$

The solution from this point proceeds as follows. Between the delta layer and the receiver, the signal propagates in free space so the equation for Γ_1 is

$$\partial\Gamma_1/\partial z - (ik_d/2k_s^2)\nabla_d^2\Gamma_1 = 0 \qquad (2\text{-}60)$$

The $\nabla_d^2\Gamma_1$ term in this equation gives the effects of diffraction on the signal as it propagates from the delta layer to the receiver. The boundary condition is $\Gamma_1 = \Gamma_2\Gamma_3$ at the point where the wave emerges from the delta layer. This equation is easily solved by taking the Fourier transform from spatial coordinates ζ and η to angular coordinates. First it is convenient to transform variables to

$$u = \zeta/z$$

$$v = \eta/z \quad .$$

24

The angular variables K_u and K_v are then independent of z. After the change in variables, the equation for Γ_1 becomes

$$\partial\Gamma_1/\partial z - (ik_d/2k_s^2 z^2)(\partial^2/\partial u^2 + \partial^2/\partial v^2)\,\Gamma_1 = 0 \quad .. \quad (2\text{-}61)$$

The Fourier transform pairs; from spatial coordinates $\vec{\rho}$ in the plane normal to the line-of-sight to angular coordinates $\vec{K}_\perp$, from carrier frequency differences ω_d to delay τ, and from time differences t_d to Doppler frequencies ω_D; are defined in this report to be

$$\hat{\Gamma}(\vec{K}_\perp) = \iint\limits_{-\infty}^{\infty} \exp(-i\vec{K}_\perp \cdot \vec{\rho})\Gamma(\vec{\rho})d^2\vec{\rho} \qquad (2\text{-}62a)$$

$$\hat{\Gamma}(\tau) = (2\pi)^{-1} \int\limits_{-\infty}^{\infty} \exp(i\omega_d \tau)\Gamma(\omega_d)d\omega_d \qquad (2\text{-}62b)$$

$$\hat{\Gamma}(\omega_D) = \int\limits_{-\infty}^{\infty} \exp(-i\omega_D t_d)\Gamma(t_d)dt_d \qquad (2\text{-}62c)$$

and

$$\Gamma(\vec{\rho}) = (2\pi)^{-2} \iint\limits_{-\infty}^{\infty} \exp(i\vec{K}_\perp \cdot \vec{\rho})\hat{\Gamma}(\vec{K}_\perp)d^2\vec{K}_\perp \qquad (2\text{-}63a)$$

$$\Gamma(\omega_d) = \int\limits_{-\infty}^{\infty} \exp(-i\omega_d \tau)\hat{\Gamma}(\omega_d)d\tau \qquad (2\text{-}63b)$$

$$\Gamma(t_d) = (2\pi)^{-1} \int\limits_{-\infty}^{\infty} \exp(i\omega_D t_d)\hat{\Gamma}(t_d)d\omega_D \quad . \qquad (2\text{-}63c)$$

Upon transforming from u and v to K_u and K_v, the equation for $\hat{\Gamma}_1$ is

$$\partial\hat{\Gamma}_1/\partial z + (ik_d/2k_s^2 z^2)(K_u^2 + K_v^2)\hat{\Gamma}_1 = 0 \quad . \qquad (2\text{-}64)$$

25

This equation is integrated from $z = z_t + L_\delta$ to $z = z_t + z_r$ which gives

$$\hat{\Gamma}_1(K_u, K_v, z_t+z_r, \omega_d, t_d) = \hat{\Gamma}_1(K_u, K_v, z_t+L_\delta, \omega_d, t_d) \times$$

$$\exp\left[-(ik_d/2k_s^2)(K_u^2+K_v^2)\gamma\right] \qquad . \qquad (2\text{-}65)$$

where

$$\gamma = \int_{z_t+L_\delta}^{z_t+z_r} z^{-2} dz = \frac{z_r - L_\delta}{(z_t+z_r)(z_t+L_\delta)} \qquad . \qquad (2\text{-}66)$$

The expression for γ may be simplified by setting L_δ to zero which is consistent with the delta layer approximation.

2.6   QUADRATIC PHASE STRUCTURE APPROXIMATION.

At this point, a formal solution of the Fourier transform of the two-position, two-frequency, two-time mutual coherence function at the receiver has been computed in terms of the structure function $A(\vec{\rho}_d, t_d)$ - A_0. As a practical matter, the quadratic phase structure approximation is required to make the exponent in Equation 2-59 quadratic in the spatial variables. This gives the resulting coherence function a tractable mathematical form. However, for the small angle, strong scattering conditions considered in this report, the correlation distance of the signal will be much smaller than the correlation distance of the electron density fluctuations. The coherence function will then be determined primarily by the values of $A(\vec{\rho}_d, t_d)$ - A_0 at small values of $\vec{\rho}_d$ and t_d. A Taylor series expansion of $A(\vec{\rho}_d, t_d)$ - A_0, keeping only the quadratic terms, will then provide a reasonably accurate mutual coherence function.

Under the frozen-in approximation, the temporal variation of $A(\vec{\rho}_d, t_d)$ is given by $A(\vec{\rho}_d-\vec{v}t_d, 0)$. It is therefore necessary to consider only the spatial form $A(\vec{\rho}_d)$. The Taylor series expansion will make the following calculations independent of the functional form of $A(\vec{\rho}_d)$ as long

26

as the second derivative of A exists for $\vec{\rho}_d$ equal to zero. A detailed discussion of $A(\vec{\rho}_d)$ will therefore be deferred to Appendix B. However, some generic properties of $A(\vec{\rho}_d)$ need to be considered here in order to specify the functional form of the quadratic terms in the Taylor series expansion.

The propagation coordinate systems are shown in Figure 2-2. The z axis is along the line-of-sight and the t axis is aligned with the geo-magnetic field lines $\vec{B}$ at the elevation of the delta layer. The r and s axes are in a plane normal to the magnetic field. The penetration angle ψ is the angle between the z axis and the $\vec{B}$ axis. In the plane of the receiver, the x axis direction is given by the cross product of the $\vec{B}$ vector and the $\hat{z}$ unit vector.

Consider now the functional form the power spectrum Φ_ξ of the electron density fluctuations in the r-s-t coordinate system. The power
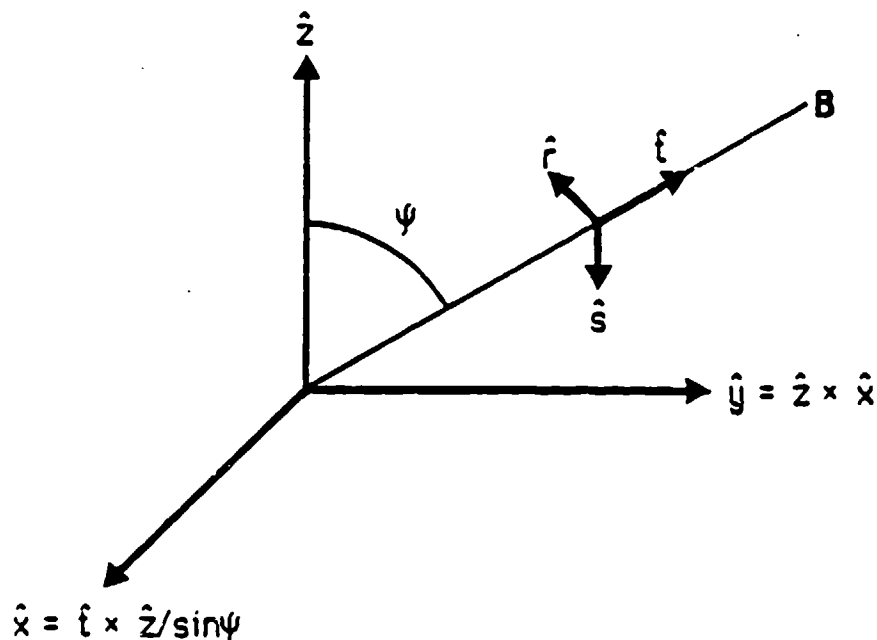
Figure 2-2. Propagation coordinate systems.

spectrum is usually assumed to be a function of the quantity $L_r^2 K_r^2 + L_s^2 K_s^2 + L_t^2 K_t^2$ where L_r, L_s, and L_t are the scale sizes of the fluctuations in the three directions. The power spectrum must be rotated into the x-y-z coordinate system in order to calculate $A(\vec{\rho}_d)$. Before performing this rotation, the usual assumption that the electron density fluctuations are elongated in the t direction and are symmetric about the t direction will be made. The scale sizes are then

$$L_r = L_s = L_o$$
$$L_t = qL_o \qquad \qquad (2\text{-}67)$$

where q $(q \geq 1)$ is the axial ratio. After the rotation, the power spectrum will be a function of the quantity (Wittwer 1979) $L_x^2 K_x^2 + L_y^2 L_y^2 + L_z^2 K_z^2 + 2L_{yz} K_y K_z$ where

$$L_x = L_o$$

$$L_y = L_o(\cos^2\psi + q^2\sin^2\psi)^{1/2} = L_o/\delta$$

$$\qquad \qquad (2\text{-}68)$$

$$L_z = L_o(\sin^2\psi + q^2\cos^2\psi)^{1/2}$$

$$L_{yz} = L_o(q^2-1)\sin\psi\cos\psi \quad .$$

The parameter δ $(1/q \leq \delta \leq 1)$ appears throughout subsequent sections of this report and is defined to be the ratio of the x and y scale sizes:

$$\delta = L_x/L_y = (\cos^2\psi + q^2\sin^2\psi)^{-1/2} \qquad . \qquad (2\text{-}69)$$

Now, the function $A(\vec{\rho}_d)$ is the two dimension Fourier transform of the power spectrum Φ_ξ:

$$A(\vec{\rho}_d) = (2\pi)^{-2} \int\int_{-\infty}^{\infty} \exp(i\vec{K}_\perp \cdot \vec{\rho}_d) \Phi_\xi(\vec{K}_\perp, K_z=0) \, d^2\vec{K}_\perp . \qquad (2\text{-}70)$$

28

Setting $K_z = 0$ in the power spectrum in this equation results in having Φ_ξ be a function of $L_x^2 K_x^2 + L_y^2 K_y^2$ and in having $A(\vec{\rho}_d)$ calculated in the $z = 0$ plane of the delta layer. After the Fourier transform is performed, A will be a function of the quantity $x^2/L_x^2 + y^2/L_y^2$ (see Appendix B) or equivalently of $(x^2 + \delta^2 y^2)/L_0^2$.

The quadratic phase structure approximation now takes the form

$$A(\vec{\rho}_d) = A_0 [1 - A_2 (x^2 + \delta^2 y^2)/L_0^2] \qquad . \qquad (2-71)$$

The coefficient A_2 is calculated in Appendix B for a K^{-4} electron density fluctuation spectrum. The coefficient A_0 is given in terms of the phase variance σ_ϕ^2 by Equation 2-52.

2.7 MUTUAL COHERENCE FUNCTION.

The mutual coherence function Γ_1 at the plane of the receiver is computed as outlined in Section 2.5. At this point, the frozen-in approximation will be used to include explicit temporal variations. In order to do this, the drift velocity must be specified. To be conservative, the drift velocity will be assumed to be along the direction with the smallest scale size for the electron density fluctuations (i.e. the x direction).

The boundary condition for Γ_1 at the delta layer is again $\Gamma_1 = \Gamma_2\Gamma_3$ evaluated at $z = L_\delta$. Using Equation 2-52 to relate A_0 to the phase variance and then setting the delta layer thickness L_δ to zero gives the following for Γ_2 and Γ_3 at the point where the wave emerges from the delta layer. From Equation 2-59 using the quadratic phase structure approximation, the diffraction term boundary condition is

$$\Gamma_2 = \exp \left\{ -\sigma_\phi^2 A_2 [(\varsigma - v_x t_d)^2 + \delta^2 \eta^2]/L_0^2 \right\} \qquad (2-72)$$

29

and from Equation 2-57, the refraction term boundary condition is

$$\Gamma_3 = \exp\left[-\sigma_\phi^2 \omega_d^2/(2\omega_0^2)\right] \qquad (2\text{-}73)$$

where $\omega_0 = ck_s$ is the carrier radian frequency. Upon changing variables in the Γ_2 equation to the dimensionless spatial coordinates u and v and performing the Fourier transform to K_u and K_v coordinates, the boundary condition for $\hat{\Gamma}_1$ is

$$\Gamma_1(K_u,K_v,z_t,\omega_d,t_d) = \left[\pi L_0^2/(\sigma_\phi^2 A_2 z_t^2 \delta)\right] \times$$

$$\exp\left[-\sigma_\phi^2 \omega_d^2/(2\omega_0^2)\right] \exp\left[iK_u(v_x t_d/z_t)\right] \times$$

$$\exp\left[-L_0^2(K_u^2+K_v^2/\delta^2)/(4\sigma_\phi^2 A_2 z_t^2)\right] \quad . \qquad (2\text{-}74)$$

The solution at the plane of the receiver is given by Equation 2-65 and this boundary condition.

After performing the inverse Fourier transform on the solution $\hat{\Gamma}_1(K_u,K_v,z_r,\omega_d,t_d)$ and converting to unnormalized distance units x and y, the mutual coherence function may be written as

$$\Gamma_1(x,y,\omega_d,t_d) = \left[(1+i\Lambda\omega_d/\omega_{coh})(1+i\Lambda\delta^2\omega_d/\omega_{coh})\right]^{-1/2} \times$$

$$\exp\left[-\sigma_\phi^2 \omega_d^2/(2\omega_0^2)\right] \times$$

$$\exp\left[-(x-v_e t_d)^2 \ell_0^{-2}/(1+i\Lambda\omega_d/\omega_{coh})\right] \times$$

$$\exp\left[-\delta^2 y^2 \ell_0^{-2}/(1+i\Lambda\delta^2\omega_d/\omega_{coh})\right] \qquad (2\text{-}75)$$

where

$$\Lambda = \left[2/(1+\delta^4)\right]^{1/2} \qquad (2\text{-}76)$$

and

$$v_e = v_x(z_t+z_r)/z_t \qquad (2\text{-}77)$$

is the effective drift velocity of the ionosphere as seen at the receiver.

30

The decorrelation distance ℓ_0 of the received electric field is defined as

$$\ell_0 = (z_t + z_r) L_0 / (z_t \sqrt{\overline{A_2}} \, \sigma_\phi) \qquad (2\text{-}78)$$

and the coherence bandwidth ω_{coh} is defined as

$$\omega_{coh} = \Lambda \omega_0^2 L_0^2 (z_t + z_r) / (2 c \sigma_\phi^2 A_2 z_t z_r) \quad . \qquad (2\text{-}79)$$

It will be shown below that ℓ_0 agrees with the usual definition of decorrelation distance and it will be seen in the next section that the coherence bandwidth is proportion to $2\pi f_0$ where f_0 is the frequency selective bandwidth of the signal. It is clear from the form of Γ_1 in Equation 2-75 that the coherence bandwidth could have been defined as $\omega_{coh} \Lambda$. The factor Λ has been included here in order to simplify the relationship between ω_{coh} and f_0.

Equations 2-78 and 2-79 are only valid under the delta layer approximation and do not reflect now these parameters are actually calculated. Wittwer (1979, 1980) has derived expressions for the decorrelation distance and the coherence bandwidth that are valid for more general scattering layer geometries. It is the expressions of Wittwer that are used in signal specifications to calculate these signal parameters. This is also true for the decorrelation time which is formally defined under the delta layer and frozen-in approximations in the next section.

For satellite communications links, the distance from the ionosphere to the satellite is typically much larger than the distance from the ionosphere to the ground. If the transmitter is on the satellite then $z_t \gg z_r$, and if the transmitter is on the ground then $z_t \ll z_r$. Because the expression for the decorrelation distance is not reciprocal in z_t and z_r, the value of ℓ_0 depends on the direction of propagation. However, the expression for the coherence bandwidth is reciprocal in z_t and z_r so ω_{coh} and the frequency selective bandwidth are independent of the propagation direction.

31

The decorrelation distance of the signal as it emerges from the delta layer is approximately equal to L_0/σ_ϕ. Under strong scattering conditions where $\sigma_\phi \gg 1$, this distance will be much smaller than the electron density fluctuation scale size and the quadratic phase structure approximation conditions are met. Conversely, under weak scattering conditions where $\sigma_\phi \sim 1$ the quadratic phase approximation will give inaccurate results for the mutual coherence function.

Consider now the mutual coherence function for two-positions, one-frequency and one-time:

$$\Gamma_1(x,y,0,0) = \exp\left[-(x/\ell_0)^2 - (\delta y/\ell_0)^2\right] \quad . \tag{2-80}$$

The distance ℓ_0 is then seen to be the $1/e$ point of $\Gamma_1(x,0,0,0)$ and is therefore the x direction decorrelation distance. The distance ℓ_0/δ is the $1/e$ point of $\Gamma_1(0,y,0,0)$ and is therefore the y direction decorrelation distance. Because δ is less than or equal to unity, the y direction decorrelation distance is always greater than or equal to ℓ_0.

2.8 GENERALIZED POWER SPECTRAL DENSITY.

The generalized power spectral density $S(\vec{K}_\perp,\tau,\omega_D)$ of the signal incident on the plane of the receiver is the Fourier transform of the mutual coherence function:

$$S(\vec{K}_\perp,\tau,\omega_D) = (2\pi)^{-1} \iint_{-\infty}^{\infty} d^2\vec{\rho} \int_{-\infty}^{\infty} d\omega_d \int_{-\infty}^{\infty} dt_d \Gamma_1(\vec{\rho},\omega_d,t_d) \times$$

$$\exp\left[-i(\vec{K}_\perp\cdot\vec{\rho}-\omega_d\tau+\omega_D t_d)\right] \tag{2-81}$$

where delay τ is the Fourier transform of frequency difference ω_D and Doppler frequency ω_D is the Fourier transform of time difference t_d. The quantity $S(\vec{K}_\perp,\tau,\omega_D)d^2\vec{K}_\perp d\tau d\omega_D$ is equal to the mean signal power arriving

within the angular interval $\vec{K}_\perp$ to $\vec{K}_\perp + d^2\vec{K}_\perp$; with delays relative to a nominal propagation time in the interval τ to $\tau + d\tau$; and with Doppler frequencies in the interval ω_D to $\omega_D + d\omega_D$. The delay spectrum of the GPSD is a consequence of the fact that different frequencies propagate differently through the ionosphere with some frequencies arriving early and some frequencies arriving late. The importance of this effect depends on the ratio of the signal bandwidth to the frequency selective bandwidth.

The indicated integrals in Equation 2-81 can all be done in closed form. If the K_x integral is done first, the distance offset results in a term with the form $\exp(iK_x v_e t_d)$ times a function of K_x. The Fourier transform from t_d to ω_D results in the delta function $2\pi\delta_F(\omega_D - K_x v_e)$. The GPSD is then the product of a Doppler term and an angular-delay term of the form

$$S(K_x, K_y, \tau, \omega_D) = S_D(\omega_D)S(K_x, K_y, \tau) \quad . \tag{2-82}$$

The angular-delay part of the GPSD is

$$S(K_x, K_y, \tau) = (\pi/2)^{1/2} \, \alpha\omega_{coh}\ell_0^2\delta^{-1} \exp\left[-(K_x^2+\delta^{-2}K_y^2)\ell_0^2/4\right] \times$$

$$\exp\left\{-(\alpha^2/2)\left[\omega_{coh}\tau - \Lambda(K_x^2+K_y^2)\ell_0^2/4\right]^2\right\} \tag{2-83}$$

where the delay parameter α is defined to be

$$\alpha = \omega_0/\sigma_\phi\omega_{coh} \quad . \tag{2-84}$$

When it is recalled that σ_ϕ is the Rayleigh phase variance, the parameter α is equal to $1/C_1$ where the notation C_1 is used by Wittwer (1980, 1982, 1986). The components of $\vec{K}_\perp$ are related to the scattering angles θ_x and θ_y about the x and y axis respectively by the relations

$$K_x = 2\pi \sin(\theta_x)/\lambda$$

$$K_y = 2\pi \sin(\theta_y)/\lambda \quad . \tag{2-85}$$

33

For the frozen-in approximation and assuming that the effective velocity is along the x direction, the Doppler spectrum is

$$S_D(\omega_D) = 2\pi\tau_o \delta_F(\omega_D\tau_o - K_x\ell_o) \quad . \tag{2-86}$$

The quantity τ_o is the decorrelation time of the signal at the receiver. It is formally defined here to be the time required for the random diffraction pattern to drift one decorrelation distance:

$$\ell_o = v_e\tau_o \quad . \tag{2-87}$$

However, as is the case for the decorrelation distance and the coherence bandwidth, the decorrelation time is calculated using the more general formalism of Wittwer.

The significance of the parameters α, ℓ_o and ω_{coh} that appear in the angular-delay part of th GPSD will be discussed in the next subsections.

2.8.1   Delay Spread and α.

The delay spread $S(\tau)$ of the signal energy arriving at a fixed angle, given by the second exponential term in Equation 2-83, has the Gaussian form

$$S(\tau) = (\alpha\omega_{coh}/\sqrt{2\pi}) \exp\left[-\alpha^2\omega^2_{coh}(\tau-t_p)^2/2\right] \tag{2-88}$$

where t_p is the additional propagation time for signals arriving at the angles K_x and K_y. To see this, the expression for t_p is expanded using the definitions for ℓ_o and ω_{coh} giving

$$t_p = (\theta^2_x+\theta^2_y)(z_t+z_r)(z_r/z_t)/2c \quad . \tag{2-89}$$

The geometry of the scattering in one plane is shown in Figure 2-3. It is clear that for small angle scattering, the angle θ_t is related to the receiver scattering angle by

34
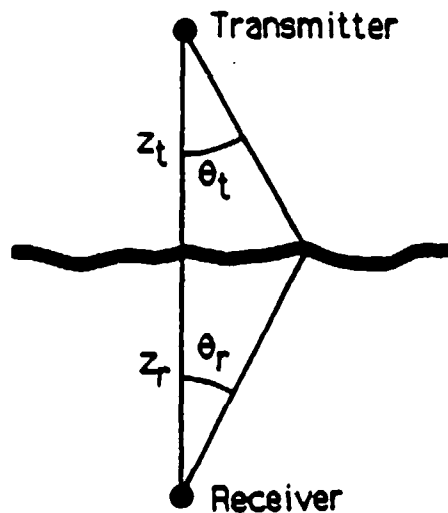
Figure 2-3. Scattering geometry

$$\theta_t = (z_r/z_t)\theta_r \quad . \tag{2-90}$$

The difference d between the line-of-sight distance and the scattered path length, for small angle scattering, is given by

$$d = (z_r^2 + z_r^2\theta_r^2)^{1/2} + (z_t^2 + z_t^2\theta_t^2)^{1/2} - (z_r + z_t) \approx (z_r/z_t)(z_r + z_t)\theta_r^2/2 \tag{2-91}$$

for scattering only in one plane. When scattering about both the x and y axes is taken into account, the total path difference is given by Equation 2-90 with θ_r^2 replaced by $\theta_x^2 + \theta_y^2$. The additional time required for the signal to propagate along the scattered path is just d/c which is equal to t_p.

For a given value of the coherence bandwidth, larger values of α mean that the signal energy arrives with a narrower distribution in delay about the time t_p. The delay parameter α is then a measure of the relative importance of diffraction or scattering and refraction with large values of α indicating strong scattering effects and small values indicating weak scattering or refractive effects (Knepp 1982). The strong scattering limit then requires that the values of α be large.

2.8.2 Frequency Selective Bandwidth and ω_{coh}.

The frequency selective bandwidth f_0 is an important measure of the effects of scintillation on the propagation of wide bandwidth signals. This quantity is defined as

$$f_0 = 1/(2\pi\sigma_\tau) \qquad (2-92)$$

where σ_τ, the time delay jitter of the received signal, is

$$\sigma_\tau^2 = \langle\tau^2\rangle - \langle\tau\rangle^2 \quad . \qquad (2-93)$$

These delay moments can be calculated directly from the angular-delay part of the GPSD using the definition

$$P_0\langle\tau^n\rangle = (2\pi)^{-2} \iint_{-\infty}^{\infty} d^2\vec{K}_\perp \int_{-\infty}^{\infty} d\tau \ \tau^n \ S(\vec{K}_\perp,\tau) \quad . \qquad (2-94)$$

It is easy to show that the mean received power P_0 is equal to unity. The first and second moments are also obtainable in closed form giving the relationship between ω_{coh} and the frequency selective bandwidth:

$$\omega_{coh} = 2\pi f_0 (1+1/\alpha^2)^{1/2} \quad . \qquad (2-95)$$

This expression is valid only under the quadratic phase structure approximation because Equation 2-94 has been evaluated using the GPSD calculated with this approximation. Yeh and Liu (1977) have calculated an expression for the time delay jitter keeping both the second order and the fourth order terms in the expansion of $A(\vec{\rho})$. This results in having more terms in the expression for the time delay jitter. However, these additional terms will be significant only when the quadratic approximation for $A(\vec{\rho})$ is invalid and therefore only when the expression for the GPSD is also invalid.

36

The $1 + 1/\alpha^2$ term in the expression for the coherence bandwidth represents the relative contributions to the time delay jitter from diffraction (1) and refraction ($1/\alpha^2$). In the limit that α is large, the time delay jitter is determined by diffractive effects alone which should be the case under strong scattering conditions.

2.8.3 Angle-of-Arrival Fluctuations and ℓ_0.

A key parameter in determining the severity of antenna filtering effects is the standard deviation σ_θ of the angle-of-arrival fluctuations of the electric field incident on the antenna. It is clear that for anisotropic scattering, the values of σ_θ for scattering about the x and y axes will differ. The variance of the angle-of-arrival fluctuations about the ξ direction is defined as

$$\sigma_{\theta\xi}^2 = (2\pi)^{-2} \iint_{-\infty}^{\infty} d^2\vec{K}_\perp \int_{-\infty}^{\infty} d\tau \; (\lambda K_\xi/2\pi)^2 S(\vec{K}_\perp, \tau) \qquad (2-96)$$

under the small angle scattering approximation that is required for the GPSD to be valid. The standard deviations of the angle-of-arrival fluctuations about the x and y axes are

$$\sigma_{\theta x} = \lambda/(\sqrt{2}\,\pi\ell_0) \qquad\qquad (2-97)$$

and

$$\sigma_{\theta y} = \lambda/(\sqrt{2}\,\pi\ell_0/\delta) \quad . \qquad\qquad (2-98)$$

For the small angle scattering to be valid, $\sigma_{\theta x}$ (which is the larger of the two) must be small relative to 1 radian. Thus the decorrelation distance ℓ_0 must be approximately equal to or greater than the RF wavelength λ. The small angle approximation has been used throughout the derivation of the GPSD, starting with the parabolic wave

37

equation. The resulting expression for the GPSD, however, does not exhibit singular behavior when the angle-of-arrival fluctuations become large and thus the small angle approximation is quite robust.

2.8.4 An Isotropic Example.

When the penetration angle is zero, δ equals unit and the scattering is isotropic about the line-of-sight. The one-dimensional generalized power spectral density is then given by the integral

$$S(K,\tau) = (2\pi)^{-1} \int_{-\infty}^{\infty} S(K,K_y,\tau) \, dK_y$$

$$= (\alpha^{1/2}\omega_{coh}\ell_0/2^{1/4}\pi^{1/2}) \exp\left[(1/2\alpha^2)-\omega_{coh}\tau\right] \times$$

$$F\{[1+\alpha^2(K^2\ell_0^2/4-\omega_{coh}\tau)]/(2^{1/2}\alpha)]\} \tag{2-99}$$

where the function F is defined as

$$F(z) = \exp(-z^2) \int_{-\infty}^{\infty} \exp(-t^4-2t^2 z) \, dt \quad . \tag{2-100}$$

The F function has been approximated by Wittwer (1980) using a polynomial expansion that is accurate to within one percent. This function may also be written in terms of $K_{1/4}$ and $I_{1/4}$ Bessel functions (Knepp 1982).

A three dimensional plot of the isotropic one-dimension GPSD with α equal to 4 is shown in Figure 2-4. This plot shows the mean received power as a function of angle K and delay τ. The vertical axis is linear with arbitrary units.

It can be seen that the power arriving at large angles is also the power arriving at long delays. The power arriving at long delays thus has higher spatial frequency components than power arriving at short

38
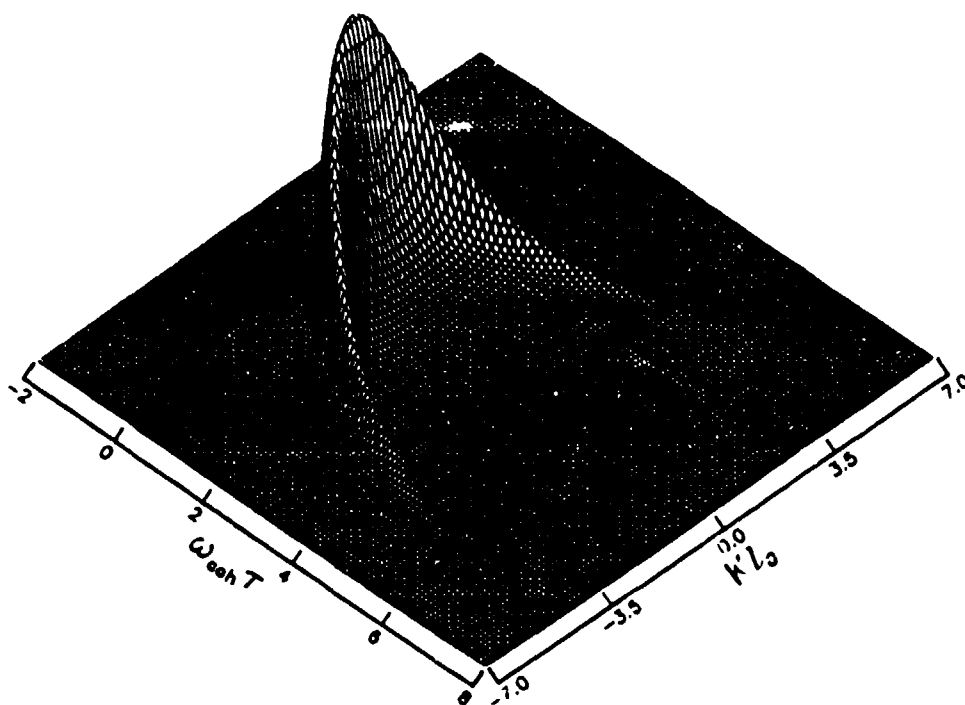
Figure 2-4. Generalized power spectral density.

delays. Under the frozen-in approximation where the ionosphere is modeled as a rigid structure drifting across the line-of-sight, these higher spatial frequency components correspond to higher Doppler frequency components. The signal energy arriving at long delays then varies more rapidly in time than the signal energy arriving at short delays under the frozen-in approximation.

2.9   TURBULENT APPROXIMATION.

Under conditions before striations have formed in the ionosphere or when there are multiple scattering layers with different velocities in the line-of-sight, the frozen-in approximation may provide a poor model of the temporal variations of the received signal. An alternative to the frozen-in approximation is the turbulent approximation where the temporal

variations and the spatial variations of the received signal are independent. The mathematical form of this approximation is that the two-position, two-frequency, two-time mutual coherence function is separable into a product of a spatial-frequency term and a time term:

$$\Gamma_1(\vec{\rho}, \omega_d, t_d) = \Gamma(\vec{\rho}, \omega_d)\Gamma(t_d) \quad . \tag{2-101}$$

The coherence function $\Gamma(\vec{\rho}, \omega_d)$ is given by Equation 2-75 with the time difference t_d set to zero. After performing the necessary Fourier transforms, the GPSD for this model has the form

$$S(\vec{K}_\perp, \tau, \omega_D) = S_D(\omega_D)S(\vec{K}_\perp, \tau) \tag{2-102}$$

where for this model the Doppler spectrum $S_D(\omega_D)$ is a function only of the Doppler frequency. Thus $S_D(\omega_D)$ does not couple angles and Doppler frequencies or, equivalently, positions and times as is the case with the frozen-in approximation. The angle-delay term in Equation 2-102 is then given by Equation 2-83.

Under the frozen-in approximation, the temporal variations of the signal at long delay are more rapid than the temporal variations of the signal arriving at short delays. Under the turbulent approximation, the Doppler spectrum is independent of delay so the temporal variations at all delays have the same rate.

In order to specify the Doppler spectrum under the turbulent approximation, the two position, two time mutual coherence function of the electron density fluctuations is needed. Detailed descriptions of the spatial variations of the electron density fluctuations are currently available (Wittwer 1986). However, detailed information on the temporal variations of the electron density fluctuations in the ionosphere is not currently available. An f^{-4} Doppler spectrum will therefore be assumed for implementation convenience in Section 5 where channel simulation techniques are discussed.

40

2.10   IMPULSE RESPONSE FUNCTION AND ANTENNA EFFECTS.

The channel impulse response function of the signal incident on the plane of the receiver and the impulse response function of the signal at the output of an aperture antenna will be discussed in this subsection.

2.10.1   Channel Impulse Response Function.

Consider a solution $U(\vec{\rho}, z_r, \omega, t)$ to the parabolic wave equation in the plane of the receiver. This represents the random effects due to the fluctuating ionosphere on the incident electric field at position $\vec{\rho}$ and time t from a transmitted monochromatic wave with angular frequency ω. The channel impulse response function of the signal in the receiver plane is (Knepp and Wittwer 1984)

$$h(\vec{\rho}, \tau, t) = (2\pi)^{-1} \int_{-\infty}^{\infty} U(\vec{\rho}, z_r, \omega + \omega_0, t) \exp\left[i\overline{\theta}(\omega) + i\omega\tau\right] d\omega \qquad (2\text{-}103)$$

where ω_0 is the carrier angular frequency and $\overline{\theta}(\omega)$ is the dispersive contribution to the impulse response function due to the mean ionization. The term $\exp\left[i\overline{\theta}(\omega)\right]$ is the transfer function of a smooth ionized plasma and is equal to the exponential term in Equation 2-16. Thus $\overline{\theta}(\omega)$ is

$$\overline{\theta}(\omega) = -\int_{-z_t}^{z_r} \overline{k}(z')dz' = -(\omega/c)\int_{-z_t}^{z_r} [1 - \overline{\omega}_p^2(z')/\omega^2]^{1/2} dz' \quad . \qquad (2\text{-}104)$$

Because the smooth plasma or dispersion effects represented by $\exp[i\overline{\theta}(\omega)]$ and the fluctuating plasma effects represented by $U(\vec{\rho}, z_r, \omega, t)$ appear as the product, it is convenient to separate these effects. The dispersive effects will be considered in Section 2.10.2.

41

If the transmitted signal is a modulated waveform $m(t)$ then the signal complex voltage incident on the plane of the receiver is the convolution of the transmitted modulation and the channel impulse response function:

$$e(\vec{\rho}, t) = \int_{-\infty}^{\infty} m(t-\tau-t_p) h(\vec{\rho}, \tau, t) \, d\tau \qquad (2\text{-}105)$$

where t_p is the nominal propagation time. If the delay spread of the impulse response function is larger than the symbol period of $m(t)$, then the convolution will encompass multiple symbols with intersymbol interference as a result. It is also clear from this equation that signal energy arriving at longer delays corresponds to symbols transmitted at earlier times.

2.10.2 Dispersive Effects.

When the dispersive term $\bar{\theta}(\omega)$ is expanded in a Taylor series about the carrier radian frequency, the result is

$$\bar{\theta}(\omega) = \bar{\theta}(\omega_0) - (\omega-\omega_0)\bar{\theta}'(\omega_0) + (\omega-\omega_0)^2 \bar{\theta}''(\omega_0)/2 + \ldots \qquad (2\text{-}106)$$

where the first three coefficients in the expansion are

$$\bar{\theta}(\omega_0) = -(\omega_0/c) \int_{-z_t}^{z_r} [1-\bar{\omega}_p^2(z')/\omega_0^2]^{1/2} \, dz' \qquad (2\text{-}107a)$$

$$\bar{\theta}'(\omega_0) = (1/c) \int_{-z_t}^{z_r} [1-\bar{\omega}_p^2(z')/\omega_0^2]^{-1/2} \, dz' \qquad (2\text{-}107b)$$

$$\bar{\theta}''(\omega_0) = -(1/c) \int_{-z_t}^{z_r} (\bar{\omega}_p^2/\omega_0^3)[1-\bar{\omega}_p^2(z')/\omega_0^2]^{-1/2} \, dz' \quad . \qquad (2\text{-}107c)$$

42

These equations may be expanded using the assumption that the carrier frequency is much larger than the plasma frequency. The first three coefficients then reduce to

$$\bar{\theta}(\omega_o) = -2\pi R/\lambda + \lambda r_e N_T \tag{2-108a}$$

$$\bar{\theta}'(\omega_o) = R/c + \lambda^2 r_e N_T/(2\pi c) \tag{2-108b}$$

$$\bar{\theta}''(\omega_o) = -\lambda^3 r_e N_T/(2\pi^2 c^2) \tag{2-108c}$$

where the free space range R and total electron content (TEC) N_T are

$$R = z_t + z_r \tag{2-109}$$

and

$$N_T = \int_{-z_t}^{z_r} \langle n_e(z') \rangle \, dz' \quad . \tag{2-110}$$

The first terms in Equations 2-108a and 2-108b are simply the free space phase shift and propagation time which are proportional to the line-of-sight distance R. The terms proportional to N_T in Equations 2-108 represent the phase shift, group delay and dispersion due to the mean ionization.

The Doppler shift f_D of the incident signal due to range and TEC dynamics is

$$f_D = (2\pi)^{-1} \, d\bar{\theta}(\omega_o)/dt = -2\pi\dot{R}/\lambda + \lambda r_e \dot{N}_T \quad . \tag{2-111}$$

Note that increasing TEC (positive $\dot{N}_T$) increases both the propagation time and the Doppler shift whereas increasing R (positive $\dot{R}$) increases the propagation time but decreases the Doppler shift.

2.10.3 Antenna Aperture Effects.

The voltage at the .t of an aperture antenna is the spatial convolution of the incident voltage and the aperture weighting function. The received voltage for an antenna located at $\vec{\rho}_0$ and pointing in the $\vec{K}_0$ direction is then given by (Knepp 1983a)

$$U_A(\vec{\rho}_0,\omega,t) = \int\int_{-\infty}^{\infty} U(\vec{\rho}',z_r,\omega,t)A_r(\vec{\rho}_0-\vec{\rho}') \exp(i\vec{K}_0\cdot\vec{\rho}') \, d^2\vec{\rho}' \qquad (2-112)$$

where the subscript A denotes the voltage at the output of the antenna. The z dependence of U_A has been suppressed because it is understood that this voltage is at the receiver plane. It is assumed that the aperture weighting function of the receiver $A_r(\vec{\rho})$ is independent of frequency. This is generally true for a range of frequencies about the carrier frequency that is larger than the signal bandwidth.

In order to relate the GPSD of U_A to the GPSD of the incident signal, the two-position, two-frequency, two-time mutual coherence function of U_A is required. The mutual coherence function of the signal out of the antenna is

$$\Gamma_A(\vec{\rho}_d,\omega_d,t_d) = \langle U_A(\vec{\rho}_1,\omega_1,t_1)U_A^*(\vec{\rho}_2,\omega_2,t_2)\rangle =$$

$$\int\int_{-\infty}^{\infty} d^2\vec{\rho}' \int\int_{-\infty}^{\infty} d^2\vec{\rho}'' \langle U(\vec{\rho}',z_r,\omega_1,t_1)U^*(\vec{\rho}'',z_r,\omega_2,t_2)\rangle \times$$

$$A_r(\vec{\rho}_1-\vec{\rho}')A_r^*(\vec{\rho}_2-\vec{\rho}'') \exp[i\vec{K}_0\cdot(\vec{\rho}'-\vec{\rho}'')] \quad . \qquad (2-113)$$

For statistically stationary processes, the expectation of $U_A U_A^*$ must be a function only of the differences $\vec{\rho}_d = \vec{\rho}_1 - \vec{\rho}_2$, $\omega_d = \omega_1 - \omega_2$, and $t_d = t_1-t_2$ and the expectation of UU^* in the integrand must be a function only

of the differences $\vec{\rho}' - \vec{\rho}''$, ω_d, and t_d. The aperture weighting function may be written in terms of the angular beam profile using the Fourier transform relationship

$$A_r(\vec{\rho}) = (2\pi)^{-2} \iint\limits_{-\infty}^{\infty} A_r(\vec{K}_\perp) \exp(i\vec{K}_\perp \cdot \vec{\rho}) \, d^2\vec{K}_\perp \qquad (2\text{-}114)$$

Upon substituting this equation for both aperture weighting functions in the expression for the mutual coherence function, changing variables from $\vec{\rho}'$ to $\vec{\rho} = \vec{\rho}' - \vec{\rho}''$, and changing the order of integration, Equation 2-113 becomes

$$\Gamma_A(\vec{\rho}_d, \omega_d, t_d) = (2\pi)^{-4} \iint\limits_{-\infty}^{\infty} d^2\vec{\rho} \; \Gamma(\vec{\rho}, z_r, \omega_d, t_d) \exp(i\vec{K}_0 \cdot \vec{\rho}) \times$$

$$\iint\limits_{-\infty}^{\infty} d^2\vec{K} \, A_r^*(\vec{K}) \exp[i\vec{K} \cdot (\vec{\rho}_1 - \vec{\rho})] \iint\limits_{-\infty}^{\infty} d^2\vec{K}' \, A_r(\vec{K}') \exp[-i\vec{K}' \cdot \vec{\rho}_2] \times$$

$$\iint\limits_{-\infty}^{\infty} d^2\vec{\rho}'' \exp[i\vec{\rho}'' \cdot (\vec{K}' - \vec{K})] \quad . \qquad (2\text{-}115)$$

The last integral in this expression is equal to $(2\pi)^2 \delta_F(\vec{K}' - \vec{K})$ and the $\vec{K}'$ integral may be performed directly. Another change in the order of integration results in

$$\Gamma_A(\vec{\rho}_d, \omega_d, t_d) = (2\pi)^{-2} \iint\limits_{-\infty}^{\infty} d^2\vec{K} \, G_r(\vec{K}) \exp(i\vec{K} \cdot \vec{\rho}_d) \times$$

$$\iint\limits_{-\infty}^{\infty} d^2\vec{\rho} \; \Gamma(\vec{\rho}, z_r, \omega_d, t_d) \exp[-i\vec{\rho} \cdot (\vec{K} - \vec{K}_0)] \quad . \qquad (2\text{-}116)$$

The quantity

$$G_r(\vec{K}) = A_r^*(\vec{K}) A_r(\vec{K}) \qquad (2\text{-}117)$$

is the power beam profile of the receiving antenna.

The mutual coherence function $\Gamma(\vec{\rho}, z_r, \omega_d, t_d)$ of the signal inci-
dent on the plane of the antenna that appears in the second integral of
Equation 2-116 is the product of the free space term Γ_0 (Equation 2-43)
and the stochastic term Γ_1. The free space term may be pulled out of the
second integral if it is assumed not to vary over the face of the antenna.
This is equivalent to assuming that any deviations from a plane wave in
the incident signal are due to scattering effects in the ionosphere and
are not due to geometrical effects. After the free space term is pulled
out of the integral, Γ_A may be assumed to represent only the stochastic
fluctuations of the received signal.

Now the GPSD of the signal out of the antenna may be computed by
taking the appropriate Fourier transforms (see Equation 2-81) from $\vec{\rho}_d$, ω_d,
and t_d to $\vec{K}_\perp$, τ, and ω_D respectively. After performing the ω_d to τ trans-
form, the angular-delay part of the GPSD at the antenna output will be

$$S_A(\vec{K}_\perp, \tau) = (2\pi)^{-2} \int\!\!\int_{-\infty}^{\infty} d^2\vec{K} \; G_r(\vec{K}) \times$$

$$\int\!\!\int_{-\infty}^{\infty} d^2\vec{\rho} \; \Gamma_1(\vec{\rho}, z_r, \tau) \exp\left[-i(\vec{K}-\vec{K}_0)\cdot\vec{\rho}\right] \int\!\!\int_{-\infty}^{\infty} d^2\vec{\rho}_d \exp\left[i(\vec{K}-\vec{K}_\perp)\cdot\vec{\rho}_d\right] \quad . \quad (2\text{-}118)$$

The last integral in this equation is just $(2\pi)^2 \delta_F(\vec{K}-\vec{K}_\perp)$ and the middle
integral gives the angular-delay GPSD of the incident voltage $S(\vec{K}-\vec{K}_0, \tau)$.
The GPSD of the signal out of the antenna is then

$$S_A(\vec{K}_\perp, \tau) = G_r(\vec{K}_\perp) S(\vec{K}_\perp - \vec{K}_0, \tau) \quad . \tag{2-119}$$

The effect of an antenna, as should be expected, is to modify with the
beam profile the mean incident power as a function of angle. This result
will be used throughout the rest of this report.

SECTION 3
ANTENNA FILTERING EFFECTS

An antenna beam profile acts as an angular filter of the re-
ceived signal energy. Because of this, the mean power, decorrelation dis-
tances, and frequency selective bandwidth of the signal at the output of
an antenna are different than those of the incident signal. The reduction
in mean power is a direct consequence of the attenuation, due to the beam
profile, of energy arriving at large angles-of-arrival relative to the
peak of the beam. The energy arriving at large angles is also the energy
arriving at long delays. The frequency selective bandwidth is an inverse
measure of the delay spread of the signal energy. Hence the frequency
selective bandwidth of the signal out of an antenna is larger than the
frequency selective bandwidth of the signal incident on the antenna. The
decorrelation distance is an inverse measure of the angle-of-arrival fluc-
tuations of the signal energy. The effect of an antenna is to reduce the
angular spread of the signal and thus to increase the decorrelation dis-
tances of the signal out of the antenna relative to the decorrelation
distances of the incident signal.

The effects of aperture antennas with arbitrary beamwidths will
be considered in this section. The antenna beam profiles for uniformly
weighted circular or rectangular apertures and for Gaussian apertures are
described in Section 3.1. The filtering equations for mean power, spatial
and temporal decorrelation properties, and frequency selective bandwidth
of the signal out of a Gaussian antenna with arbitrary beamwidths are
derived in Section 3.2. Then a comparison of the antenna filtering
effects of a Gaussian antenna and a uniformly weighted circular antenna is
made in Section 3.3 to assess the accuracy of the Gaussian approximation.

47

3.1   ANTENNA DESCRIPTIONS.

The coordinate systems for the propagation and the antenna are shown in Figure 3-1. The z axis is along the line-of-sight between the transmitter and the receiver and the direction with the minimum decorrelation distance is along the x axis. The antenna u-v coordinate system, in this case for a rectangular antenna, is in the x-y plane. The rotation angle χ is the angle between the x axis and the u axis.

In general, the face of the antenna will not lie in the x-y plane. However, for satellite communication links it is usual for the satellite position to be known accurately through ephermeris data and for an antenna to be dedicated to a single link. Thus the rotation angles of the antenna out of the x-y plane will be small in most cases and the cosine squared effects of these angles may be ignored. If these rotation
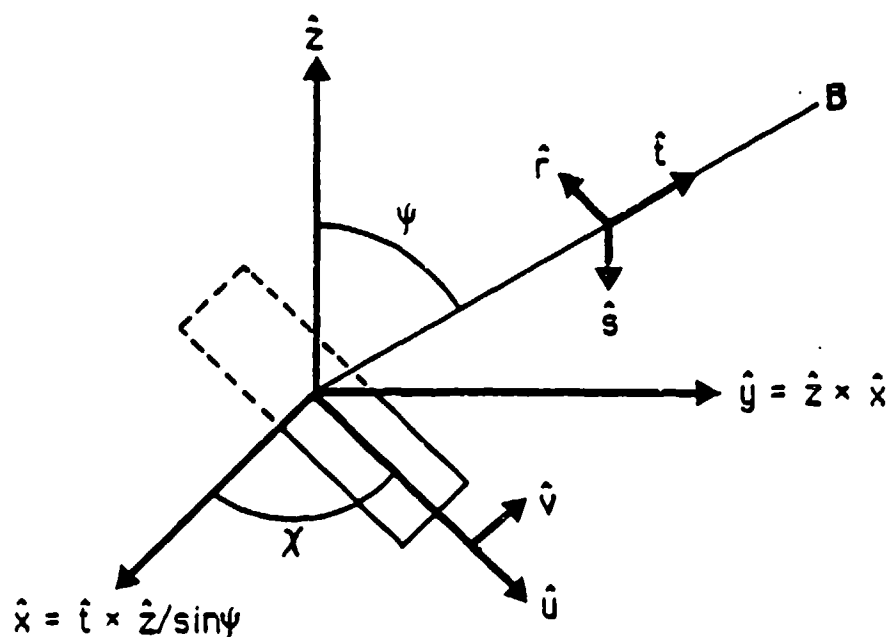
Figure 3-1. Propagation and antenna coordinate systems.

48

angles are not small, then in the developments that follow the antenna size is the projection in the x-y plane and the antenna beamwidths must include the effects of beam broadening as the beam is pointed away from boresight.

3.1.1   Gaussian Beam Profiles.

The antenna beam profile is assumed to be separable in the u-v coordinate system. The Gaussian antenna beam profile is then

$$G(K_u, K_v) = \exp\left(-\alpha_u^2 K_u^2 - \alpha_v^2 K_v^2\right) \quad . \tag{3-1}$$

The peak gain $G(0,0)$ has been set to unity because this value is usually included in the calculation of the mean received power. For either the u or the v direction, the antenna beam profile can also be written as

$$G(\theta) = \exp\left[-(\ln 2)(2\theta/\theta_0)^2\right] \tag{3-2}$$

where θ_0 is the 3 dB beamwidth (i.e. full width at half maximum). Equating these two profiles gives

$$\alpha_\xi^2 = (\ln 2)\lambda^2/(\pi^2 \theta_{0\xi}^2) \tag{3-3}$$

where $\theta_{0\xi}$ is the 3 dB beamwidth in the $\xi = u$ or the $\xi = v$ direction.

The beam profile is required in the x-y coordinate system of the propagation. Using the transformation

$$K_u = K_x \cos\chi + K_y \sin\chi$$
$$K_v = -K_x \sin\chi + K_y \cos\chi \tag{3-4}$$

gives

49

$$G(K_x, K_y) = \exp\left[-(\alpha_u^2\cos^2 x + \alpha_v^2\sin^2 x)K_x^2\right] \times$$

$$\exp\left[-2(\alpha_u^2 - \alpha_v^2)\sin x\cos x K_x K_y\right] \times$$

$$\exp\left[-(\alpha_u^2\sin^2 x + \alpha_v^2\cos^2 x)K_y^2\right] \quad . \tag{3-5}$$

The coefficients α_u and α_v will be related to the sizes of uniformly weighted apertures in the next subsections. If α_u and α_v are equal, then the Gaussian beam profile is independent of the rotation angle and is referred to as isotropic in subsequent sections.

3.1.2 Uniformly Weighted Circular Apertures.

For a uniformly weighted circular aperture, the aperture weighting function without pointing errors is

$$A_x(\vec{\rho}) = \begin{cases} 1/a & \text{if } |\vec{\rho}| < D/2, \\ \\ 0 & \text{otherwise} \end{cases} \tag{3-6}$$

where D is the diameter of the circular aperture and where $x = r$ for a receiving antenna and $x = t$ for a transmitting antenna. The value of a is chosen so that the peak antenna gain $G(0)$ is unity. The voltage antenna gain pattern $A_x(\vec{K})$ is related to the aperture distribution function by the Fourier transform

$$A_x(\vec{K}) = \int\int_{-\infty}^{\infty} \exp(-i\vec{K}\cdot\vec{\rho})A_x(\vec{\rho})d^2\vec{\rho} \quad . \tag{3-7}$$

The coordinate system for this transformation is shown in Figure 3-2. The antenna is pointed along the line-of-sight in the z direction and $\vec{\rho}$ is chosen to be along the x axis. The beam profile for a circular antenna
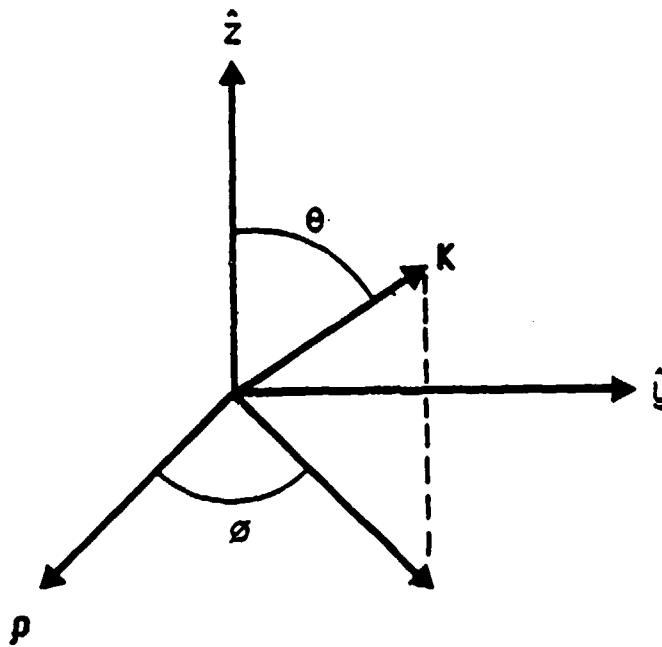
Figure 3-2. Circular antenna coordinate system.

will then be a function only of the elevation angle θ. In this coordinate system, the dot product $\vec{K} \cdot \vec{\rho}$ is

$$\vec{K} \cdot \vec{\rho} = kr \sin\theta \sin\phi \tag{3-8}$$

where $k = |\vec{K}| = 2\pi/\lambda$ and $r = |\vec{\rho}|$. The Fourier transform then becomes

$$A_x(\theta) = a^{-2} \int_0^{D/2} dr\, r \int_{-\pi}^{\pi} d\phi \, \exp(-ikr \sin\theta \sin\phi) \quad . \tag{3-9}$$

Performing the indicated integrals results in the well known form for the power beam profile

$$G_x(\theta) = A_x(\theta) A_x^{\star}(\theta) = \frac{4 J_1{}^2[\pi(D/\lambda)\sin\theta]}{[\pi(D/\lambda)\sin\theta]^2} \tag{3-10}$$

51

where J_1 is the Bessel function and where $G(0) = 1$ when the value of a is chosen to be the area of the aperture $\pi D^2/4$. The factor of 4 in the expression for $G_x(\theta)$ is required because the limit of $J_1^2(\xi)/\xi^2$ as ξ approaches zero is $1/2$. The 3 dB full width at half maximum beamwidth [i.e. $G(\theta_0/2) = 1/2$] is given by solving the equation

$$4J_1^2(\xi)/\xi^2 = 1/2 \qquad (3-11)$$

with the result $\xi = 1.616340$. Assuming that the beamwidth is small so $\sin(\theta_0/2) \approx \theta_0/2$, the beamwidth in terms of the diameter D is

$$\theta_0 = 1.02899 \, (\lambda/D) \text{ radians} \quad . \qquad (3-12)$$

If this beam profile is approximated by a Gaussian profile with the same 3 dB beamwidth, then the α coefficients that appear in Equation 3-1 are

$$\alpha_u^2 = \alpha_v^2 = (\ln 2)D^2/(1.02899\pi)^2 \quad . \qquad (3-13)$$

3.1.3 Uniformly Weighted Rectangular Apertures.

For uniformly weighted rectangular apertures, the aperture weighting function without pointing errors is

$$A_x(u,v) = \begin{cases} 1/a \text{ if } |u| < D_u/2 \text{ and } |v| < D_v/2 \\ \\ 0 \text{ otherwise} \end{cases} \qquad (3-14)$$

where D_u and D_v are the lengths of the aperture in the u and v directions respectively. In this case, the Fourier transform indicated in Equation 3-7 can be done directly with the result

$$G_x(\theta_u, \theta_v) = G_x(\theta_u)G_x(\theta_v) \qquad (3-15)$$

where $G_x(\theta_\xi)$ for $\xi = u$ or $\xi = v$ has the familiar $\sin^2(x)/x^2$ form

$$G_x(\theta_\xi) = \frac{\sin^2[\pi(D_\xi/\lambda)\sin\theta_\xi]}{[\pi(D_\xi/\lambda)\sin\theta_\xi]^2} \quad . \qquad (3-16)$$

52

The normalization a of the weighting function is just the area $D_u D_v$ of the rectangular antenna. The 3 dB beamwidth is given by solving the equation

$$\sin^2(\xi)/\xi^2 = 1/2 \qquad\qquad (3\text{-}17)$$

with the result $\xi = 1.391557$. The ξ direction beamwidth in terms of the antenna size D_ξ is then

$$\theta_{o\xi} = 0.885893 \, (\lambda/D_\xi) \text{ radians} \qquad\qquad (3\text{-}18)$$

assuming that $\sin(\theta_{o\xi}/2) \approx \theta_{o\xi}/2$. If this beam profile is approximated by a Gaussian profile with the same 3 dB beamwidth, the α coefficients that appear in Equation 3-1 are

$$\alpha_\xi^2 = (\ln 2)D_\xi^2/(0.885893\pi)^2 \quad . \qquad\qquad (3\text{-}19)$$

3.2   FILTERING EQUATIONS.

The filtering equations relate the statistics of the signal at the outputs of one or more antennas to the statistics of the signal incident on the antennas. The statistics that are considered in this section are the mean power, frequency selective bandwidth, decorrelation distances, and decorrelation times of the signal out of an antenna and the cross correlation of the signals out of two separate antennas. A Gaussian beam profile is used because this approximation leads to closed form expressions for the filtering equations. The accuracy of this approximation is investigated in Section 3.3.

The power impulse response function $G_A(\tau)$ of the signal out of an antenna is also calculated in this section in the limit that the parameter α is equal to infinity. The quantity $G_A(\tau)d\tau$ is equal to the mean received power in the delay interval τ to $\tau + d\tau$. This function will be used in Section 5 which describes channel simulation techniques.

53

The severity of the filtering effects is determined by the relative size of the standard deviation of the angle-of-arrival fluctuations σ_θ and the antenna beamwidths. When σ_θ is small compared to the antenna beamwidths, the signal arrives essentially at the peak of the beam profile, if the pointing error is small, and the filtering effects are small. However, if σ_θ is large compared to the beamwidths, much of the signal energy arrives at angles outside of the main lobe of the antenna beam profile and the filtering effects are large. Equivalently, large values of the ratio σ_θ/θ_0 correspond to situations where the decorrelation distance of the incident signal is small compared to the antenna size and the incident electric field as seen by the aperture is no longer a plane wave. In this situation, the induced voltages across the face of the aperture do not add coherently when summed together by the antenna with a loss in signal power as a result.

3.2.1   Orthogonalized GPSD.

The delay moments of the signal out of an antenna pointing at the transmitter are given by

$$P_A\langle\tau^n\rangle = (2\pi)^{-3} \iint_{-\infty}^{\infty} d^2\vec{K}_\perp \, G_r(\vec{K}_\perp) \int_{-\infty}^{\infty} d\tau \, \tau^n \int_{-\infty}^{\infty} d\omega_D \, S(\vec{K}_\perp,\tau,\omega_D) \qquad (3\text{-}20)$$

where P_A is the mean power of the signal out of the antenna and is equal to the $n = 0$ delay moment. The Doppler integral is just

$$S(\vec{K}_\perp,\tau) = \int_{-\infty}^{\infty} S(\vec{K}_\perp,\tau,\omega_D) d\omega_D \qquad (3\text{-}21)$$

where $S(\vec{K}_\perp,\tau)$ is the angular-delay part of the GPSD of the incident signal given by Equation 2-83.

When Equations 2-83, 2-119, and 3-5 are combined, the resulting GPSD of the signal out of the antenna in the x-y coordinate system is

$$S_A(K_x, K_y, \tau) = (\pi/2)^{1/2} \alpha \omega_{coh} \ell_0^2 \delta^{-1} \exp \left\{ -(\alpha^2/2) [\omega_{coh} \tau - \Lambda(K_x^2 + K_y^2) \ell_0^2/4]^2 \right\} \times$$

$$\exp \left[-\Delta_x^2 K_x^2 \ell_0^2/4 \right] \exp \left[-\Delta_y^2 K_y^2 \ell_0^2/4\delta^2 \right] \exp \left[-\Delta_{xy}^2 K_x K_y \ell_0^2/4\delta \right] \qquad (3-22)$$

where the Δ coefficients are

$$\Delta_x^2 = 1 + 4\alpha_u^2 \cos^2 \chi / \ell_0^2 + 4\alpha_v^2 \sin^2 \chi / \ell_0^2$$

$$\Delta_y^2 = 1 + 4\delta^2 \alpha_u^2 \sin^2 \chi / \ell_0^2 + 4\delta^2 \alpha_v^2 \cos^2 \chi / \ell_0^2$$

$$\Delta_{xy}^2 = 8\delta(\alpha_u^2 - \alpha_v^2) \sin \chi \cos \chi / \ell_0^2 \quad . \qquad (3-23)$$

The cross term $K_x K_y$ in the last exponent of Equation 3-22 significantly complicates the evaluation of the angular integrals. However, this term may be eliminated by performing the integration in a rotated p-q coordinate system where the GPSD is orthogonal (i.e. contains only K_x^2 and K_y^2 terms). The rotation is defined by

$$K_x = K_p \cos\theta + K_q \sin\theta$$
$$K_y = -K_p \sin\theta + K_q \cos\theta \qquad (3-24)$$

where $dK_p dK_q = dK_x dK_y$ and $K_p^2 + K_q^2 = K_x^2 + K_y^2$. The angle θ, chosen so that the coefficient of $K_p K_q$ is zero, is

$$\theta = (1/2)\tan^{-1} [2\delta\Delta_{xy}^2 / (\delta^2 \Delta_x^2 - \Delta_y^2)] \quad . \qquad (3-25)$$

In the rotated coordinate system, the GPSD at the antenna output takes the form

$$S_A(K_p, K_q, \tau) = (\pi/2)^{1/2} \, \alpha\omega_{coh}\ell_0^2\delta^{-1} \exp\left\{-(\alpha^2/2)[\omega_{coh}\tau - \Lambda(K_p^2+K_q^2)\ell_0^2/4]^2\right\} \times$$

$$\exp\left[-\Delta_p^2 K_p^2\ell_0^2/4\right] \exp\left[-\Delta_q^2 K_q^2\ell_0^2/4\delta^2\right] \quad . \tag{3-26}$$

The Δ coefficients are now

$$2\Delta_p^2 = \Delta_x^2 + \Delta_y^2/\delta^2 + [(\Delta_x^2 - \Delta_y^2/\delta^2)^2 + 4\Delta_{xy}^4/\delta^2]^{1/2}$$

$$2\Delta_q^2 = \delta^2\Delta_x^2 + \Delta_y^2 - [(\delta^2\Delta_x^2 - \Delta_y^2)^2 + 4\delta^2\Delta_{xy}^4]^{1/2} \quad . \tag{3-27}$$

After the rotation, the delay moments are given by

$$P_A\langle\tau^n\rangle = (2\pi)^{-2} \int_{-\infty}^{\infty} dK_p \int_{-\infty}^{\infty} dK_q \int_{-\infty}^{\infty} d\tau \; \tau^n \, S_A(K_p, K_q, \tau) \quad . \tag{3-28}$$

3.2.2 Scattering Loss.

The mean power of the signal out of the antenna is calculated from Equation 3-28 with $n = 0$ and is

$$P_A = 1/\Delta_p\Delta_q = 1/L_S \tag{3-29}$$

where L_S is the scattering loss. After some manipulations, the square of the scattering loss becomes

$$L_S^2 = (1+4\delta^2\alpha_u^2/\ell_0^2)(1+4\alpha_v^2/\ell_0^2)\sin^2\chi + (1+4\alpha_u^2/\ell_0^2)(1+4\delta^2\alpha_v^2/\ell_0^2)\cos^2\chi \quad . \tag{3-30}$$

The terms in parenthesis occur frequently in the filtering equations. Thus for notational convenience, define

$$G_{ux} = 1 + 4\alpha_u^2/\ell_0^2 \quad = 1 + (8\ln 2)(\sigma_{\theta x}/\theta_{ou})^2$$

$$G_{uy} = 1 + 4\delta^2\alpha_u^2/\ell_0^2 = 1 + (8\ln 2)(\sigma_{\theta y}/\theta_{ou})^2$$

$$G_{vx} = 1 + 4\alpha_v^2/\ell_0^2 \quad = 1 + (8\ln 2)(\sigma_{\theta x}/\theta_{ov})^2$$

$$G_{vy} = 1 + 4\delta^2\alpha_v^2/\ell_0^2 = 1 + (8\ln 2)(\sigma_{\theta y}/\theta_{ov})^2 \tag{3-31}$$

where equations 2-97 and 2-98 have been used to write ℓ_0 and ℓ_0/δ in terms of the variance of the angle-of-arrival fluctuations $\sigma_{\theta x}$ and $\sigma_{\theta y}$ and where Equation 3-3 has been used to write α_u and α_v in terms of the 3 dB beam-widths θ_{cu} and θ_{ov}. With these definitions, the scattering loss takes the simpler form

$$L_S = [G_{uy}G_{vx}\sin^2\chi + G_{ux}G_{vy}\cos^2\chi]^{1/2} \quad . \tag{3-32}$$

The scattering loss is a function of the ratios of the widths of the angle-of-arrival fluctuations σ_θ and the antenna beamwidths θ_0 with the scattering loss approaching unity for $\sigma_\theta \ll \theta_0$. It can be seen that the dependence on the rotation angle disappears if the scattering is isotropic (i.e. $\delta = 1$ and $\sigma_{\theta x} = \sigma_{\theta y}$) or if the antenna is isotropic (i.e. $\theta_{ou} = \theta_{ov}$).

Now consider the case of an isotropic antenna where $G_{ux} = G_{vx}$ and $G_{uy} = G_{vy}$. When the scattering is also isotropic (penetration angle $= 0°$), $G_{ux} = G_{uy}$ and the scattering loss is $L_S = G_{ux}$. However when the penetration angle is 90°, the y direction decorrelation distance will be q (q=15) times larger than the x direction decorrelation distance. Then under most circumstances, $G_{uy} \approx 1$ and the scattering loss is $L_S \approx \sqrt{G_{ux}}$. The scattering loss is therefore a sensitive function of the penetration angle.

3.2.3   Frequency Selective Bandwidth.

The frequency selective bandwidth has been defined in terms of the time delay jitter of the signal in Section 2.8.2. The required delay moments are

$$\omega_{coh}\langle\tau\rangle = (\Lambda/2)\left[\Delta_p^{-2}+\delta^2\Delta_q^{-2}\right] \tag{3-33}$$

and

$$\omega_{coh}^2\langle\tau^2\rangle = \left[\alpha^{-2}+(3\Lambda^2/4\Delta_p^4) + (\Lambda^2\delta^2/2\Delta_p^2\Delta_q^2) + (3\Lambda^2\delta^4/4\Delta_q^4)\right] \quad . \tag{3-34}$$

The time delay jitter is then given by

$$\sigma_\tau^2 = \omega_{coh}^{-2}\left[\alpha^{-2}+(\Lambda^2/2)(\Delta_p^{-4}+\delta^4\Delta_q^{-4})\right] \quad . \tag{3-35}$$

The α^{-2} term in the expression for σ_τ^2 represents the effects of refraction on the time delay jitter. In the limit that diffraction effects dominate the signal fluctuations, the time delay spread of the signal is determined by the spread of propagation times as a function of the angle-of-arrival of the signal with the largest delays corresponding to the largest angles-of-arrival. The effect of an antenna then is to preferentially attenuate the signal energy at large angles and thereby to reduce the delay spread of the signal and to increase the frequency selective bandwidth. In the limit of a large angle-of-arrival variance, or equivalently of a small decorrelation distance, only energy arriving near zero angle is received at the output of the antenna and the time delay jitter of the output signal approaches zero. The value of α must be set large enough that the time delay jitter of the signal out of the antenna is not limited by α under the most severely disturbed propagation conditions. The expressions below for the frequency selective bandwidth of the signal out of the antenna are therefore calculated with α set to infinity.

58

The ratio of the frequency selective bandwidth of the signal out of the antenna to that of the incident signal is just

$$f_A/f_o = \sigma_\tau(\text{without antenna})/\sigma_\tau(\text{with antenna}) \quad . \quad (3\text{-}36)$$

The numerator of this expression may be obtained from Equation 3-35 with Δ_p and Δ_q set to unity. The resulting equation for the ratio is

$$f_A/f_o = [(1+\delta^4)/(1/\Delta_p^4+\delta^4/\Delta_q^4)]^{1/2} \quad . \quad (3\text{-}37)$$

After some manipulations, this expression may be rewritten as

$$f_A/f_o = \frac{(1+\delta^4)^{1/2} \, L_S^2}{[(\delta^4 G_{ux}^2+G_{vy}^2)\cos^2\chi + (G_{uy}^2+\delta^4 G_{vx}^2)\sin^2\chi]^{1/2}} \quad . \quad (3\text{-}38)$$

3.2.4   Two-Position Mutual Coherence Function.

It will be convenient in further developments to have the two-position mutual coherence function of the signal out of the antenna calculated in the x-y coordinate system. The coherence function is defined as

$$\Gamma_A(x,y) = (2\pi)^{-2} \int_{-\infty}^{\infty} dK_x \int_{-\infty}^{\infty} dK_y \int_{-\infty}^{\infty} d\tau \, \exp(iK_x x+iK_y y)S_A(K_x,K_y,\tau) \quad (3\text{-}39)$$

where Equation 3-22 is used for the GPSD. In this case, the integral may be done in closed form with the result

$$\Gamma_A(x,y) = P_A \exp\{-[(G_{uy}\sin^2\chi+G_{vy}\cos^2\chi)/L_S^2]x^2/\ell_o^2\} \times$$

$$\exp\{-[(G_{ux}\cos^2\chi+G_{vx}\sin^2\chi)/L_S^2]\delta^2 y^2/\ell_o^2\} \times$$

$$\exp\{-[2(G_{ux}-G_{vx})\sin\chi\cos\chi/L_S^2]\delta^2 xy/\ell_o^2\} \quad . \quad (3\text{-}40)$$

59

3.2.5   Decorrelation Distances and Time.

The x direction decorrelation distance of the signal out of the antenna is given by the 1/e point of $\Gamma_A(x,0)/P_A$ and the y direction decorrelation distance is given by the 1/e point of $\Gamma_A(0,y)/P_A$. These quantities are

$$\ell_{Ax}/\ell_0 = L_S[G_{uy}\sin^2 x + G_{vy}\cos^2 x]^{-1/2} \tag{3-41}$$

and

$$\ell_{Ay}/\ell_0 = \delta^{-1} L_S[G_{ux}\sin^2 x + G_{vx}\cos^2 x]^{-1/2} \quad . \tag{3-42}$$

Recall that under the frozen-in approximation the drift direction is chosen to be along the x axis and the decorrelation time of the signal is related to the decorrelation distance by the effective velocity (Equation 2-87). The decorrelation time τ_A of the signal out of the antenna will then be given in terms of the decorrelation time τ_0 of the incident signal by

$$\tau_A/\tau_0 = \ell_{Ax}/\ell_0 \quad . \quad \text{(Frozen-in Approximation)} \tag{3-43}$$

The filtering of the decorrelation time is a reflection of the fact that signal energy arriving at large angles varies more rapidly than energy arriving at small angles. However, under the turbulent approximation, the decorrelation time of the signal is independent of its angle-of-arrival (see Equation 2-100). For this approximation, there is no filtering of the decorrelation time by the antenna and

$$\tau_A/\tau_0 = 1 \quad . \quad \text{(Turbulent Approximation)} \tag{3-44}$$

3.2.6   Power Impulse Response Function.

The power impulse response function gives the mean power received in the delay interval τ to $\tau + d\tau$ from a transmitted impulse. At the output of an antenna, this function is

$$G_A(\tau) = (2\pi)^{-2} \iint\limits_{-\infty}^{\infty} d^2\vec{K}_\perp \, G_r(\vec{K}_\perp) S(\vec{K}_\perp, \tau) \quad . \tag{3-45}$$

This integral cannot be done in closed form for general anisotropic scattering and antennas and for arbitrary values of the parameter α. However, using the fact that

$$\underset{\alpha \to \infty}{\text{Limit}} \; \alpha \exp(-\alpha^2 x^2) = \sqrt{\pi} \, \delta_F(x) \quad , \tag{3-46}$$

allows an analytic result to be obtained. In this limit, the GPSD of the electric field incident on the plane of the receiver becomes

$$S(K_x, K_y, \tau) = (\pi/\sqrt{2}) \, \omega_{coh} \ell_0^{2\delta-1} \exp\left[-(K_x^2 + \delta^{-2}K_y^2)\ell_0^2/4\right] \times$$

$$\delta_F\left\{\left[\omega_{coh}\tau - \Lambda(K_x^2 + K_y^2)\ell_0^2/4\right]/\sqrt{2}\right\} \quad . \tag{3-47}$$

This geometric optics limit then results in a delta function relationship between angle and delay and requires that τ be greater than or equal to zero in order for the GPSD to be non-zero.

The power impulse response function for general anisotropic scattering and antennas now becomes

$$G_A(\tau) = \begin{cases} (\omega_{coh}/\delta\Lambda) \exp(-g_1\omega_{coh}\tau) \, I_0(g_2\omega_{coh}\tau), & \tau \geq 0 \\ \\ 0 & , \; \tau < 0 \end{cases} \tag{3-48}$$

61

where I_0 is the modified Bessell function of order 0 and where

$$g_1 = [(\delta^2 G_{ux} + G_{vy})\cos^2\chi + (\delta^2 G_{vx} + G_{uy})\sin^2\chi]/(2\delta^2\Lambda)$$

$$g_2 = [(G_{uy} - \delta^2 G_{vx})^2\sin^2\chi + (G_{vy} - \delta^2 G_{ux})^2\cos^2\chi]^{1/2}/(2\delta^2\Lambda) \quad . \quad (3\text{-}49)$$

It is easy, if not somewhat tedious to show that

$$\int_0^\infty G_A(\tau)d\tau = P_A \tag{3-50}$$

which is equal to the mean received power at the output of the antenna.

In the limit that both the scattering and the antenna are iso-tropic, the expression for the power impulse response function reduces to

$$G_A(\tau) = \begin{cases} \omega_{coh} \exp(-G\omega_{coh}\tau) & , \quad \tau \geq 0 \\ \\ 0 & , \quad \tau < 0 \end{cases} \tag{3-51}$$

where, in terms of the standard deviation of the angle-of-arrival fluctuations σ_θ and the 3 dB beamwidth θ_0,

$$G = 1.0 + (8\ln 2)(\sigma_\theta/\theta_0)^2 \quad . \tag{3-52}$$

Under these conditions, the quantity G is equal to the scattering loss.

The cumulative delay distribution $C(\tau)$ of signal energy may be defined as

$$C(\tau) = \int_0^\tau [G_A(t)/P_A]dt \quad . \tag{3-53}$$

This function gives the fraction of received signal energy arriving with a delay less than or equal to τ. For isotropic scattering and for an iso-tropic antenna, the cumulative delay distribution is

$$C(\tau) = 1.0 - \exp(-G\omega_{coh}\tau) \quad . \tag{3-54}$$

Without an antenna, the value of $C(\tau)$ is equal to 0.8 for $\omega_{coh}\tau = 1.61$. With an antenna, as the value of G or the scattering loss increases, the 80 percent point on the distribution occurs for smaller values of $\omega_{coh}\tau$.

3.3 COMPARISON OF UNIFORMLY WEIGHTED CIRCULAR AND GAUSSIAN ANTENNA FILTERING EFFECTS.

The filtering equations presented in the previous sections are for antennas with a Gaussian beam profiles which do not have sidelobes. It is of interest to evaluate the filtering equations for implementable antenna beam profiles in order to assess the effects of sidelobes on the statistics of the signal out of an antenna and to assess the accuracy of the Gaussian beam profile filtering equations.

To facilitate this calculation, uniformly weighted circular antennas and isotropic scattering will be assumed. With these assumptions, the moments of delay defined in Equation 3-28, the equation for the spatial coherence function (Equation 3-39) and the cumulative distribution of the received signal energy (Equation 3-53) can all be written in terms of a set of single integrals which can be evaluated numerically. From these integrals, the scattering loss and the ratios f_A/f_0 and ℓ_A/ℓ_0 can be calculated. These quantities are a function only of the ratio D/ℓ_0 where D is the diameter of the circular antenna.

Under isotropic scattering conditions and for the isotropic antennas considered here, the filtering equations for Gaussian antennas reduce to

$$L_S = G$$

$$\ell_A/\ell_0 = \sqrt{G} \tag{3-55}$$

$$f_A/f_0 = G$$

where the function G is defined in Equation 3-52 in terms of the standard deviation of the angle-of-arrival fluctuations and the 3 dB antenna beamwidth. For uniformly weighted circular or square apertures,

$$G = \begin{cases} 1.0 + 0.265(D/\ell_0)^2 & \text{(Circular Antenna)} \\ 1.0 + 0.358(D/\ell_0)^2 & . \quad \text{(Square Antenna)} \end{cases} \quad (3\text{-}56)$$

Figures 3-3, 3-4, and 35 show the scattering loss, decorrelation distance, and frequency selective bandwidth respectively at the outputs of Gaussian (solid lines) and uniformly weighted (dots) circular antennas. Figure 3-6 shows the value of $\omega_{coh}\tau$ for which the cumulative delay distribution is equal to 0.8.

As can be seen from the figures, there is good agreement in the scattering losses and the decorrelation distances between the Gaussian approximation and the uniformly weighted aperture antennas over the range of D/ℓ_0 from 0.1 to 100 shown in the figures. The scattering loss is primarily determined by the fraction of signal energy that is scattered out of the main beam of the antenna (Dana 1981) and is insensitive to the sidelobe structure for antennas with sidelobes that are less than or equal to those of uniformly weighted apertures. Under conditions where $D \gg \ell_0$, an antenna must only be displaced approximately a distance D for the signal out of the antenna to decorrelate. Thus under these conditions, the decorrelation distance depends primarily on the aperture size and is insensitive to the sidelobe structure.

The frequency selective bandwidth of the signals out of uniformly weighted circular antennas agree with the Gaussian approximation values only for D/ℓ_0 less than 3. For values of this ratio greater than 3, there is less filtering of the frequency selective bandwidth with the uniformly weighted aperture with sidelobes than there is with the Gaussian antenna without sidelobes. This can be understood by considering Equation 3-28 for the delay moments of the received signal. The GPSD, $S_A(K_x, K_y, \tau)$,
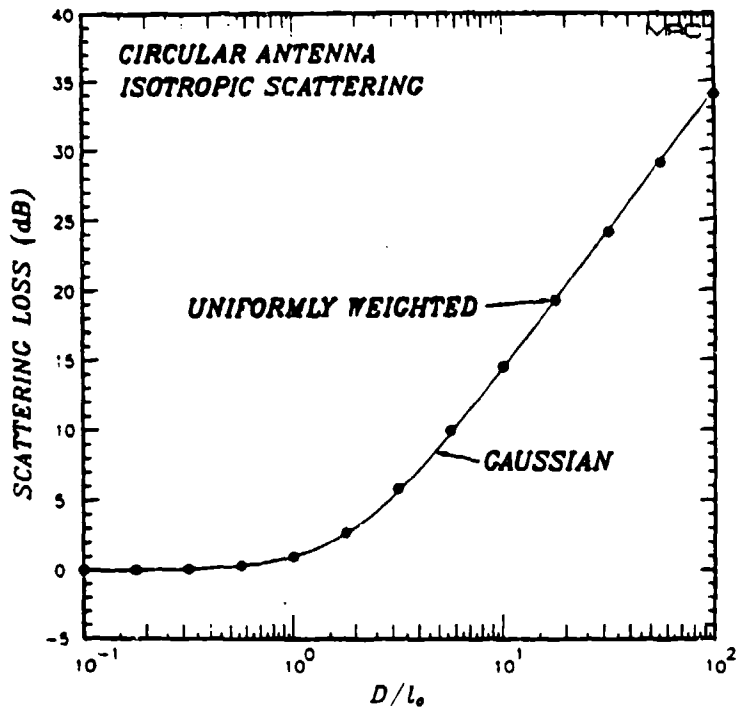
64

Figure 3-3. Scattering loss for Gaussian and uniformly weighted circular antennas.
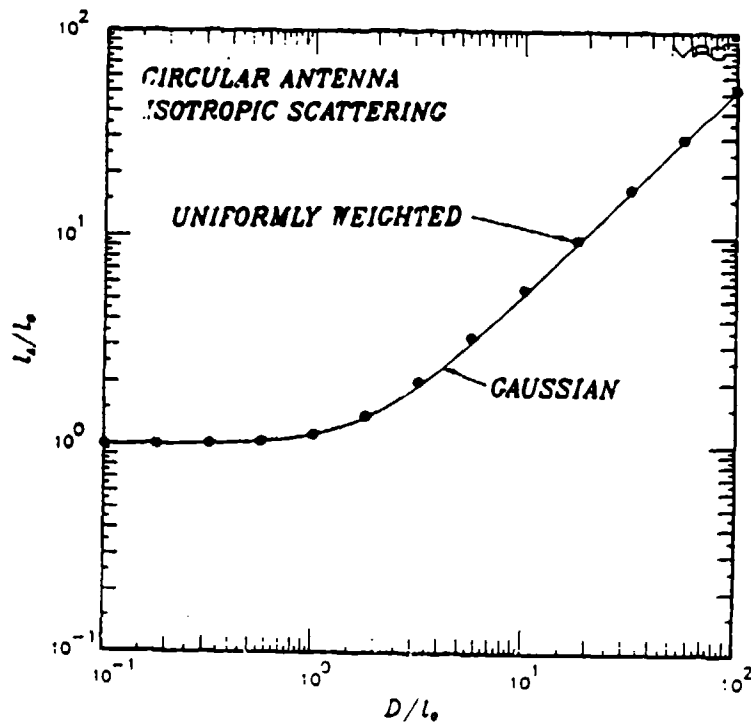

Figure 3-4. Decorrelation distance for Gaussian and uniformly weighted circular antennas.

65

in this equation couples delay and angle by requiring that the signal arriving at long delays also arrive at large angles. The moments of delay $\langle \tau^n \rangle$ then become more sensitive to the details of S_A at large angles, and therefore to the sidelobe structure of the antenna, as n increases. As D/ℓ_0 increases, more of the signal energy is scattered out of the main beam and into the sidelobes of the antenna. Although this energy contributes little to the total received power, it does increase the values of the delay moments of the output signal relative to those of the signal out of an antenna without sidelobes and thereby decreases the frequency selective bandwidth.

The frequency selective bandwidth is intended to reflect how the bulk of the signal energy arrives in delay. To see how the uniformly weighted circular antenna affects the delay distribution of the received signal energy, the 80 percent point of the cumulative delay distribution (i.e. the value of $\omega_{coh} \tau$ for which $C(\omega_{coh} \tau) = 0.8$) is plotted in Figure 3-6 for both Gaussian and uniformly weighted antennas. Over the entire range of D/ℓ_0 values from 0.1 to 100, there is close agreement between the Gaussian antenna values and the uniformly weighted antenna values indicating that at least 80 percent of the signal energy is received with a similar distribution in delay. Even for the largest value of D/ℓ_0, more than 80 percent of the received signal energy is received in the main lobe. Thus the agreement in the 80 percent values is a reflection of the fact that a Gaussian function provides a good approximation to $4J_1^2(\xi)/\xi^2$ within its main lobe. The large difference in the filtered values of the frequency selective bandwidth ratio seen in Figure 3-5 is then attributed to large differences in the delay distribution of no more than 20 percent of the received signal energy. The Gaussian values of f_A/f_0 will therefore provide an accurate description of the delay distribution of the bulk of the received signal energy and should be used for all antennas provided a reasonable fit can be made to the main lobe using the Gaussian approximation.
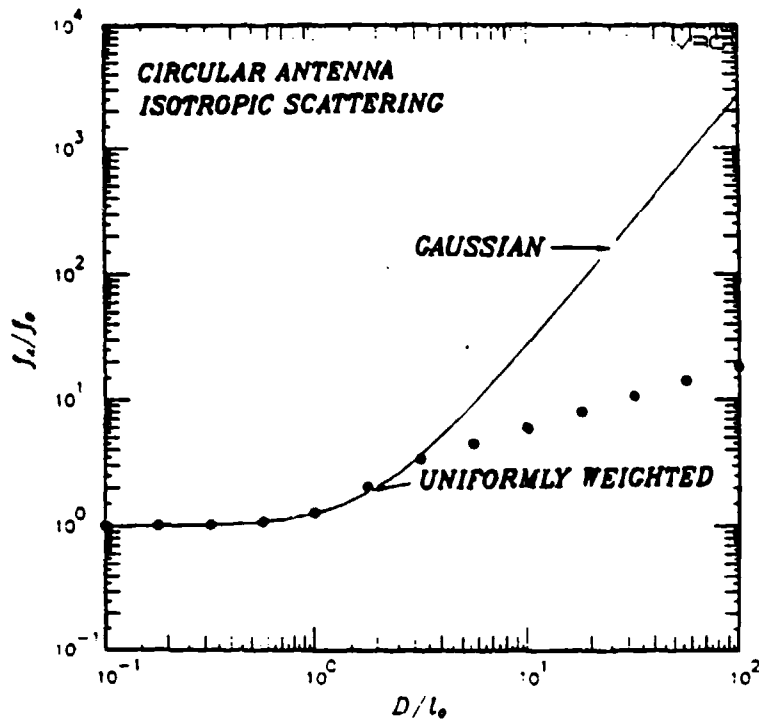
66

Figure 3-5. Frequency selective bandwidth for Gaussian and uniformly weighted circular antennas.
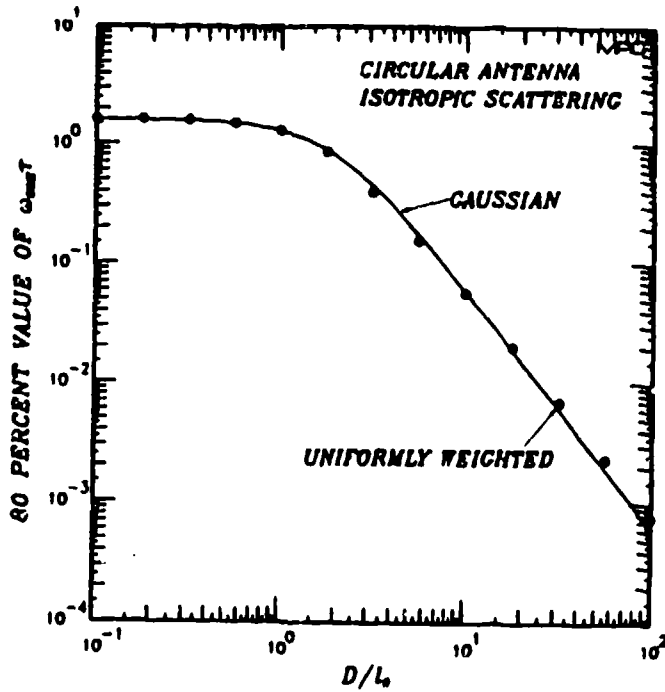

Figure 3-6. Cumulative delay distribution 80 percent value for Gaussian and uniformly weighted circular antennas.

SECTION 4
TRANSPONDER COMMUNICATION LINKS

The filtering equations for a transponder communication link
with four antennas and two uncorrelated propagation paths will be pre-
sented in this section. The mean power, decorrelation distances, decor-
relation time, and frequency selective bandwidth of the received signal
will be calculated. In order to simplify the calculations, it will be
assumed that all antennas are isotropic and are pointed without error,
that the transponder is ideal (i.e. the transmitted signal is identical to
the received signal), and that both propagation paths suffer strong scat-
tering effects. With this latter assumption, the mutual coherence func-
tion derived in Section 2 applies separately to each path.

The bistatic transponder propagation geometry is shown in
Figure 4-1. Although they are not indicated in the figure, it is assumed
that both the uplink from the sender to the transponder and the downlink
from the transponder to the receiver have transmitting and receiving
antennas.

The mutual coherence function of the signal out of the receivers
antenna will be used to calculate the filtering equations. With the
assumption that the scattering effects on the two propagation paths are
uncorrelated, the mutual coherence function can be written down directly
as the product of the coherence functions of the two paths. However, some
insight can be gained by constructing the received voltage and then by
calculating its mutual coherence function so this procedure will be used.
The frozen-in approximation will be used to model the temporal fluctua-
tions and to calculate the decorrelation time of the received signal.

68
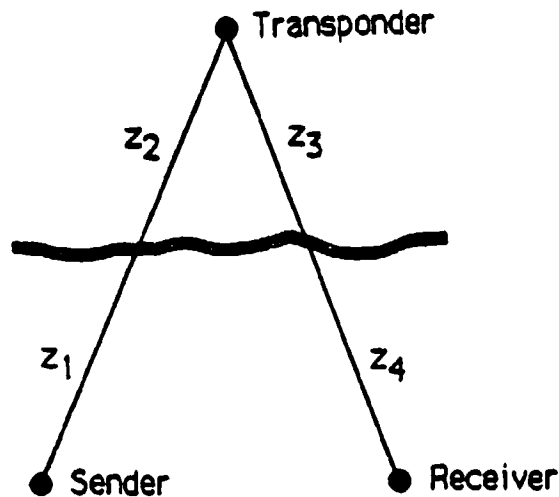
Figure 4-1. Bistatic transponder link geometry.

4.1   MUTUAL COHERENCE FUNCTION.

Consider a monochromatic wave $U_u(\vec{\xi},\omega,t)$ with RF angular frequency ω that has propagated along the uplink path from the sender and that is incident on the plane of the transponder at time t and at position $\vec{\xi}$. The effects of the sender's transmitting antenna are implicitly contained in U_u. The voltage at the output of the transponder receiving antenna, without pointing errors, can be written as

$$e_u(\vec{\xi},\omega,t) = \iint\limits_{-\infty}^{\infty} A_{ru}(\vec{\xi}-\vec{\xi}')U_u(\vec{\xi}',\omega,t)d^2\vec{\xi}' \qquad (4-1)$$

where A_{ru} is the aperture weighting function of the receiving antennna on the uplink. If a monochromatic wave is transmitted by the transponder, then the incident voltage on the plane of the receiver at position $\vec{\zeta}$ after propagating along the downlink path from the transponder to the receiver

69

will be $U_d(\vec{\zeta},\omega,t)$. Again, the effects of the transponders transmitting antenna are implicitly included in U_d. If, however, the voltage $e_u(\vec{\xi},\omega,t)$ is transmitted, then the incident voltage at the receiver will be $U_d(\vec{\zeta},\omega,t)e_u(\vec{\xi},\omega,t-t_p)$ where t_p is the nominal propagation time from the transponder to the receiver. The voltage at the output of the receiving antenna is

$$e_d(\vec{\zeta},\omega,t) = \int\limits_{-\infty}^{\infty}\!\!\!\int A_{rd}(\vec{\zeta}-\vec{\zeta}')U_d(\vec{\zeta}',\omega,t)e_u(\vec{\xi},\omega,t-t_p)\ d^2\vec{\zeta}' \qquad (4-2)$$

where A_{rd} is the aperture weighting function of the receiving antenna on the downlink.

The two-position, two-frequency, two-time mutual coherence function of the received signal is then given by calculating the expectation

$$\Gamma_b(\vec{\rho},\omega_d,t_d) = \langle e_d(\vec{\zeta}_1,\omega_1,t_1)e_d^{\ *}(\vec{\zeta}_2,\omega_2,t_2)\rangle \qquad (4-3)$$

which, for statistically stationary processes, must be a function only of the difference $\vec{\rho} = \vec{\zeta}_1 - \vec{\zeta}_2$, $\omega_d = \omega_1 - \omega_2$, and $t_d = t_1 - t_2$. The subscript b denotes the coherence function of the bistatic signal that has propagated from the sender up to the transponder and then down to the receiver.

The transponder acts as a point source for the receiver just as the sender is a point source of the signal incident at the transponder. Then because the coherence function for either one-way path is independent of the point of origin, the coherence function of the bistatic signal depends only on the distances z_i $(i=1,4)$ and on $\vec{\rho}$ and is independent of the positions of the sender or the transponder as long as the z_i distances are held constant.

At this point, it is convenient to include the frozen-in approximation explicitly in the formulation by writing the voltages U_u and U_d as

70

$$U_u(\vec{\xi},\omega,t) = U_u(\vec{\xi}-\vec{v}_u t,\omega,0) \qquad (4\text{-}4a)$$

and

$$U_d(\vec{\zeta},\omega,t) = U_d(\vec{\zeta}-\vec{v}_d t,\omega,0) \qquad (4\text{-}4b)$$

where $\vec{v}_u$ and $\vec{v}_d$ are the effective drift velocities of the random diffraction patterns as seen respectively at the transponder on the uplink and at the receiver on the downlink.

by combining Equations 4-1 through 4-4, the coherence function can be written as

$$\Gamma_b(\vec{\rho},\omega_d,t_d) = \iint_{-\infty}^{\infty} d^2\vec{\xi}_1 \; A_{ru}(\vec{\xi}-\vec{\xi}_1) \iint_{-\infty}^{\infty} d^2\vec{\xi}_2 \; A_{ru}^*(\vec{\xi}-\vec{\xi}_2) \times$$

$$\langle U_u[\vec{\xi}_1-\vec{v}_u(t_1-t_p),\omega_1,0]U_u^*[\vec{\xi}_2-\vec{v}_u(t_2-t_p),\omega_2,0]\rangle \times$$

$$\iint_{-\infty}^{\infty} d^2\vec{\zeta}_1 \; A_{rd}(\vec{\zeta}_1-\vec{\zeta}_1') \iint_{-\infty}^{\infty} d^2\vec{\zeta}_2' \; A_{rd}^*(\vec{\zeta}_2-\vec{\zeta}_2') \times$$

$$\langle U_d(\vec{\zeta}_1'-\vec{v}_d t_1,\omega_1,0)U_d^*(\vec{\zeta}_2'-\vec{v}_d t_2,\omega_2,0)\rangle \quad . \qquad (4\text{-}5)$$

The two terms in the brackets $\langle \; \rangle$ are recognized as the ͡functions of U_u and U_d.

Consider for the moment the received signal wi͡ ectional antennas at the sender, transponder, and receiver. The received signal will then be just the product $U_u U_d$ and bec͡se the propagation effects on the two paths are assumed to be uncorrelated, $\Gamma_b = \Gamma_u \Gamma_d$. As was done in Section 2, the functions Γ_u and Γ_d can be written as the product of a free space term Γ_0 and a scintillation term Γ_1. If the bis͡ ͡ee space term is set equal to $\Gamma_{uo}\Gamma_{do}$, the bistatic scin͡ ͡lati͡ ͡ will be $\Gamma_{b1} = \Gamma_{u1}\Gamma_{d1}$. In what follows, only the contri͡ ͡ ͡ the received

73

voltage due to scintillation will be considered and an expression for Γ_{b1} will be derived in terms of the uplink and downlink GPSDs and the four antennas.

Equation 4-5 can be split into an uplink factor Γ_{Au} times a downlink factor Γ_{Ad} where the downlink factor is

$$\Gamma_{Ad}(\vec{\rho},\omega_d,t_d) = \iint_{-\infty}^{\infty} d^2\vec{\zeta}_1' \; A_{rd}(\vec{\zeta}_1-\vec{\zeta}_1') \iint_{-\infty}^{\infty} d^2\vec{\zeta}_2' \; A_{rd}^*(\vec{\zeta}_2-\vec{\zeta}_2') \times$$

$$\Gamma_{d1}[(\vec{\zeta}_1'-\vec{\zeta}_2')-\vec{v}_d t_d,\omega_d,0] \quad . \tag{4-6}$$

The subscripts Ad and Au are used to denote the coherence functions at the outputs of the receiving antennas on the uplink and downlink. It is understood that Γ_{Ad} and Γ_{Au} represent the coherence functions of the scintillation part of the signal. This equation can be further reduced by writing the aperture weighting function in terms of its Fourier transform (see Equation 2-114). After changing the order of integration, Γ_{Ad} becomes

$$\Gamma_{Ad}(\vec{\rho},\omega_d,t_d) = (2\pi)^{-4} \iint_{-\infty}^{\infty} d^2\vec{K}_1 \; A_{rd}(\vec{K}_1) \iint_{-\infty}^{\infty} d^2\vec{K}_2 \; A_{rd}^*(\vec{K}_2) \times$$

$$\iint_{-\infty}^{\infty} d^2\vec{\zeta}_1' \; \exp[i\vec{K}_1\cdot(\vec{\zeta}_1-\vec{\zeta}_1')] \iint_{-\infty}^{\infty} d^2\vec{\zeta}_2' \; \exp[-i\vec{K}_2\cdot(\vec{\zeta}_2-\vec{\zeta}_2')] \times$$

$$\Gamma_{d1}(\vec{\zeta}_1'-\vec{\zeta}_2'-\vec{v}_d t_d,\omega_d,0) \quad , \tag{4-7}$$

and after a change of variables from $\vec{\zeta}_1'$ to $\vec{\zeta} = \vec{\zeta}_1 - \vec{\zeta}_2' \cdot \vec{v}_d t_d$,

$$\Gamma_{Ad}(\vec{\rho},\omega_d,t_d) = (2\pi)^{-4} \int\limits_{-\infty}^{\infty}\!\!\int d^2\vec{K}_1 \; A_{rd}(\vec{K}_1) \; \exp[i\vec{K}_1\cdot(\vec{\xi}_1 - \vec{v}_d t_d)] \; \times$$

$$\int\limits_{-\infty}^{\infty}\!\!\int d^2\vec{K}_2 \; A^\star_{rd}(\vec{K}_2) \; \exp(-i\vec{K}_2\cdot\vec{\xi}_2) \int\limits_{-\infty}^{\infty}\!\!\int d^2\vec{\xi}_2' \; \exp[i\vec{\xi}_2'\cdot(\vec{K}_2 - \vec{K}_1)] \; \times$$

$$\int\limits_{-\infty}^{\infty}\!\!\int d^2\vec{\xi} \; \exp(-i\vec{K}_1\cdot\vec{\xi}) \; \Gamma_{d1}(\vec{\xi},\omega_d,0) \quad . \tag{4-8}$$

The last integral, which will be denoted $\hat{S}_{Ad}(\vec{K}_1,\omega_d)$, is the Fourier transform of the angular-delay part of the GPSD for the downlink signal. The subscript A is attached because $\hat{S}_{Ad}$ includes the effects of the transponder's transmitting antenna. The integral over $\vec{\xi}_2'$ results in the delta function $(2\pi)^2 \delta_F(\vec{K}_2 - \vec{K}_1)$. With these substitutions, the coherence function for the downlink is

$$\Gamma_{Ad}(\vec{\rho},\omega_d,t_d) = (2\pi)^{-2} \int\limits_{-\infty}^{\infty}\!\!\int d^2\vec{K}_d \; G_{rd}(\vec{K}_d)\hat{S}_{Ad}(\vec{K}_d,\omega_d) \; \exp[i\vec{K}_d\cdot(\vec{\rho}-\vec{v}_d t_d)] \tag{4-9}$$

where G_{rd} is the beam profile of the receiving antenna on the downlink.

In a similar fashion, the coherence function Γ_{Au} can be derived. However, it can also be written down directly from Equation 4-9 with the following two observations. First, the bistatic mutual coherence function is the expectation of received voltage for two positions of the receiver but for only one position of the transponder. Thus the uplink contribution to Γ_{b1} contains only carrier frequency and time differences. Second, the expectation of $U_u U_u^\star$ that appears in Equation 4-5 depends only on the argument differences and is therefore independent of the nominal propagation time t_p. The uplink coherence function is then given by

73

$$\Gamma_{Au}(\omega_d, t_d) = (2\pi)^{-2} \iint_{-\infty}^{\infty} d^2\vec{K}_u \ G_{ru}(\vec{K}_u)\hat{S}_{Au}(\vec{K}_u, \omega_d) \exp \ (-i\vec{K}_u \cdot \vec{v}_u t_d) \quad (4\text{-}10)$$

where G_{ru} is the gain function of the receiving antenna on the uplink and $\hat{S}_{Au}$ is the Fourier transform of the angular-delay GPSD for the uplink including the effects of the sender's transmitting antenna.

The effect of a transmitting antenna is to filter, as a function of angle, the angular-delay GPSD of the signal at the receiver. Thus the angular-delay GPSD of the incident signal on the plane of the receiver including the effects of the transmitting antenna pointed at the receiver is

$$S_t(\vec{K}, \tau) = G_t(\kappa\vec{K})S(\vec{K}, \tau) \quad (4\text{-}11)$$

where $S(\vec{K}, \tau)$ is the GPSD for an omnidirectional transmitter, G_t is the beam profile of the transmitting antenna and $\kappa = z_r/z_t$ is a scale factor that transforms angles at the transmitter to angles at the receiver (see Figure 2-3 and Equation 2-90).

The mutual coherence function of the signal out of the receiver for a transponder communications link is now given by

$$\Gamma_{bl}(\vec{\rho}, \omega_d, t_d) = \Gamma_{Au}(\omega_d, t_d)\Gamma_{Ad}(\vec{\rho}, \omega_d, t_d) =$$

$$(2\pi)^{-2} \iint_{-\infty}^{\infty} d^2\vec{K}_u \ G_{tu}(\kappa_u\vec{K}_u)G_{ru}(\vec{K}_u)\hat{S}_u(\vec{K}_u, \omega_d) \exp \ (-i\vec{K}_u \cdot \vec{v}_u t_d) \times$$

$$(2\pi)^{-2} \iint_{-\infty}^{\infty} d^2\vec{K}_d \ G_{td}(\kappa_d\vec{K}_d)G_{rd}(\vec{K}_d)\hat{S}_d(\vec{K}_d, \omega_d) \exp \ [(i\vec{K}_d \cdot (\vec{\rho} \cdot \vec{v}_d t_d)]$$

where G_{tu} is the beam profile of the transmitting antenna on the uplink and G_{td} is the beam profile of the transmitting antenna on the downlink. The κ scale factors are

74

$$\kappa_u = z_2/z_1 \tag{4-13a}$$

and

$$\kappa_d = z_4/z_3 \quad . \tag{4-13b}$$

For satellite transponders, the distance from the satellite to the ionosphere will usually be much greater than the distance from the ionosphere to the ground. Therefore, $\kappa_u \gg 1$ and $\kappa_d \ll 1$ under most circumstances.

4.2 SCATTERING LOSS.

The scattering loss suffered on the transponder communications link depends on the GPSDs of the two propagation paths and on the beam profiles of the four antennas. Under the assumption that the two propagation paths are uncorrelated, the total scattering loss will be the product of an uplink contribution and a downlink contribution.

The mean received power for the bistatic path is

$$
\begin{aligned}
P_b &= \Gamma_{bl}(\vec{0},0,0) = P_u P_d \\[2mm]
&= (2\pi)^{-2} \iint\limits_{-\infty}^{\infty} d^2\vec{K}_1 \; G_{tu}(\kappa_u\vec{K}_1)G_{ru}(\vec{K}_1)\hat{S}_u(\vec{K}_1,0) \times \\[2mm]
&\quad (2\pi)^{-2} \iint\limits_{-\infty}^{\infty} d^2\vec{K}_2 \; G_{td}(\kappa_d\vec{K}_2)G_{rd}(\vec{K}_2)\hat{S}_d(\vec{K}_2,0)
\end{aligned} \tag{4-14}
$$

where P_u is equal to the first integral and where P_d is equal to the second integral. The function $\hat{S}_\xi(\vec{K},0)$ is

$$
\begin{aligned}
\hat{S}_\xi(\vec{K},0) &= \int\limits_{-\infty}^{\infty} S_\xi(\vec{K},\tau)d\tau \\[2mm]
&= (\pi \ell_{o\xi}^2/\delta_\xi) \exp\left[-(K_x^2\ell_{o\xi}^2/4) - (K_y^2\ell_{o\xi}^2/4\delta_\xi^2)\right]
\end{aligned} \tag{4-15}
$$

where $S_\xi(\vec{K},\tau)$ is the angular-delay part of the GPSD for the uplink ($\xi=u$) or the downlink ($\xi=d$). In the developments that follow, each path will have its own decorrelation distance at the receiver $\ell_{o\xi}$, frequency selective bandwidth $f_{o\xi}$, and penetration angle and scale size ratio δ_ξ. Also, there will be no assumed relationship between the orientations of the x axes on the two paths.

The antenna beam profiles for this calculation are assumed to be isotropic and Gaussian and to be pointed without error. The combined transmitting and receiving beam profiles may then be written as

$$G_{t\xi}(\kappa_\xi\vec{K})G_{r\xi}(\vec{K}) = \exp\left[-(\alpha_{t\xi}^2\kappa_\xi^2 + \alpha_{r\xi}^2)K_x^2\right]\exp\left[-(\alpha_{t\xi}^2\kappa_\xi^2 + \alpha_{r\xi}^2)K_y^2\right] \quad (4\text{-}16)$$

where $\alpha_{t\xi}$ and $\alpha_{r\xi}$ are given in terms of the transmitting and receiving antenna beamwidths respectively by Equation 3-3. The combined beam profile is again Gaussian with a beamwidth that is smaller than either of the two antennas.

The scattering loss the ξ path is

$$L_{S\xi} = P_\xi^{-1} = \left[G_{x\xi}G_{y\xi}\right]^{1/2} \quad (4\text{-}17)$$

where

$$G_{x\xi} = 1 + 4\alpha_{t\xi}^2\kappa_\xi^2/\ell_{o\xi}^2 + 4\alpha_{r\xi}^2/\ell_{o\xi}^2 \quad (4\text{-}18a)$$

and

$$G_{y\xi} = 1 + 4\delta_\xi^2\alpha_{t\xi}^2\kappa_\xi^2/\ell_{o\xi}^2 + 4\delta_\xi^2\alpha_{r\xi}^2/\ell_{o\xi}^2 \quad . \quad (4\text{-}18b)$$

If the antennas are uniformly weighted circular apertures, then the G functions become

$$G_{x\xi} = 1 + 0.265\left[\kappa_\xi^2(D_{t\xi}/\ell_{o\xi})^2 + (D_{r\xi}/\ell_{o\xi})^2\right] \quad (4\text{-}19a)$$

and

$$G_{y\xi} = 1 + 0.265\,\delta_\xi^2\left[\kappa_\xi^2(D_{t\xi}/\ell_{o\xi})^2 + (D_{r\xi}/\ell_{o\xi})^2\right] \quad (4\text{-}19b)$$

76

where $D_{t\xi}$ and $D_{r\xi}$ are the transmitting and receiving antenna diameters respectively. The total loss of the bistatic transponder link is

$$L_S = L_{Su}L_{Sd} = [G_{xu}G_{yu}G_{xd}G_{yd}]^{1/2} \quad . \tag{4-20}$$

The decorrelation distance $\ell_{0\xi}$ in these expressions is that of the signal incident on the plane of the receiving antenna when an omnidirectional signal is transmitted. Recall from Section 2 that the decorrelation distance is not a reciprocal quantity. If an omnidirectional signal were transmitted at the receiver's location, the decorrelation distance of the signal at the plane of the transmitter would be $\ell_{0\xi}/\kappa_\xi$. On the uplink to a geosynchronous satellite transponder, $\kappa_u \gg 1$ and the uplink scattering loss is determined primarily by the loss due to the transmitting antenna. However on the downlink, $\kappa_d \ll 1$ and the downlink scattering loss is determined primarily by the loss due to the receiving antenna. In either case, it is the antenna closest to the ionosphere that determines the scattering loss of the link.

4.3 FREQUENCY SELECTIVE BANDWIDTH

The time delay jitter of the bistatic signal at the output of the receiver can be calculated from the power impulse response function

$$P_b(\tau) = (2\pi)^{-1} \int_{-\infty}^{\infty} \Gamma_{b1}(\vec{0},\omega_d,0) \exp(i\omega_d\tau)d\omega_d \tag{4-21}$$

where $P_b(\tau)d\tau$ is the fraction of signal energy arriving in the delay interval τ to $\tau + d\tau$. The nth delay moment of the signal energy is

$$P_b\langle\tau^n\rangle = \int_{-\infty}^{\infty} \tau^n P_b(\tau)d\tau \tag{4-22}$$

where P_b is the $n = 0$ moment and is equal to the mean received power. The evaluation of the delay moments is simplified by considering the form of $P(\tau)$. The power impulse response function can be written as

77

$$P_b(\tau) = (2\pi)^{-1} \int_{-\infty}^{\infty} \Gamma_{Au}(\omega_d,0)\Gamma_{Ad}(\vec{0},\omega_d,0) \, \exp(i\omega_d\tau)d\omega_d \quad . \tag{4-23}$$

This integral can also be written in the delay domain as a convolution:

$$P_b(\tau) = \int_{-\infty}^{\infty} P_u(\tau')P_d(\tau-\tau')d\tau' \tag{4-24}$$

where $P_u(\tau)$ and $P_d(\tau)$ are the power impulse response functions of the up-link and downlink paths respectively. These functions are

$$P_u(\tau) = (2\pi)^{-1} \int_{-\infty}^{\infty} \Gamma_{Au}(\omega_d,0) \, \exp(i\omega_d\tau)d\omega_d \tag{4-25}$$

and

$$P_d(\tau) = (2\pi)^{-1} \int_{-\infty}^{\infty} \Gamma_{Ad}(\vec{0},\omega_d,0) \, \exp(i\omega_d\tau)d\omega_d \quad . \tag{4-26}$$

Now the delay moments of the received signal can be evaluated in terms of the delay moments of each of the paths:

$$P_\xi \langle \tau_\xi^n \rangle = \int_{-\infty}^{\infty} \tau^n \, P_\xi(\tau)d\tau \tag{4-27}$$

for $\xi = u$ or $\xi = d$. The mean received power is

$$P_b = \int_{-\infty}^{\infty} P_b(\tau)d\tau = \int_{-\infty}^{\infty} d\tau \int_{-\infty}^{\infty} d\tau' P_u(\tau')P_d(\tau-\tau') \tag{4-28}$$

which after some manipulations reduces to the previous result, given in Section 4.2, that $P_b = P_u P_d$. Using this formalism, it is easy to show that the first two delay moments of the bistatic signal are

$$\langle \tau_b \rangle = \langle \tau_u \rangle + \langle \tau_d \rangle \tag{4-29}$$

and

$$\langle \tau_b^2 \rangle = \langle \tau_u^2 \rangle + 2\langle \tau_u \rangle\langle \tau_d \rangle + \langle \tau_d^2 \rangle \quad . \tag{4-30}$$

The time delay jitter of the bistatic signal is then

$$\sigma_{\tau b}^2 = \sigma_{\tau u}^2 + \sigma_{\tau d}^2$$

and the frequency selective bandwidth of the bistatic signal out of the receiver's antenna is

$$f_{Ab} = 1/(2\pi\sigma_{\tau b}) \quad . \tag{4-32}$$

The problem has now been reduced to that of finding the frequency selective bandwidths of the signals at the outputs of the receiving antennas for the one-way paths. This result was presented in Section 3.2.3 for one-way paths with a receiving antenna only. However, it is a simple matter to generalize those results to include the effects of a Gaussian transmitting antenna. The frequency selective bandwidth of the signal out of the receiving antenna for either one-way path is

$$f_{A\xi}/f_{O\xi} = \frac{(1+\delta_\xi^4)^{1/2} L_{S\xi}^2}{[\delta_\xi^4 G_{x\xi}^2 + G_{y\xi}^2]^{1/2}} \tag{4-33}$$

where $\xi = u$ or $\xi = d$. This expression is valid only for isotropic antennas. The quantity $f_{O\xi}$ is the frequency selective bandwidth of the signal incident on the plane of the receiving antenna for a transmitted impulse and for an omnidirectional transmitter antenna. The time delay jitter for either path is given by

$$\sigma_{\tau\xi} = 1/(2\pi f_{A\xi}) \quad . \tag{4-34}$$

Finally, the frequency selective bandwidth of the bistatic signal at the output of the receiving antenna is

$$f_{Ab} = [f_{Au}^{-2} + f_{Ad}^{-2}]^{-1/2} \quad . \tag{4-35}$$

79

If both the uplink and the downlink have the same filtered frequency selective bandwidths, then f_{Ab} is equal to $f_{A\xi}/\sqrt{2}$. If, however, one of the links has a much smaller frequency selective bandwidth than the other, then f_{Ab} is equal to the smaller value of $f_{A\xi}$.

4.4 DECORRELATION DISTANCES AND TIME.

The decorrelation distances of the signal at the receiver depend only on the downlink path and are given by the 1/e points of $\Gamma_{Ad}(\vec{\rho},0,0)/P_d$. The downlink two-position mutual coherence function is calculated using Equation 4-9 and is equal to

$$\Gamma_{Ad}(\vec{\rho},0,0) = P_d \exp\left[-(x/\ell_{od})^2/G_{xd}\right] \exp\left[-(\delta_d y/\ell_{od})^2/G_{yd}\right] \quad . \quad (4-36)$$

The antenna filtered decorrelation distances at the receiver are then given by

$$\ell_{Ax}/\ell_{od} = \sqrt{G_{xd}} \quad (4-37)$$

and

$$\ell_{Ay}/\ell_{od} = \sqrt{G_{yd}}/\delta_d \quad . \quad (4-38)$$

The decorrelation time does depend on both the uplink and the downlink. It is convenient to calculate the two-time mutual coherence function $\Gamma_{A\xi}(\vec{0},0,t_d)$ of each path separately and then to construct this function for the bistatic path. As has been done previously, it will be assumed that the effective drift velocities are aligned with the x axes. For the downlink, the function Γ_{Ad} is calculated from Equation 4-9 and is equal to

$$\Gamma_{Ad}(\vec{0},0,t_d) = P_d \exp\left[-(v_d t_d)^2/(G_{xd}\ell_{od}^2)\right]$$

$$= P_d \exp\left[-(t_d/\tau_{Ad})^2\right] \quad (4-39)$$

60

where

$$\tau_{Ad} = \ell_{od} \sqrt{G_{xd}}/v_d \qquad\qquad (4\text{-}40)$$

is the antenna filtered decorrelation time due to the downlink only and where v_d is the effective downlink drift velocity along the downlink x axis. A similar set of expressions hold for the uplink two-time coherence function and decorrelation time:

$$\Gamma_{Au}(\vec{0},0,t_d) = P_u \exp[-(v_u t_d)^2/(G_{xu}\ell_{ou}^2)]$$

$$= P_u \exp[-(t_d/\tau_{Au})^2] \qquad\qquad (4\text{-}41)$$

where

$$\tau_{Au} = \ell_{ou}\sqrt{G_{xu}}/v_u \qquad\qquad (4\text{-}42)$$

is the antenna filtered decorrelation time due to the uplink only and where v_u is the effective uplink drift velocity along the uplink x axis. The bistatic path has a two-time mutual coherence function given by

$$\Gamma_{Ab}(\vec{0},0,t_d) = \Gamma_{Au}(\vec{0},0,t_d)\Gamma_{Ad}(\vec{0},0,t_d)$$

$$= P_u P_d \exp[-(\tau_{Au}^{-2} + \tau_{Ad}^{-2})t_d^2] \quad . \qquad\qquad (4\text{-}43)$$

The bistatic path decorrelation time τ_{Ab} under the frozen-in approximation is then given by

$$\tau_{Ab} = (\tau_{Au}^{-2} + \tau_{Ad}^{-2})^{-1/2} \quad . \quad \text{(Frozen-in Approximation)} \qquad (4\text{-}44)$$

The decorrelation time for the turbulent approximation can be obtained from this expression by noting that under this approximation, the decorrelation time is not filtered by the antennas. Therefore, the bistatic decorrelation time becomes

$$\tau_{ob} = (\tau_{ou}^{-2} + \tau_{od}^{-2})^{-1/2} \quad . \quad \text{(Turbulent Approximation)} \qquad (4\text{-}45)$$

where τ_{ou} and τ_{od} are the uplink and downlink decorrelation times without antenna effects. This expression is valid only if the Doppler frequency spectrum is Gaussian. If this is not the case, then a slightly different relationship holds between the bistatic path decorrelation time and the decorrelation times of the two individual paths (Dana 1982).

If both the uplink and the downlink have the same decorrelation time at the outputs of the receiving antennas, then under the frozen-in (turbulent) approximation, $\tau_{Ab}(\tau_{ob})$ is equal to $\tau_{A\xi}/\sqrt{2}$ $(\tau_{o\xi}/\sqrt{2})$. If however, one of the links has a much smaller decorrelation time than the other, then $\tau_{Ab}(\tau_{ob})$ is equal to the smaller value of $\tau_{A\xi}(\tau_{o\xi})$.

SECTION 5
CHANNEL SIMULATION

The purpose of this section is to describe a statistical channel simulation technique that allows realizations of the impulse response functions to be generated at the outputs of multiple antennas with spatial and temporal correlation properties given by the GPSD derived in Section 2 and with Rayleigh amplitude statistics. The realizations generated with this technique represent only the diffractive part of the received voltage and they are valid only under strong scattering conditions where the GPSD is valid and where Rayleigh statistics apply. Under these conditions however, they represent a solution of Maxwell's equations for propagation of RF waves through randomly structured ionization.

The basic formalism to generate statistical realizations of the channel impulse response function without antenna effects explicitly included was developed by Wittwer (1980) for isotropic irregularities and was extended by Knepp (1982) to the case of elongated irregularities. (The elongated case corresponds to a 90° penetration angle and to an infinite axial ratio.) The channel simulation technique has been generalized in this report to include the effects of anisotropic scattering and the effects of multiple receiving antennas and has resulted in a new DNA software channel simulator for antenna applications (Dana and Wittwer, 1985).

83

It will be assumed in this section for the sake of limiting the discussion that the multiple antennas are identical in beam profile, orientation, and pointing angle. It is also assumed that the antenna centers are colinear. These restrictions may be easily lifted by using the more general formalism reported by Wittwer (1986).

The frozen-in approximation will be used in most of the developments in this section to describe the temporal fluctuations of the incident signal. The generalization of the channel simulation technique to the turbulent approximation is discussed in Section 5.2 along with a second technique proposed by Wittwer (1986) that is valid in the α equal infinity limit. A comparison of realizations generated under the frozen-in and turbulent approximations is made in Section 5.4.

The scattering of the signal is described in the x-y coordinate system shown in Figure 5-1, which is normal to the line-of-sight. The x axis corresponds to the direction with the minimum decorrelation distance
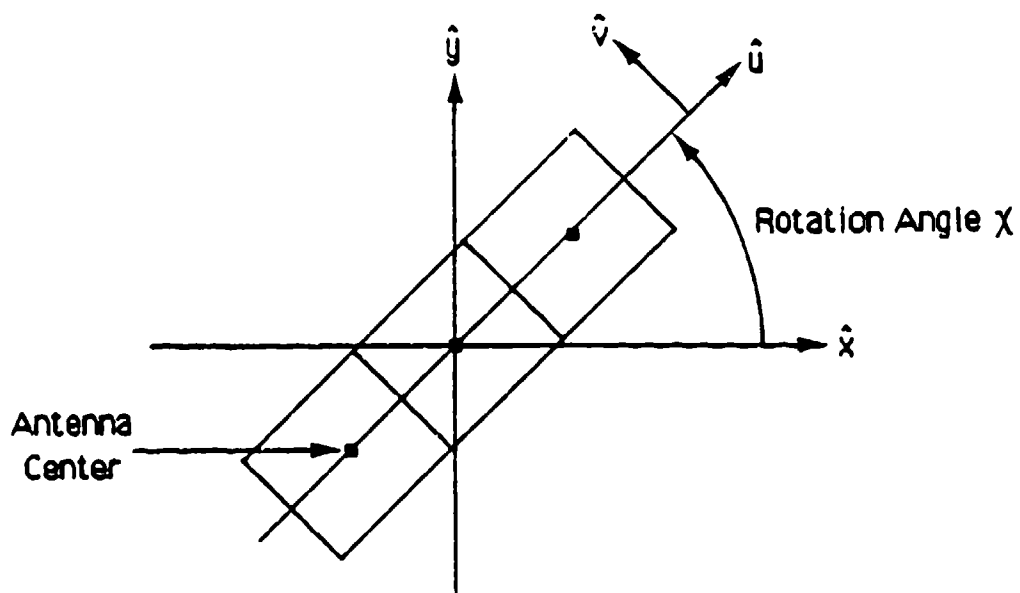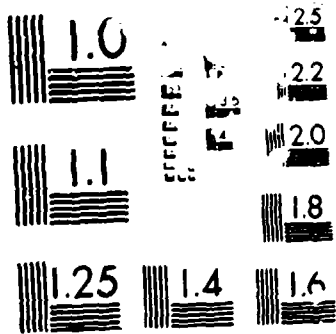

Figure 5-1. Scattering and antenna coordinate systems.

84

1.0

1.1

1.25   1.4   1.6

2.5

2.2

2.0

1.8

MICROCOPY RESOLUTION TEST CHART

which, to be conservative, is chosen to be the direction of the effective velocity between the antennas and the random diffraction pattern. The antennas are described in the u-v coordinate system, which lies in the x-y plane, where the antenna centers lie along the u axis. The angle χ $(0 \leq \chi \leq \pi/2)$ is the rotation angle between the scattering coordinate system and the antenna coordinate system. In the figure, one of the antennas is depicted at the origin of the x-y coordinate system. The mth antenna is specified by $\vec{\rho}_m$ where $\vec{\rho}_m$ is a position vector in the x-y plane that points to the mth antenna center.

5.1   GENERATION OF REALIZATIONS (FROZEN-IN APPROXIMATION).

The technique for generating the realizations of the impulse response function at the outputs of multiple antennas is outlined below. For a given signal delay, random samples of the impulse response function at the outputs of the antennas are generated on the two dimensional x-y grid shown schematically in Figure 5-2. The y coordinates of the grid correspond to the y coordinates of the multiple antenna centers y_m. The x coordinates of the grid correspond to the x positions of the antenna centers x_m as a function of time due to the effective velocity of the antenna relative to the random diffraction pattern.

5.1.1   Discrete Evaluation of the GPSD.

The first step in generating the impulse response function at the output of an antenna is the evaluation of the GPSD on a discrete K_x - K_y - τ grid. The angular-delay grid centers are defined by

$$K_x = k\Delta K_x$$

$$K_y = l\Delta K_y$$

$$\tau_j = \tau_s + j\Delta\tau \qquad (5-1)$$

85
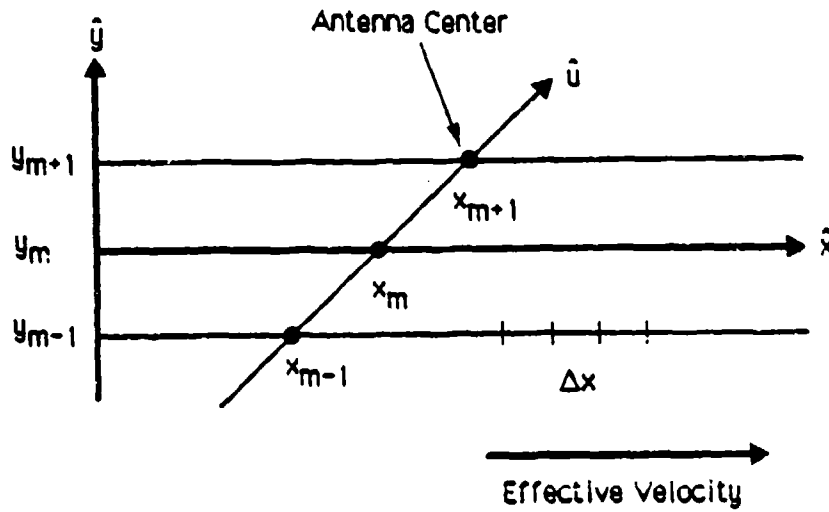
Figure 5-2. x-y grid of impulse response function.

where k, 1, and j are integers. The starting delay τ_s and the angular and delay grid sizes will be defined in Section 5.1.3. The mean signal energy at each grid point is

$$E_{k,1,j} = (2\pi)^{-2} \int\limits_{(k-1/2)\Delta K_x}^{(k+1/2)\Delta K_x} dK_x \int\limits_{(1-1/2)\Delta K_y}^{(1+1/2)\Delta K_y} dK_y \int\limits_{\tau_j-\Delta\tau/2}^{\tau_j+\Delta\tau/2} d\tau \; S_A(K_x,K_y,\tau) \qquad (5-2)$$

where $S_A(K_x,K_y,\tau)$ is given by Equation 3-22 in the x-y coordinate system. The mean signal power in the jth delay bin is

$$P_j = \sum_k \sum_1 E_{k,1,j} \qquad (5-3)$$

and the total mean power in the grid is

$$P_G = \sum_j P_j \quad . \qquad (5-4)$$

These two quantities are useful in verifying the statistics of random realizations as discussed in Section 5.3.

86

The integral over delay in Equation 5-2 can be done in closed form with the result that the mean signal energy in the k-l-j grid cell is

$$
E_{k,l,j} = [\ell_0^2/(8\pi\delta)] \int_{(k-1/2)\Delta K_x}^{(k+1/2)\Delta K_x} dK_x \exp(-K_x^2\ell_0^2/4) \times
$$

$$
\int_{(l-1/2)\Delta K_y}^{(l+1/2)\Delta K_y} dK_y \exp(-K_y^2\ell_0^2/4\delta^2) \, G(K_x,K_y) \, E_j(K_x,K_y) \quad (5\text{-}5)
$$

where

$$
E_j(K_x,K_y) = \mathrm{erf}\{\alpha[\omega_{coh}(\tau_j+\Delta\tau/2) - \Lambda(K_x^2+K_y^2)\ell_0^2/4]/\sqrt{2}\} -
$$

$$
\mathrm{erf}\{\alpha[\omega_{coh}(\tau_j-\Delta\tau/2) - \Lambda(K_x^2+K_y^2)\ell_0^2/4]/\sqrt{2}\} \quad (5\text{-}6)
$$

and where erf is the error function. Because the antenna beam profile appears explicitly in the integrand of Equation 5-5, $E_{k,l,j}$ is valid only for an antenna with beam profile $G(K_x,K_y)$. However, at this point the location of the antenna is arbitrary as long as the beam profile remains fixed. If the different antennas have different beam profiles (or the same profile with different pointing angles), then a separate $E_{k,l,j}$ must be calculated for each different $G(K_x,K_y)$.

The value of α in Equation 5-6 is chosen to be large enough so that under the most disturbed propagation conditions the antenna filtering of the frequency selective bandwidth is not limited by the value of α. The procedure for choosing α is as follows. The ratio f_A/f_0 under conditions where the decorrelation distance approaches zero is obtained by combining Equations 3-35 and 3-36 with the result

$$
\underset{\ell_0 \to 0}{\mathrm{Limit}} \ f_A/f_0 = \alpha^2 + 1 \quad . \quad (5\text{-}7)
$$

Using the minimum decorrelation distance, the maximum value of f_A/f_0 is obtained from Equation 3-38 for α set equal to infinity. The value of α is then chosen so that the difference between $\alpha^2 + 1$ and the maximum value of f_A/f_0 is small. As discussed by Knepp (1982), it is possible to set α to infinity. However, the resulting discontinuities in the GPSD present numerical difficulties in the signal generation process that are avoided with a finite value of α. An alternative channel simulation technique which depends on α being infinite is discussed in Section 5.2.2. This latter technique was developed to generate signal realizations under the turbulent approximation but it could be applied to the generation of frozen-in approximation realizations as well.

5.1.2   Random Realizations.

The impulse response functions will be generated one delay at a time starting with the smallest delay ($j=0$) and working to the largest value of delay ($j=j_{max}$). For each delay, the steps that are performed are outlined in this subsection.

The Fourier transform $\bar{h}_A$ of the impulse response function at the output of an antenna is

$$\bar{h}_A(k\Delta K_x, l\Delta K_y, \tau_j) = (4\pi^2/\Delta K_x \Delta K_y \Delta\tau)\xi_{k,l,j}\sqrt{E_{k,l,j}} \qquad . \qquad (5-8)$$

The normalization factor $(4\pi^2/\Delta K_x \Delta K_y \Delta\tau)$ has been chosen so that after $\bar{h}_A$ is Fourier transformed from the angular $K_x - K_y$ domain to the spatial domain, $h_A\Delta\tau$ will represent the voltage received during the delay interval $\tau_j - \Delta\tau/2$ to $\tau_j + \Delta\tau/2$. The quantity $\xi_{k,l,j}$ is a complex, zero mean, Gaussian random variable with the properties

$$\langle \xi_{k,l,j}\xi^*_{\alpha,\beta,\gamma}\rangle = \delta_{k,\alpha}\delta_{l,\beta}\delta_{j,\gamma}$$

$$\langle \xi_{k,l,j}\rangle \qquad = 0$$

$$\langle \xi_{k,l,j}\xi_{\alpha,\beta,\gamma}\rangle = 0 \qquad\qquad\qquad (5-9)$$

where $\delta_{m,n}$ is the Kronecker delta symbol. The random numbers ξ may be generated using the equation

$$\xi = \sqrt{-\ln u_1} \, \exp(2\pi i u_2) \qquad (5\text{-}10)$$

where u_1 and u_2 are independent random numbers uniformly distributed on the interval $[0,1)$.

There is no explicit y coordinate since realizations will be generated only at y coordinates corresponding to antenna centers. This is accomplished by first generating N_y samples of $\bar{h}_A$ in the K_y domain and then by Fourier transforming $\bar{h}_A$ to the y domain using discrete Fourier transforms (DFTs). One DFT is performed at each K_x coordinate grid point for each unique antenna center y coordinate. In continuous notation, this transform is

$$\bar{h}_{A,m}(K_x,\tau) = (1/2\pi) \int_{-\infty}^{\infty} \bar{h}_A(K_x,K_y,\tau) \, \exp(iK_y y_m) dK_y \qquad (5\text{-}11)$$

where y_m is the y coordinate of the mth antenna center. The DFT equivalent of this equation is

$$\bar{h}_{A,m}(k\Delta K_x,\tau_j) = (\Delta K_y/2\pi) \sum_{l=-N_y/2}^{N_y/2-1} \exp(il\Delta K_y y_m) \, \bar{h}_A(k\Delta K_x, l\Delta K_y, \tau_j) \, . \qquad (5\text{-}12)$$

Now the K_x to x Fourier transform is performed for each antenna. In this case, a fast Fourier transform (FFT) may be used. In continuous notation

$$h_{A,m}(x,\tau) = (1/2\pi) \int_{-\infty}^{\infty} \exp(iK_x x) \, \bar{h}_{A,m}(K_x,\tau) dK_x \, . \qquad (5\text{-}13)$$

89

The discrete equivalent of this equation is

$$h_{A,m}(k\Delta x, \tau_j) = (\Delta K_x/2\pi) \sum_{k'=-N_x/2}^{N_x/2-1} \exp(ik'\Delta K_x k\Delta x) \, \tilde{h}_{A,m}(k'\Delta K_x, \tau_j) \qquad (5\text{-}14)$$

where N_x is the number of x coordinate grid points.

The quantity $h_{A,m}(k\Delta x, \tau_j)$ is the impulse response function at the output of the mth antenna when that antenna is located at x position $k\Delta x$. Under the frozen-in approximation, a time step Δt may be associated with Δx using the effective velocity:

$$\Delta t = \Delta x (\tau_0/\ell_0) \qquad (5\text{-}15)$$

where τ_0 is the decorrelation time of the incident signal. The quantity $h_{A,m}(k\Delta x, \tau_j)$ then also represents the impulse response function at the output of the mth antenna at time $k\Delta t$.

5.1.3   Grid Sizes.

The grid sizes of the channel simulator are chosen on the basis of the statistics of the signal out of the antennas which are given by the filtering equations in Section 3.2. The angular grid sizes are chosen so the antenna filtered GPSD will be small or zero at the edges of the angular grid and so there will be a sufficient number of samples per decorrelation distance to resolve the fades of the Rayleigh amplitude distribution. The delay grid size $\Delta \tau$ is chosen on the basis of the sampling period of the receiver and the number of delay samples N_D of the realizations is chosen so the total delay spread of the realization $N_D \Delta \tau$ will encompass at least 95 percent of the delayed signal energy.

5.1.3.1 The $\Delta x - \Delta K_x$ Grid. The x grid spacing is

$$\Delta x = \ell_{Ax}/N_0 \qquad (5-16)$$

where ℓ_{Ax} is the filtered x direction decorrelation distance (Equation 3-41). The quantity N_0 is the number of samples per decorrelation distance or time where N_0 should have a value of 10 or larger in order for the realization to accurately represent the duration and separation of the fades of the Rayleigh amplitude distribution (Dana 1982).

The number of x grid points N_x is subject to two constraints: First, N_x should be a power of 2 so a fast Fourier transform can be used to transform from the K_x domain to the x domain. Second, N_x should be greater than or equal to 100 N_0. Equivalently, there should be at least 100 x direction decorrelation distances in the realization in order for the realization to represent a reasonable sample of the random process. Under the frozen-in approximation, 100 decorrelation distances corresponds to an elapsed time of 100 decorrelation times.

Here reasonable is defined in terms of the application. Typically, the realizations are used to exercise simulations of transionospheric communications links and each realization with $N_x/N_0 = 100$ can be used to calculate receiver performance averaged over 100 decorrelation times. The resulting receiver performance measures will have some statistical variation due to the finite time duration of the simulation. This variation can be reduced by either using lo er realizations or by using several realizations with the same signal , meters but with different random numbers and by averaging the results from the multiple realizations. This latter approach allows an estimate of the statistical variation in the receiver performance to be made.

Returning to the grid spacing, the x direction distance spanned by the realization is $L_x = N_x \Delta x$ and ΔK_x is

$$\Delta K_x = 2\pi/L_x = 2\pi/N_x \Delta x \qquad . \qquad (5\text{-}17)$$

The functional dependence of the GPSD on K_x is given approximately by

$$\epsilon = \exp[-(K_x \ell_{Ax}/2)^2] \qquad . \qquad (5\text{-}18)$$

In discrete notation, $K_x = k\Delta K_x$ where $|k|$ has a maximum value of $N_x/2$. Using the maximum value for K_x of $N_x \Delta K_x/2$, the value of ϵ at the edge of the K_x grid is $\exp[-(\pi N_0/2)^2]$ which is essentially zero for N_0 equal to 10.

5.1.3.2 The ΔK_y Grid. The number of K_y grid points is determined by requiring that the GPSD is small at both ends of the K_y grid. The functional dependence of the GPSD on K_y is given approximately by

$$\epsilon = \exp[-(K_y \ell_{Ay}/2)^2] \qquad (5\text{-}19)$$

A convenient minimum value of ϵ is $\exp(-\pi^2) = 5.2 \times 10^{-5}$. Using this value results in the following condition on N_y:

$$N_y > 4\pi/(\Delta K_y \ell_{Ay}) \qquad . \qquad (5\text{-}20)$$

It is desirable to minimize the number of K_y samples generated to minimize computer memory and execution time requirements for signal generation. A reasonable minimum value for N_y is 32.

The ΔK_y grid spacing is then

$$\Delta K_y = 2\pi/L_y \qquad (5\text{-}21)$$

where the length of the realization in the y direction is chosen as

$$L_y = \text{maximum} \left[16\ell_{A,y}; \ 4 \text{ maximum} \left(|y_m| \right) \right] \qquad . \qquad (5\text{-}22)$$

92

The first condition, $L_y = 16\ell_{A,y}$, results from letting $N_y = 32$ in Equation 5-20. The second condition, $L_y = 4$ maximum $(|y_m|)$, is chosen to minimize aliasing of the impulse response functions of the antenna with the largest value of y_m and the antenna with the smallest value of y_m. If the value of L_y is determined by this latter condition, then the value of N_y will need to be larger than 32 in order to satisfy the condition on N_y given by Equation 5-20.

5.1.3.3   The Delay Grid $\Delta\tau$.   The delay grid size is usually chosen so there are an integer number of delay samples in a sample period of the communications link receiver.   There should be at least two delay samples per symbol in order to represent the frequency spectrum of the symbols. The number of delay samples is chosen so the delay spread of the realiza- tion $N_D\Delta\tau$ will encompass at least 95 percent of the delayed signal energy.   However, the delay spread of the signal depends on the anisotropy of the signal, on the value of α, and on the antenna filtering.   For a given frequency selective bandwidth of the incident signal, the delay spread of the signal out of an antenna increases as the antenna filtering is reduced (or as ℓ_0 is increased), as the value of α is decreased, and as the penetration angle is reduced (as the incident signal becomes more isotropic).   Without antenna filtering, 95 percent of the signal energy under isotropic scattering conditions arrives with delays in the range $-0.25 < \omega_{coh}\tau < 3.45$ when α is set at its minimum value of 4 (Wittwer 1980).   To be conservative, this same criterion is applied under all conditions   The minimum delay spread of the impulse response function realizations must therefore satisfy the condition

$$-0.25 < 2\pi f_A \tau < 3.45 \quad . \tag{5-23}$$

The minimum number of delay samples required is then

$$N_D > 1 + 3.7/(2\pi f_A \Delta\tau) \tag{5-24}$$

where the first delay bin (j=0) has a center delay of

$$\tau_s = -0.25/(2\pi f_A) \quad .$$

(5-25)

5.2 GENERATION OF REALIZATIONS (TURBULENT APPROXIMATION).

The GPSD developed in Section 2 has the form given by Equation 2-102 which is reproduced here:

$$S(\vec{K}_\perp, \tau, \omega_D) = S_D(\omega_D) S(\vec{K}_\perp, \tau) \quad .$$

(2-102)

Under the turbulent approximation, the Doppler frequency spectrum $S_D(\omega_D)$ is independent of the angular-delay part of the GPSD $S(\vec{K}_\perp, \tau)$. The Doppler frequency spectrum and therefore the decorrelation time of the signal is then the same for any angle and any delay.

Two techniques for generating realizations of the impulse response function under the turbulent approximation will be discussed in this section. The first technique is a generalization of the technique used for frozen-in approximation realizations and is valid for appropriately chosen large but finite values of the parameter α. The second technique, proposed by Wittwer (1985), is valid only for infinite values of α. However, for reasons described in Section 2.8.1, this limitation does not reduce the usefulness of Wittwer's technique. Indeed, it has the advantage of requiring less computer storage and cpu time to generate realizations than are required with the first technique. Both techniques are somewhat different than that described in Section 5.1.

5.2.1 Finite α Technique.

The starting point of this generation technique is Equation 5-8 which is rewritten as

94

$$\bar{h}_A(k\Delta K_x, l\Delta K_y, \tau_j, t_n) = (4\pi^2/\Delta K_x \Delta K_y \Delta\tau)\xi_{k,l,j}(t_n)\sqrt{\overline{E_{k,l,j}}} \qquad (5\text{-}26)$$

where t_n are discrete times for which the impulse response functions will be calculated. The temporal variation of the impulse response function is given by the temporal variation of the random numbers $\xi_{k,l,j}(t_n)$. These random numbers must still satisfy the conditions given by Equation 5-9. The grid sizes ΔK_y and $\Delta\tau$ are calculated using the criteria given in Sections 5.1.3.2 and 5.1.3.3 respectively. The grid size ΔK_x for this model is chosen using the same arguments that were used to select ΔK_y. That is, the number N_x of K_x grid points is first chosen to be 32 and then Equations 5-21 and 5-22 (with y replaced by x) are used to calculate ΔK_x.

The impulse response functions at the outputs of multiple antennas are calculated in a manner similar to that outlined in Section 5.1.2. At a given time, the impulse response function for the mth antenna, with center coordinates x_m and y_m, is calculated from $\bar{h}_A$ using a two dimensional Fourier transform. In continuous notation,

$$h_{A,m}(t,\tau) = (2\pi)^{-2} \int_{-\infty}^{\infty} dK_x \int_{-\infty}^{\infty} dK_y \exp(iK_x x_m + iK_y y_m)\, \bar{h}_A(t, K_x, K_y, \tau) . \qquad (5\text{-}27)$$

The discrete equivalent of this equation is

$$\bar{h}_{A,m}(\tau_j, t_n) = (\Delta K_x \Delta K_y / 4\pi^2) \times$$

$$\sum_{k=-N_x/2}^{N_x/2-1} \sum_{l=-N_y/2}^{N_y/2-1} \exp(ik\Delta K_x x_m + il\Delta K_y y_m)\, \bar{h}_A(k\Delta K_x, l\Delta K_y, \tau_j, t_n) . \qquad (5\text{-}28)$$

This operation is repeated for each set of unique antenna center coordinates and then for each delay.

At the next time step $t_{n+1} = t_n + \Delta t$ (where $\Delta t = \tau_0/N_0$), the random numbers $\xi_{k,l,j}$ are recalculated according to the Doppler frequency spectrum. A convenient form for the Doppler spectrum is an f^{-4} power spectrum because it can be readily synthesized using two-pole low-pass filters. The noise sample $\xi_{k,l,j}(t_{n+1})$ can then be obtained directly from $\xi_{k,l,j}(t_n)$ and a complex white Gaussian noise sample. Once the noise samples ξ have been updated, the impulse response functions at time t_{n+1} are calculated using the above equations.

5.2.2 Infinite α Technique.

This technique will utilize the delta function relationship between angle and delay given by Equation 3-47 for the infinite α limit. For the jth delay bin, the GPSD will be non-zero only for the angles that satisfy the condition

$$\omega_{coh}(\tau_j - \Delta\tau/2) \leq \Lambda(K_x^2 + K_y^2)\lambda_0^2/4 < \omega_{coh}(\tau_j + \Delta\tau/2) \quad . \tag{5-29}$$

In this limit, ω_{coh} is related to the frequency selective bandwidth as

$$\omega_{coh} = 2\pi f_0 \quad . \tag{5-30}$$

The impulse response function may now be generated in the angular domain without regard to delay. Once this has been done, Equation 5-29 may be used to assign an annulus in the $K_x - K_y$ plane to each delay bin.

The starting point for this technique is then the energy in a $K_x - K_y$ grid cell:

$$E_{k,l} = (2\pi)^{-2} \int_{(k-1/2)\Delta K_x}^{(k+1/2)\Delta K_x} dK_x \int_{(l-1/2)\Delta K_y}^{(l+1/2)\Delta K_y} dK_y \; G(K_x, K_y) S(K_x K_y) \tag{5-31}$$

where the angular power spectral density is

$$S(K_x, K_y) = \int_{-\infty}^{\infty} S(K_x, K_y, \tau) d\tau$$

$$= (\tau \ell_0^2 / \delta) \exp\left[-(K_x^2 \ell_0^2 / 4) - (K_y^2 \ell_0^2 / 4\delta^2)\right] \qquad (5\text{-}32)$$

The random angular spectrum of the signal at discrete time t_n is rewritten from Equation 5-26 as

$$\bar{h}_A(k\Delta K_x, l\Delta K_y, t_n) = (4\pi^2 / \Delta K_x \Delta K_y) \xi_{k,1}(t_n) \sqrt{\overline{E_{k,1}}} \qquad . \qquad (5\text{-}33)$$

For the jth delay bin, the Fourier transform of the impulse response function at time t_n is

$$\bar{h}_A(k\Delta K_x, l\Delta K_y, \tau_j, t_n) = \begin{cases} \bar{h}_A(k\Delta K_x, l\Delta K_y, t_n)/\Delta\tau & , \text{ if Equation 5-29} \\ \\ 0 & , \text{ otherwise } . \end{cases} \qquad (5\text{-}34)$$

The impulse response functions at the outputs of multiple antennas are then generated from $\bar{h}_A(k\Delta K_x, l\Delta K_y, \tau_j, t_n)$ using Equation 5-28.

The savings in computer resources between this technique and that described in Section 5.2.1 is the result of the fact that only the random angular spectrum instead of the random angular-delay spectrum is required at each discrete time for the latter technique. Thus $E_{k,1}$ is stored rather than $E_{k,1,j}$ and at each discrete time the random numbers $\xi_{k,1}(t_n)$ are updated and stored rather than $\xi_{k,1,j}(t_n)$.

For this technique, the mean signal power in the grid is

$$P_G = \sum_k \sum_1 E_{k,1} \qquad (5\text{-}35)$$

and the mean power in the jth delay bin is

$$P_j = \int_{\tau_j - \Delta\tau/2}^{\tau_j + \Delta\tau/2} G_A(\tau')d\tau' \qquad (5\text{-}36)$$

where $G_A(\tau)$ is the power impulse response function given in Equation
3-48. For general anisotropic scattering and antennas, this integral must
be performed numerically.

5.3   REALIZATION PARAMETERS.

A check can be made of the generated realizations of the impulse
response function by computing the mean signal power in the grid, scatter-
ing loss, frequency selective bandwidth, x direction decorrelation dis-
tance, and the cross correlation between antennas and then by comparing
these quantities with their ensemble values which are given in Section
3.2. The realization signal power in each delay bin may also be compared
with the ensemble values to ensure that the realization has the proper
delay distribution of signal energy. For reasons discussed below, this is
often a better check than comparing the realization and ensemble frequency
selective bandwidths.

Because each realization contains a finite number of decorrela-
tion distances or times, the agreement between the realization parameters
and the ensemble values will not be exact. In addition, the realization
parameters will also vary from antenna to antenna. However, as the reali-
zations are made longer in distance (i.e. N_x is increased while N_o is kept
fixed) the agreement will improve.

An exception to this is the frequency selective bandwidth which
requires both a long realization in distance or time and a fine gridding
in delay to make an accurate measurement. In particular, if the delay

98

grid size $\Delta\tau$ is chosen so there are only a few delay bins encompassing the delay spread of the signal, then the measurement of the time delay jitter will be limited by the delay grid size. The resulting frequency selective bandwidth, which is computed from the time delay jitter, will be inaccurate. An accurate measurement of the frequency selective bandwidth requires on the order of 20 to 30 delay bins in the delay region which encompasses 95 percent of the signal power (see Equation 5-21). Because the delay sample size $\Delta\tau$ is often chosen on the basis of a channel symbol period rather than to achieve an accurate measurement of the frequency selective bandwidth, a comparison of the signal power in each delay bin with the ensemble values may be a better check that the realization has the proper delay distribution.

The accuracy with which the GPSD is evaluated can be checked by computing the mean power P_G in the K_x - K_y - τ grid (Equation 5-3 or 5-35). The mean power out of an antenna should be equal to $1/L_S$ where L_S is the ensemble scattering loss of the antenna. The difference in the values of P_G and $1/L_S$ is equal to the amount of delayed signal power that is not included in the delay grid if the integrals involved in the evaluation of the mean signal power in each grid cell are done with sufficient accuracy. If the minimum delay criterion given by Equation 5-21 is met, then these two values should agree to within a few percent.

The following subsections describe the algorithms used to measure the realization parameters.

5.3.1   Scattering Loss.

The mean power of the realizations will be, in general, less than unity because of the signal attenuation caused by the antenna beam profile. The difference between the mean power of the realization and unity is equal to the scattering loss. The steps for computing the scattering loss of a realization are as follows:

99

1. Compute the impulse response function integrated over all signal delays. In continuous notation, this is

$$h_{A,m}(x) = \int_{-\infty}^{\infty} h_{A,m}(x,\tau)d\tau \quad . \tag{5-37}$$

This integral is evaluated in the channel simulator as

$$h_{A,m}(k\Delta x) = \Delta\tau \sum_{j} h_{A,m}(k\Delta x, j\Delta\tau) \tag{5-38}$$

where the sum is over all delay bins. The quantity $h_{A,m}(k\Delta x)$ represents the voltage that would be received by the antenna under flat fading conditions (e.g. when the transmitted modulation is turned off).

2. The power P_m of the impulse response function is averaged over the realization:

$$P_m = (1/N_x) \sum_{k=1}^{N_x} \left| h_{A,m}(k\Delta x) \right|^2 \quad . \tag{5-39}$$

3. The scattering loss in dB is computed for the mth antenna:

$$L_{S,m} = -10 \log_{10}(P_m) \quad . \tag{5-40}$$

5.3.2 Frequency Selective Bandwidth and Delay Distribution.

The frequency selective bandwidth is computed by calculating the time delay jitter of the signal. Sufficient delay resolution is required to do this computation accurately. The realization delay distribution is given by the mean power of the jth delay bin. These values may be compared with the approximate ensemble values given by Equation 5-3 or 5-36. The algorithms for computing the frequency selective bandwidth and the delay distribution are as follows:

1. Calculate the first two moments of delay:

$$P_m\langle\tau^n\rangle = (1/N_x) \sum_k \sum_j (j\Delta\tau)^n \left|\Delta\tau h_{A,m}(k\Delta x, j\Delta\tau)\right|^2 \quad . \quad (5\text{-}41)$$

This is evaluated for $n=1$ and for $n=2$.

2. The time delay jitter is

$$\sigma_\tau = \left[\langle\tau^2\rangle - \langle\tau\rangle^2\right]^{1/2} \quad . \quad (5\text{-}42)$$

3. The frequency selective bandwidth of the realization is computed from σ_τ as

$$f_{A,m} = 1/(2\pi\sigma_\tau) \quad . \quad (5\text{-}43)$$

4. Calculate the mean power in the jth delay bin:

$$P_{j,m} = (1/N_x) \sum_k \left|\Delta\tau h_{A,m}(k\Delta x, j\Delta\tau)\right|^2 \quad . \quad (5\text{-}44)$$

5.3.3 X Direction Decorrelation Distance or Time.

The x direction decorrelation distance or the decorrelation time is computed by finding the 1/e point of the autocorrelation function of the impulse response function. The algorithm used to compute the decorrelation distance or time is:

1. Calculate the power spectrum of the realization. In continuous notation this is

$$S_m(K_x) = \left|(1/L_x) \int_{-L_x/2}^{L_x/2} h_{A,m}(x) \exp(-iK_x x)dx\right|^2 \quad (5\text{-}45)$$

where x is replaced by t to compute the decorrelation time. The discrete equivalent of this equation is

101

$$S_m(k\Delta K_x) = \left|(1/N_x) \sum_{k'} h_{A,m}(k'\Delta x) \exp(-ik\Delta K_x k'\Delta x)\right|^2. \quad (5-46)$$

2. Next calculate the autocorrelation function as the Fourier transform of the power spectrum. In continuous notation,

$$P_0 \rho_m(x) = \int_{-\infty}^{\infty} S_m(K_x) \exp(iK_x x)dK_x \quad (5-47)$$

and in discrete notation

$$P_0 \rho_m(k\Delta x) = (\Delta K_x/2\pi) \sum_{k'} S_m(k'\Delta K_x) \exp(ik'\Delta K_x k\Delta x) \quad (5-48)$$

where

$$P_0 = (\Delta K_x/2\pi) \sum_{k'} S_m(k'\Delta K_x) \quad . \quad (5-49)$$

3. Finally, find the value of $\ell_{A,x}$ or τ_A where

$$\rho_m(\ell_{A,x}) = \rho_m(\tau_A) = 1/e \quad . \quad (5-50)$$

5.3.4   Cross Correlation Between Antennas.

The x direction spatial correlation properties of the realizations may be verified by computing the x direction decorrelation distance and comparing with the ensemble value. Another important and measurable quantity is the cross correlation of the realizations of two antennas.

The algorithm for measuring the antenna cross correlation is

$$\rho_A(m,n) = \sum_{k=1}^{N_x} h_{A,m}(k\Delta x)h_{A,n}^*[(k+k_s)\Delta x]/[N_x\sqrt{\overline{P_m P_n}}] \quad (5-51)$$

102

where k_s, the relative index of the two antenna centers, is given by

$$k_s = (x_n - x_m)/\Delta x \quad . \tag{5-52}$$

Here x_n and x_m are the relative x coordinates for the antenna centers.

5.4 EXAMPLES.

In this section, examples are presented of the channel simulation techniques outlined in Section 5.1. First a comparison is made between the ensemble signal parameters and the values obtained from random realizations of the impulse response function at the output of an antenna. These results show that the random realizations do indeed have signal parameter values that are close to the ensemble values. Then some examples of the voltage amplitude at the output of a matched filter to a transmitted square pulse are shown to illustrate some of the effects and techniques that have been discussed in this report. It is assumed in this section that mean ionization or dispersive effects are negligible in comparison to stochastic diffraction effects. It is further assumed that the penetration angle is zero so the scattering is isotropic about the line-of-sight.

5.4.1 Signal Parameters of Random Realizations.

The signal parameters at the outputs of the square, Gaussian antennas without pointing errors and without sidelobes are considered here. The random realizations of the impulse response function were generated at the outputs of two antennas whose centers are displaced by the distance D where D is the length of a side of one antenna. The rotation angle was chosen to be 45°. The configuration is similar to that depicted in Figure 5-1 except that there are only two arrays rather than the three shown in the figure. The algorithms presented in Section 5.3 were then used to compute the realization signal parameters.

Under these conditions, Equations 3-55 give the ensemble scattering loss, ℓ_A/ℓ_o, and f_A/f_o. The cross correlation of the impulse response functions out of the two antennas is, from Equation 3-40,

$$\rho_A = \exp\left[-(D/\ell_o)^2(\ell_o/\ell_A)^2\right] \quad . \tag{5-53}$$

Figure 5-3a through 5-3d present, respectively, the ensemble (solid lines) and realization (dots) values of the scattering loss, frequency selective bandwidth, x-direction decorrelation distance, and the voltage cross correlation ρ_A of the impulse response functions at the outputs of the two antennas. Except for the cross correlation, the realization values plotted are the average of the values for the two antennas.

Because of the finite length of the realizations, the agreement between the realization values and the ensemble values is not exact. However, over the range of D/ℓ_o shown from 0.1 to 5, the agreement of the scattering loss and the ratio f_A/f_o with the ensemble values is quite good. Somewhat more scatter about the ensemble values is seen in the values of the ratio ℓ_A/ℓ_o and the cross correlation function. The ratio ℓ_A/ℓ_o appears to be biased to the high side which is attributed to the linear interpolation algorithm used to solve Equation 5-50 for the 1/e point of the realization autocorrelation function.

5.4.2   Received Voltage.

This final section presents examples of the received voltage out of an integrate and dump filter that is matched to a transmitted square pulse. These examples are intended to illustrate the effects of frequency selectivity and antenna filtering on a transionospheric communications link and to illustrate the differences in the structure of the received signal depending on whether the frozen-in or turbulent approximation is
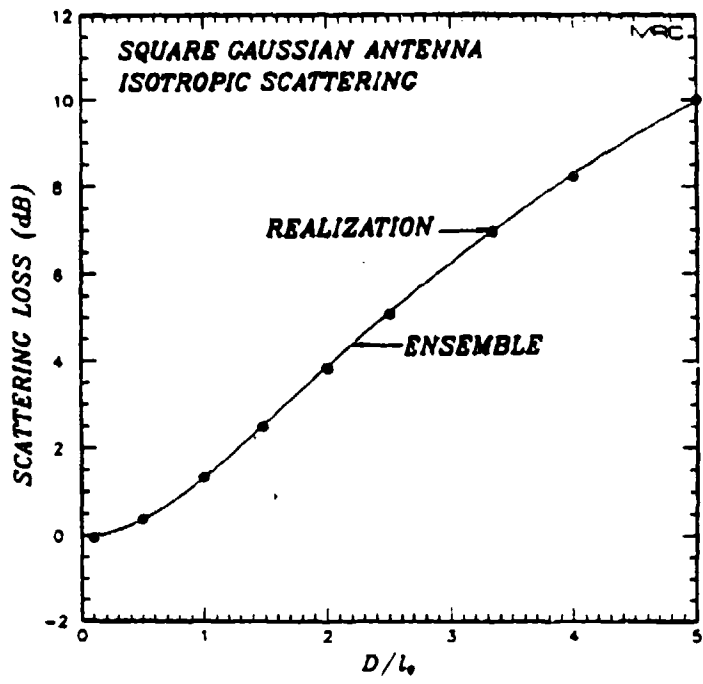
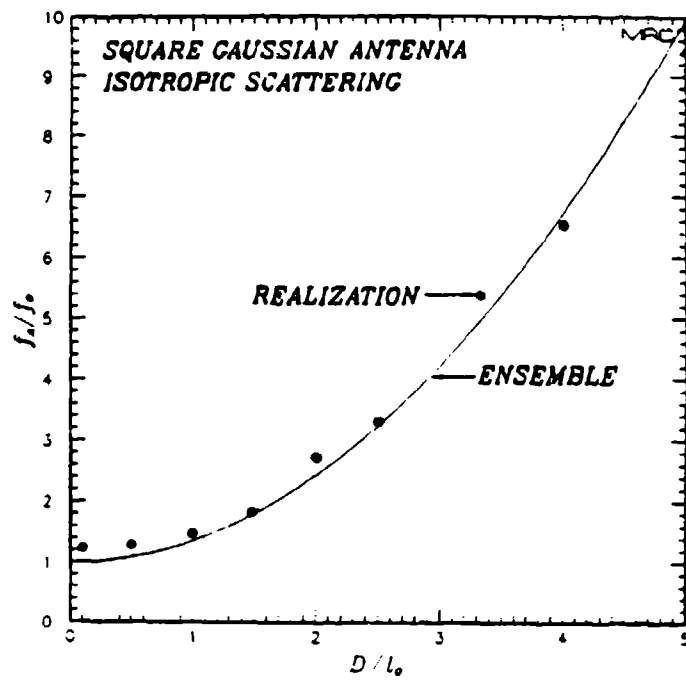Figure 5-3a. Realization and ensemble scattering loss.
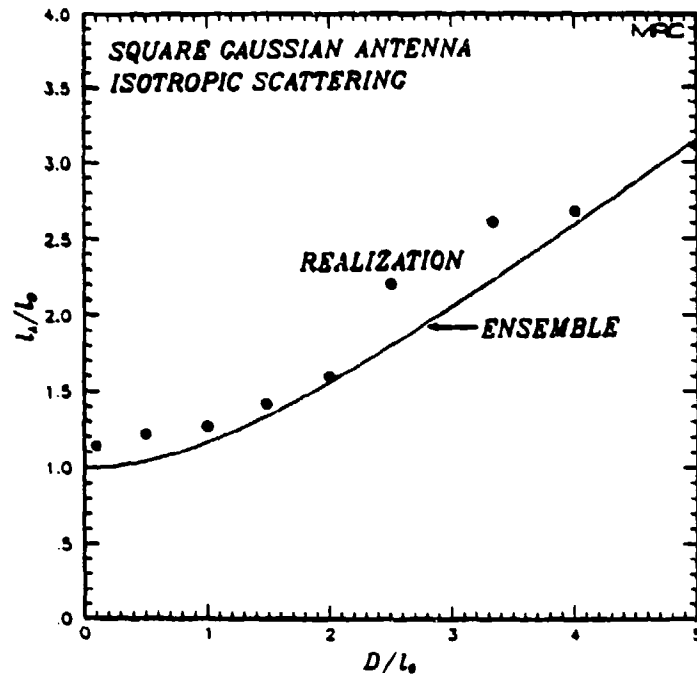

Figure 5-3b. Realization and ensemble values of f_A/f_o.

105

Figure 5-3c. Realization and ensemble values of ℓ_A/ℓ_o.
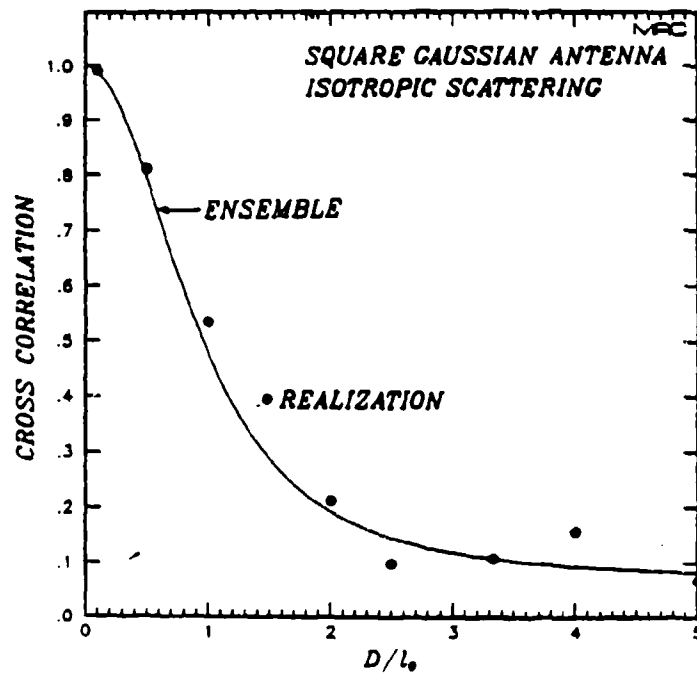

Figure 5-3d. Realization and ensemble values of ρ_A.

106

used to generate the impulse response function realizations. The follow-
ing calculation will also illustrate how the received voltage can be con-
structed from the impulse response function realizations in a digital sim-
ulation of the link. Additional examples for specific system applications
may be found in Bogusch, et al. (1981) and in Bogusch, Guigliano, and
Knepp (1983).

The received time-varying, complex voltage from a transmitted
impulse under conditions where the mean ionization effects are negligible
is given by the inverse of Equation 2-103:

$$U(\omega+\omega_0,t) = \int_{-\infty}^{\infty} h(\tau,t) \exp(-i\omega\tau)d\tau \qquad (5\text{-}54)$$

where $h(\tau,t)$ is the impulse response function and ω_0 is the carrier fre-
quency. The quantity $U(\omega+\omega_0,t)$ then represents the voltage at a relative
frequency ω out of an antenna at time t. For a transmitted square pulse
with a chip duration T_c, the voltage out of the matched filter at time t
can be written as

$$e(\tau,t) = (1/2\pi) \int_{-\infty}^{\infty} M(\omega)U(\omega+\omega_0,t) \exp(i\omega\tau)d\omega \qquad (5\text{-}55)$$

where τ is the relative time delay of the matched filter and where

$$M(\omega) = T_c\sin^2(\omega T_c/2)/(\omega T_c/2)^2 \qquad (5\text{-}56)$$

is the combined spectrum of the square pulse and the matched filter.

In an actual simulation, these two integrals are performed at
baseband ($\omega_0=0$) and must be performed discretely. If the impulse response
function is generated with N_D delay samples of size $\Delta\tau$, then the dis-
crete frequency domain voltage at time t is

$$U(k\Delta\omega,t) = \sum_{j=0}^{N_D-1} \Delta\tau h(j\Delta\tau,t) \exp\left[-ik\Delta\omega(\tau_s+j\Delta\tau)\right] \qquad (5\text{-}57)$$

where $\Delta\omega = 2\pi/N_D\Delta\tau$. Here the delay τ_s defines the start of the delay grid upon which the impulse response function is generated (Equation 5-1). However this delay may be ignored at this point because it will be accounted for when the received voltage is constructed. The range of the index k in this equation is from 0 to N_D-1 so the range of frequencies represented is from 0 to $(N_D-1)\Delta\omega$. The zero frequency of $U(k\Delta\omega,t)$ must correspond to the smallest frequency of $M(\omega)$ within the receiver bandwidth. The discrete received voltage is then given by

$$e(\tau,t) = (\Delta\omega T_c/2\pi) \sum_{k=0}^{N_D-1} \frac{\sin^2\left[(k-N_D/2)\Delta\omega T_c/2\right]}{\left[(k-N_D/2)\Delta\omega T_c/2\right]^2} U(k\Delta\omega,t) \exp\left[ik\Delta\omega(\tau-\tau')\right] .$$
$$(5\text{-}58)$$

If $\Delta\tau$ is chosen to be $T_c/2$, then $\Delta\omega T_c/2 = 2\pi/N_D$ and $e(\tau,t)$ represents a signal that is band-limited to the frequency range $-1/T_c$ to $+1/T_c$. Note also that $e(\tau,t)$ is unambiguous in delay only over the interval from 0 to $(N_D-1)\Delta\tau$. The arbitrary starting delay τ' is included in Equation 5-49 to account for the delay τ_s which may have been ignored in Equation 5-48 and to ensure that $e(\tau,t)$ is not aliased in delay.

In the examples that follow, the random realizations of the impulse response function were generated with a delay sample size of $T_c/2$ and with 32 delay samples. The chip rate $R_c = 1/T_c$ was set at 1 MHz. However, the frequency selective effects depend only on the ratio of the frequency selective bandwidth to the chip rate f_0/R_c. Then the voltage out of a matched filter was calculated from the impulse response functions using Equations 5-48 and 5-49. The amplitude of this voltage is plotted as a function of the delay of the matched filter and as a function of time.

108

The effect of frequency selectivity on the received voltage amplitude is shown in the next set of figures. The impulse response functions used for these signals were generated using the frozen-in approximation and an omnidirectional antenna. Delay in chips is plotted on the abscissa of the figures and time or antenna position is directed into the figure. The total time duration of the plots is $10 \tau_0$.

The signal in Figure 5-4a where $f_0/R_c = 1.0$ clearly shows the effect of signal fading as the peak amplitude rises and falls with time. The matched filter output in the figure is somewhat rounded rather than being a triangle because the signal is band-limited to the frequency range between the first nulls of the transmitted spectrum. Some minor distortion of the output waveform is seen but for the most part the signal is contained within the period of one transmitted symbol. For this channel the fading is nearly flat which means that all frequency components within the signal bandwidth propagate essentially the same way through the disturbed ionosphere and there is very little time delay spreading of the received signal.

Figure 5-4b shows a signal generated with $f_0/R_c = 0.5$. The impulse response function of this signal was generated using the same set of random numbers and the same angular-delay grid that was used for the impulse response function of the signal in the previous figure. The only difference in the two impulse response functions is the distribution of signal energy within the delay bins. Thus there is strong correlation in the signal structures seen in the two figures. For this smaller value of the frequency selective bandwidth, more of the signal energy is arriving at longer delays. There is one time about three quarters of the way into the figure where there are two distinct peaks in the matched filter output amplitude. It is these sort of structures that can cause delay tracking algorithms in receivers to lose lock and that cause intersymbol interference which can degrade demodulation performance.
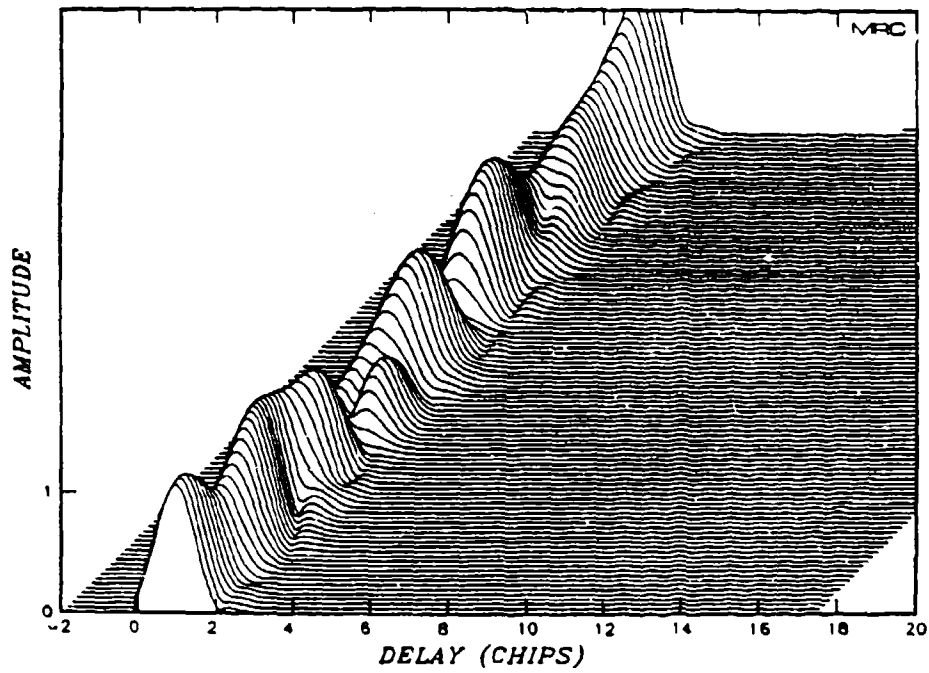
109

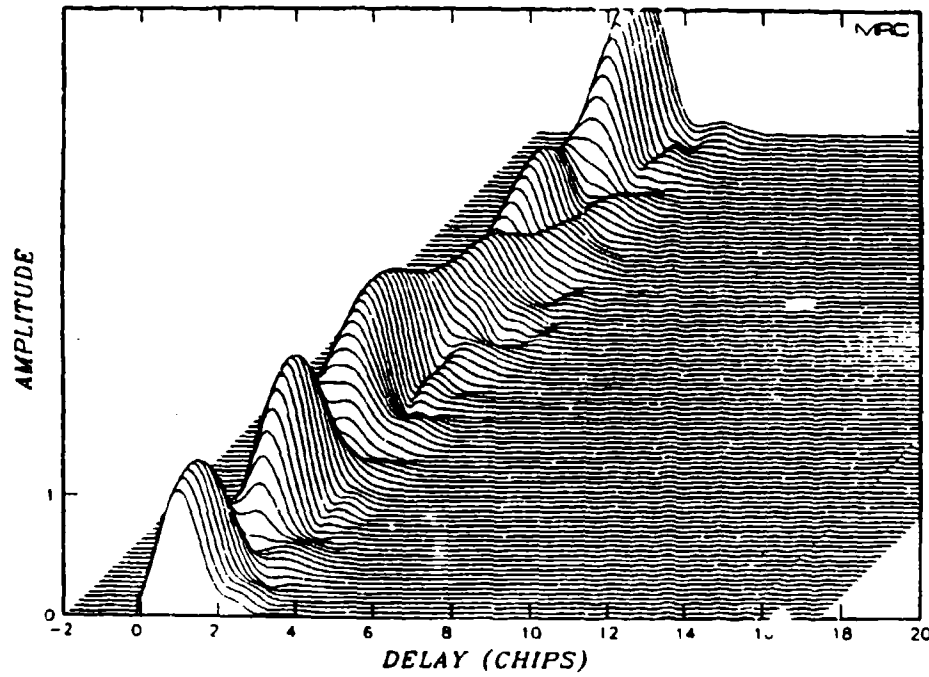Figure 5-4a. Matched filter output amplitude for $f_0/R_C = 1.0$.

Figure 5-4b. Matched filter output amplitude for $f_0/R_C = 0.5$.

110

The matched filter output amplitudes for f_0/R_c equal to 0.2 and 0.1 are shown in Figures 5-4c and 5-4d respectively. The signals in these figures are much more distorted than the signals in the previous two figures with the signal energy being spread out over multiple chips. This amount of multipath delay spread produces severe intersymbol interference and reduces the amplitude out of the matched filter at a given delay.

Another effect that is evident in these signals is that the signal received at long delays varies more rapidly in time than the signal received at shorter delays. This is a result of the frozen-in approximation. Figure 5-5 shows a signal with $f_0/R_c = 0.1$ whose impulse response function was generated using the turbulent approximation. Again 10 decorrelation times of the signal are plotted. It should be remembered when comparing the signals in Figure 5-4d and 5-5 that the Doppler spectrum has a Gaussian form for the frozen-in approximation and an f^{-4} form for the turbulent approximation. It is this fact that accounts for the more spikey appearance of the turbulent approximation signal. Also the impulse response function generation techniques are sufficiently different so there is no correlation between features seen in the two figures. The thing to note about the turbulent approximation signal is that the features at long and short delays have the same decorrelation time.

Finally, the effect of an antenna on the received signal amplitude is shown in the last set of figures. The impulse response functions used for these signals were generated using the frozen-in approximation and a square Gaussian antenna. As is the case for all signals plotted in this section, the scattering is isotropic about the line-of-sight. All of these signals have the ratio f_0/R_c set at 0.1 while the ratio D/λ_0 is varied. Again the signal amplitude out of the matched filter is plotted versus delay with time directed into the figure. The total time duration of the plots is 10 τ_0.
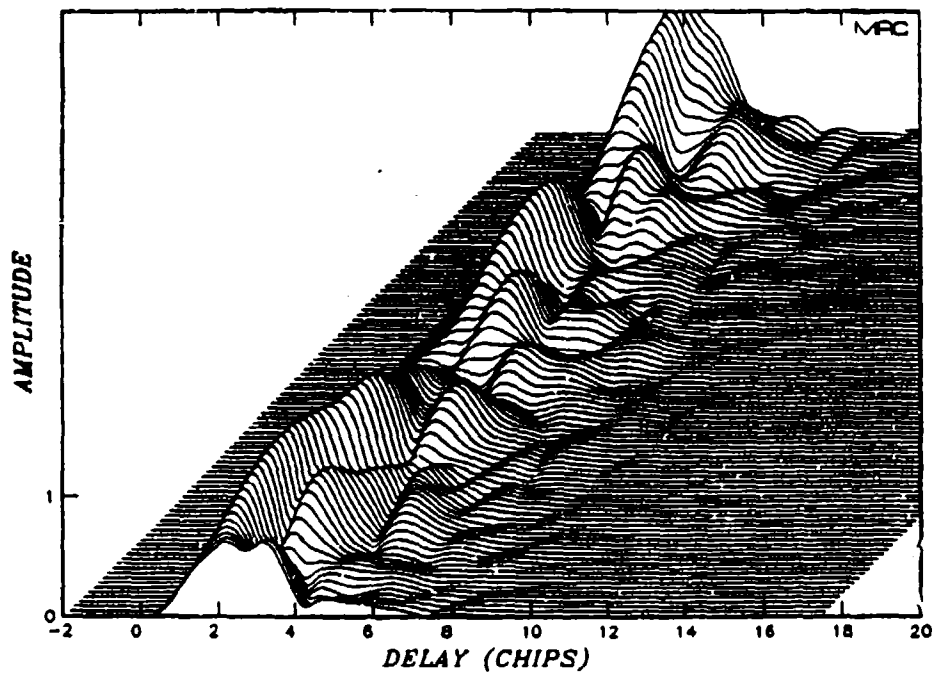
111

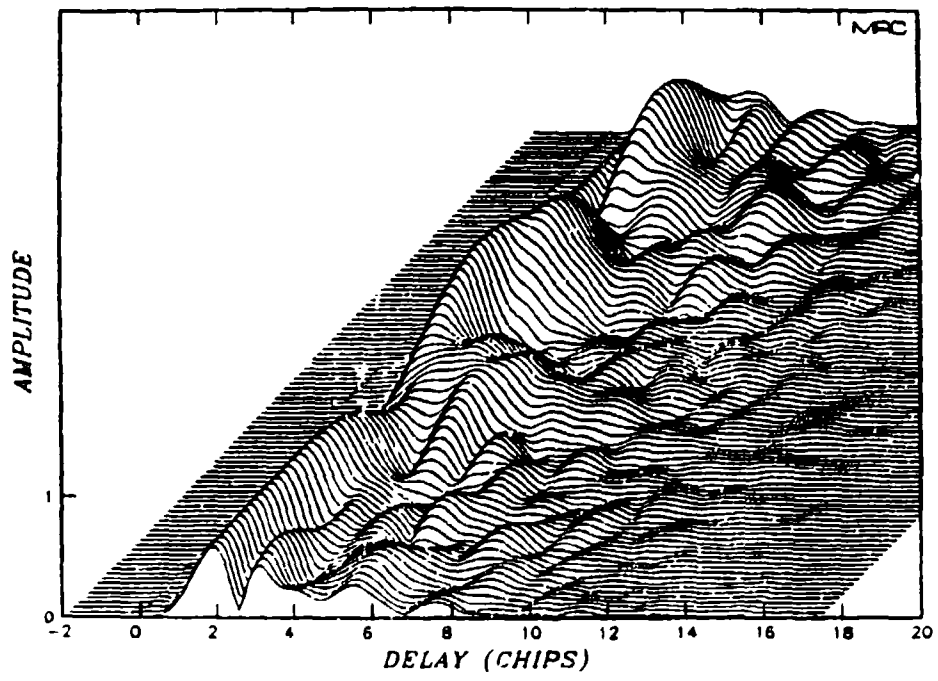Figure 5-4c. Matched filter output amplitude for $f_0/R_c = 0.2$.

Figure 5-4d. Matched filter output amplitude for $f_0/R_c = 0.1$.
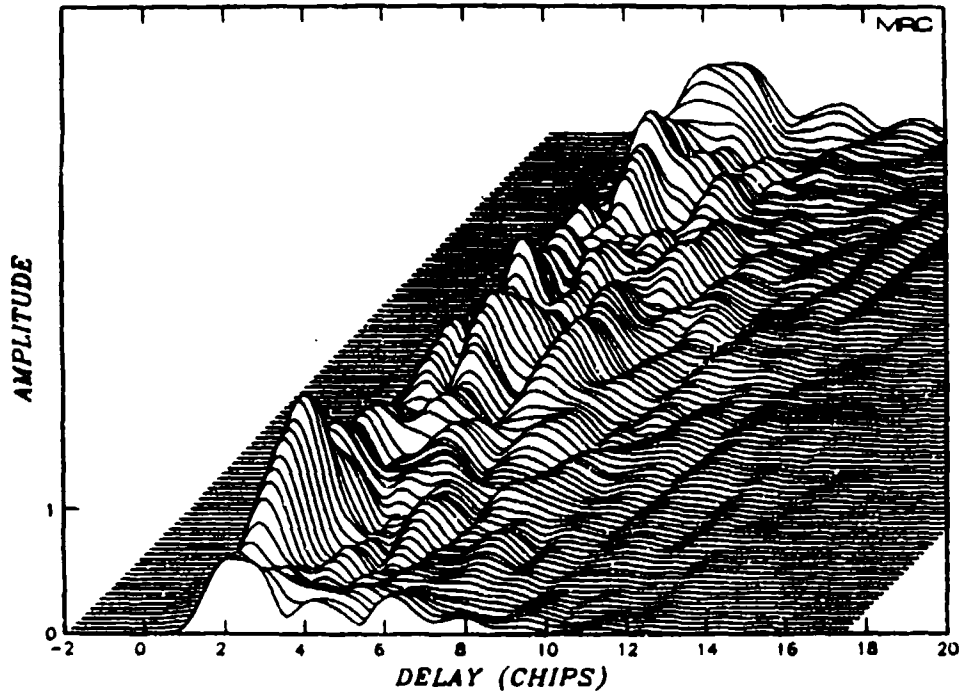
112

Figure 5-5. Matched filter output amplitude for a signal generated using the turbulent approximation ($f_0/R_c = 0.1$).

Figure 5-6a shows the matched filter output amplitude for a Gaussian square antenna with $D/\ell_0 = 0.5$. For this antenna and isotropic scattering, the ensemble scattering loss is 0.4 dB. This signal is not identical to that shown in Figure 5-4d, although similarities can be seen, because of the antenna filtering and because the angular-delay grid sizes depend on the ensemble signal parameters at the antenna output. Figures 5-6b through 5-6d show respectively the matched filter output amplitude for D/ℓ_0 equal to 1.0 (ensemble scattering loss equal to 1.3 dB), 2.0 (ensemble scattering loss equal to 3.9 dB), and 5.0 (ensemble scattering loss equal to 10.0 dB).

The effects of an antenna on the signal parameters are readily apparent from these figures as the ratio D/ℓ_0 is reduced. The signal
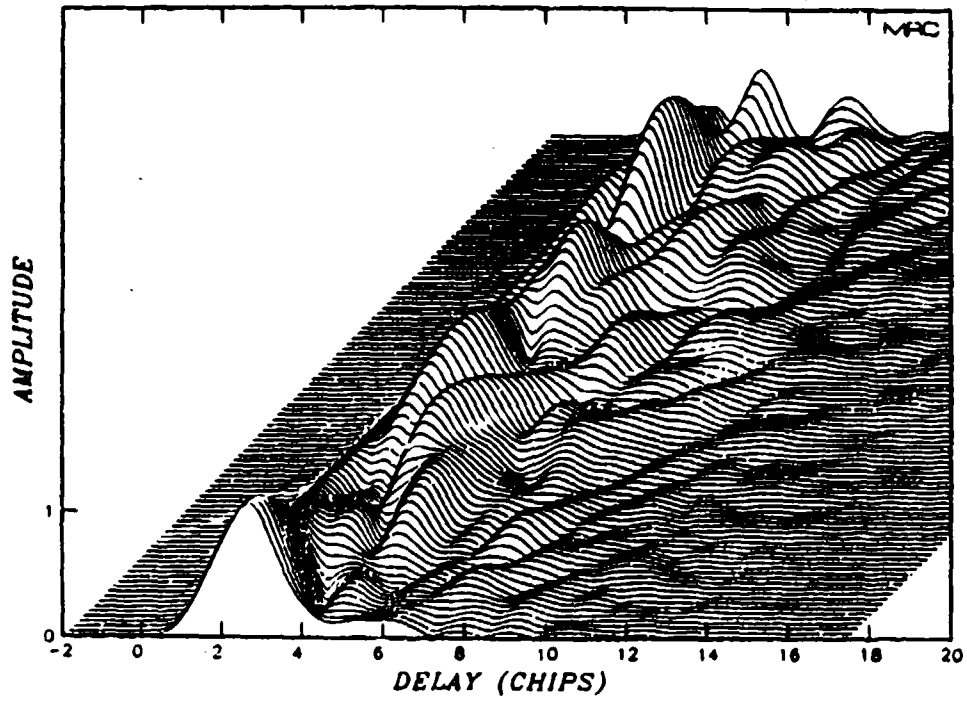
113

Figure 5-6a. Matched filter output amplitude for $D/\lambda_0 = 0.5$.
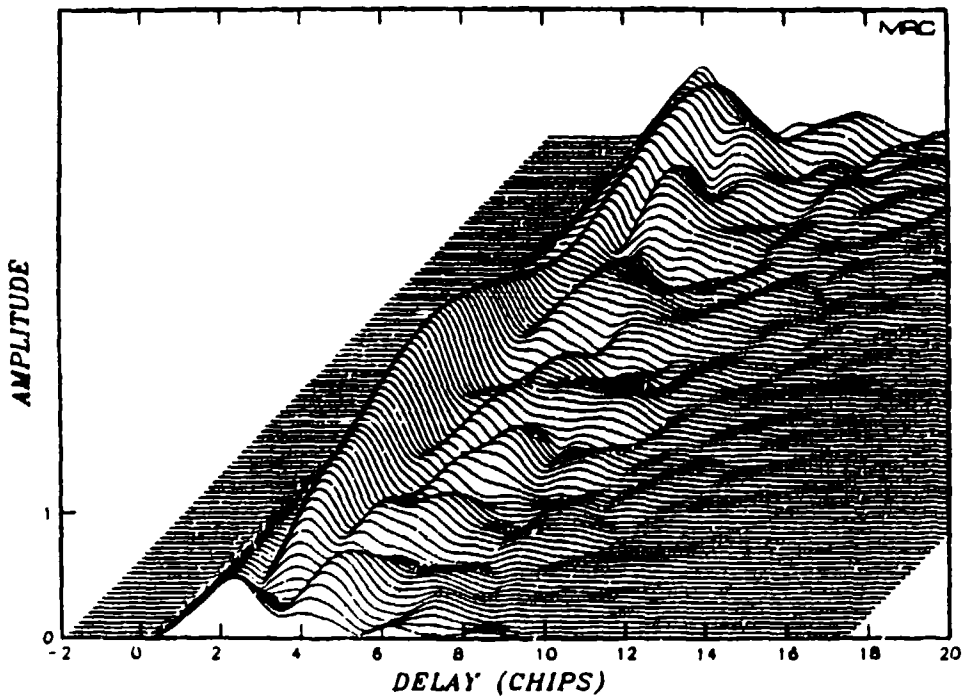
Figure 5-6b. Matched filter output amplitude for $D/\lambda_0 = 1.0$.

114
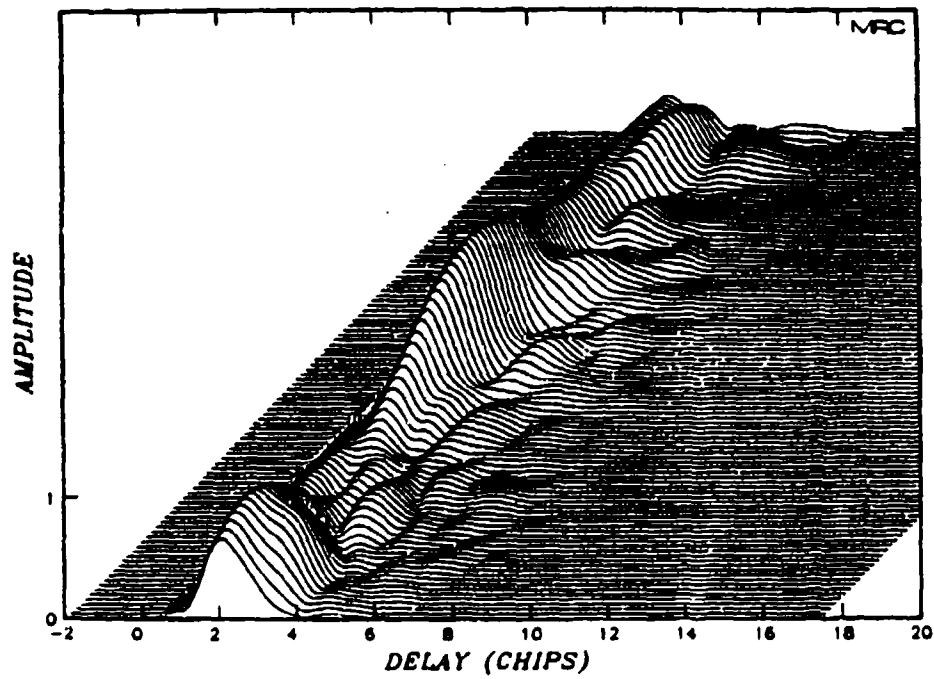
Figure 5-6c. Matched filter output amplitude for $D/\ell_0 = 2.0$.
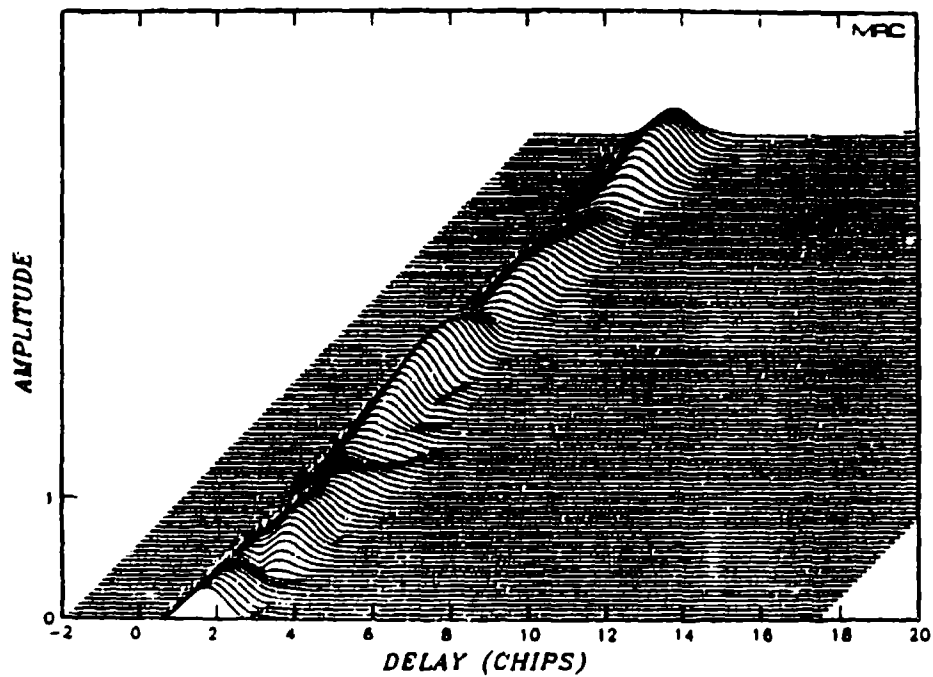
Figure 5-6d. Matched filter output amplitude for $D/\ell_0 = 5.0$.

115

energy arriving at longer delays is preferentially suppressed by the antenna. For D/ℓ_0 equal to 5.0, the output signal looks almost flat with very little distortion of the matched filter output. However, the output signal amplitude is 10 dB smaller on the average than it was without antenna filtering. Also, the decorrelation time or distance of the signals is seen to increase as the antenna filtering increases.

SECTION 6
LIST OF REFERENCES

Arendt, P. R., and H. Soicher, "Effects of Arctic Nuclear Explosions on Satellite Radio Communication," Proc. IEEE, Vol. 52, No. 6, pp. 672-676, June 1964.

Bogusch, R. L., F. W. Guigliano, D. L. Knepp, and A. H. Michelet, "Frequency Selective Propagation Effects on Spread-Spectrum Receiver Tracking," Proc. IEEE, Vol. 69, No. 7, pp. 787-796, July 1981.

Bogusch, R. L., F. W. Guigliano, D. L. Knepp, "Frequency Selective Scintillation Effects and Decision Feedback Equalization in High Data-Rate Satellite Links," Proc. IEEE, Vol. 71, No. 6, pp. 754-767, June 1983.

Dana, R. A., Beam Profile Loss Due to Angle-of-Arrival Fluctuations, MRC-N-497, Mission Research Corporation, August 1981.

Dana, R. A., Temporal Statistics of Scintillation for Satellite Communication and Radar Systems, DNA-TR-81-129, MRC-R-692, Mission Research Corporation, April 1982.

Davis, T. N., G. J. Romick, E. M. Westcott, R. A. Jeffries, D. M. Kerr, and H. M. Peek, "Observations of the Developmment of Striations in Large Barium Clouds," Planet. Space Science, Vol. 22, p. 67, 1974.

Ishimaru, A., Wave Propagation and Scattering in Random Media, Academic Press, New York, 1978.

King, M. A., and P. B. Fleming, "An Overview of the Effets of Nuclear Weapons on Communications Capabilities," Signal, pp. 59-66, January 1980.

Knepp, D. L., Propagation of Wide Bandwidth Signals Through Strongly Turbulent Ionized Media, DNA-TR-81-78, MRC-R-671, Mission Research Corporation, March 1982.

Knepp, D. L., The Effect of Aperture Antennas After Propagation Through Anisotropic Ionized Media, DNA-TR-81-254, MRC-R-744, Mission Research Corporation, March 1983(a).

Knepp, D. L., "Analytic Solution for the Two-frequency Mutual Coherence Function for Spherical Wave Propagation," Radio Science, Vol. 18, No. 4, pp. 535-549, July 1983(b).

Knepp, D. L., "Aperture Antenna Effects After Propagation Through Strongly Disturbed Random Media," IEEE Trans. Antennas Propagat., Vol. AP33, No. 10, pp. 1074-1084, October 1985.

LIST OF REFERENCES (Concluded)

Knepp, D. L. and L. A. Wittwer, "Simulation of Wide Bandwidth Signals That Have Propagated Through Random Media," Radio Science, Vol. 19, No. 1, pp. 303-318, January 1984.

Lee, L. C., and J. R. Jokipii, "Strong Scintillation in Astrophysics. I. The Markov Approximation, Its Validity and Application to Angular Broadening," Astrophys. J., Vol. 196, No. 3, pp. 695-707, March 1975(a).

Lee, L. C., and J. R. Jokipii, "Strong Scintillation in Astrophysics. II. A Theory of Temporal Broadening of Pulses," Astrophys. J., Vol. 201, No. 2, pp. 532-543, October 1975(b).

Tatarskii, V. I., The Effects of the Turbulent Atmosphere on Wave Propagation, translated by Isreal Program for Scientific Translations, National Technical Information Service, U.S. Department of Commerce, 1971.

Wittwer, L. A., Radio Wave Propagation in Structured Ionization for Satellite Applications, DNA 5304D, Defense Nuclear Agency, January 1979.

Wittwer, L. A., A Trans-Ionospheric Signal Specification for Satellite C^3 Applications, DNA 5662D, Defense Nuclear Agency, December 1980.

Wittwer, L. A., Radio Wave Propagation in Structured Ionization for Satellite Applications II, DNA-IR-82-02, Defense Nuclear Agency, August 1982.

Wittwer, L. A., Private Communication, 1985.

Wittwer, L. A., A Trans-Ionospheric Signal Specifiction for Satellite C^3 and Radar Applictions, DNA-IR-86-XXXX, Defense Nuclear Agency, in Preparation, 1986

Wolcott, J. H., D. J. Simons, T. E. Eastman, and T. J. Fitzgerald, "Characteristics of Late-Time Striations Observed During Operation STRESS," Effect of the Ionosphere on Space Terrestrial Systems, edited by J. M. Goodman, pp. 602-613, U. S. Government Printing Office, 1978.

Yek, K. C. and C. H. Liu, "An Investigation of Temporal Moments of Stochastic Waves," Radio Science, Vol. 12, No. 5, pp. 671-680, September 1977.

APPENDIX A
PHASE VARIANCE DUE TO ELECTRON DENSITY FLUCTUATIONS

A relationship between the phase variance imparted on the wave as it propagates through the ionization layer and the electron density fluctuations will be derived in this appendix. This relationship is given by Equation 2-51 which was derived using the Markov approximation. However, it will be shown here that the relationship requires only that the layer thickness be large compared to the decorrelation distance of the electron density fluctuations along the line-of-sight.

It was shown in Section 2 that the total phase change of the wave as it propagates through the ionization layer is

$$\phi = r_e \lambda \langle n_e \rangle \int \xi(\vec{\rho}, z, t) dz \quad . \tag{A-1}$$

The autocorrelation function of the phase fluctuations is then

$$\langle \phi(\vec{\rho}, t) \phi(\vec{\rho}'t') \rangle = (r_e \lambda \langle n_e \rangle)^2 \int_0^L dz \int_0^L dz' \ \langle \xi(\vec{\rho}, z, t) \xi(\vec{\rho}', z', t') \rangle \tag{A-2}$$

where L is the thickness of the scattering layer. For spatially and temporally stationary random electron density fluctuations, the expectation must be a function of the differences $\Delta\vec{\rho}$, $z-z'$ and Δt only. Denoting the autocorrelation of $\xi(\vec{\rho}, z, t)$ by $B_\xi(\Delta\vec{\rho}, z-z', \Delta t)$ and the autocorrelation of $\phi(\vec{\rho}, t)$ by $B_\phi(\Delta\vec{\rho}, \Delta t)$, Equation A-2 becomes

$$B_\phi(\Delta\vec{\rho}, \Delta t) = (r_e \lambda \langle n_e \rangle)^2 \int_0^L dz \int_0^L dz' \ B_\xi(\Delta\vec{\rho}, z-z', \Delta t) \quad . \tag{A-3}$$

119

This double integral may be reduced to a single integral by changing the order of integration with the result

$$B_\phi(\Delta\vec{\rho},\Delta t) = (r_e\lambda\langle n_e\rangle)^2 L \int_{-L}^{L} (1 - |z|/L)B_\xi(\Delta\vec{\rho},z,\Delta t)dz \quad . \qquad (A-4)$$

If the correlation distance of $B_\xi(\Delta\vec{\rho},z,\Delta t)$ along the z direction is small compared to L, then $B_\xi(\Delta\vec{\rho},z,\Delta t)$ will become small before $|z|/L$ approaches unity in the integral and the $|z|/L$ term may be ignored. The limits of the integral may then be set to $\pm\infty$ and the integral reduces to

$$B_\phi(\Delta\vec{\rho},\Delta t) = (r_e\lambda\langle n_e\rangle)^2 L \int_{-\infty}^{\infty} B_\xi(\Delta\vec{\rho},z,\Delta t)dz \quad . \qquad (A-5)$$

The remaining integral is denoted by $A(\Delta\vec{\rho},\Delta t)$ so the autocorrelation of the phase fluctuations is

$$B_\phi(\Delta\vec{\rho},\Delta t) = (r_e\lambda\langle n_e\rangle)^2 L \, A(\Delta\vec{\rho},\Delta t) \qquad (A-6)$$

which is the same as the final expression in Equation 2-51.

APPENDIX B
SIGNAL PARAMETERS FOR K^{-4} ELECTRON DENSITY FLUCTUATIONS

In this appendix, the expansion coefficients A_0 and A_2 are calculated using the quadratic approximation of the correlation function $A(\vec{\rho}_d)$ of the electron density fluctuations and using the delta layer approximation. From these coefficients, the phase variance, decorrelation distance, and the coherence bandwidth of the signal incident on the plane of the receiver are written in terms of physical parameters. However, these signal parameters are computed from a disturbed ionosphere model using the more general formalism of Wittwer (1979, 1980) which accounts for the finite thickness of the scattering region and other complicating effects. The purpose of this appendix is only to illustrate the dependence of the signal parameters on geometrical and electron density fluctuation parameters.

A power-law form of the PSD for the three dimensional electron density fluctuations is assumed:

$$\Phi_\xi(\vec{K}) = \frac{8\pi^{3/2} L_r L_s L_t \langle \Delta n_e^2 \rangle \Gamma(n)}{\langle n_e \rangle^2 \Gamma(n-3/2)(1+\vec{K}\cdot\vec{L}\cdot\vec{K})^n} \tag{B-1}$$

where

$$\vec{L} = \begin{bmatrix} L_x^2 & 0 & 0 \\ 0 & L_y^2 & L_{yz} \\ 0 & L_{yz} & L_z^2 \end{bmatrix} \tag{B-2}$$

121

The scales L_r, L_s, L_t and L_y, L_z, L_{yz} are defined in Section 2.6 in terms of the outer scale L_0, the penetration angle ψ, and the axial ratio q. The root mean square value of the electron density fluctuations is $\langle \Delta n_e^2 \rangle$. For $K \cdot L \cdot K \gg 1$, Φ_ξ is proportional to K^{-2n}. Thus a K^{-4} PSD for the three dimensional electron density fluctuations corresponds to the n = 2 case.

The correlation function $A(\vec{\rho}_d)$ under the delta layer approximation is given by Equation 2-70 which is reproduced here:

$$A(\vec{\rho}_d) = (2\pi)^{-2} \iint_{-\infty}^{\infty} \exp(i\vec{K}_\perp \cdot \vec{\rho}_d) \Phi_\xi(\vec{K}_\perp, K_z = 0) d^2\vec{K}_\perp \quad . \qquad (2\text{-}70)$$

Using Equations B-1 and B-3 and performing the angular integral, Equation B-3 reduces to

$$A(\vec{\rho}_d) = \frac{4\sqrt{\pi}\, q\delta L_0 \Gamma(n) \langle \Delta n_e^2 \rangle}{\Gamma(n-3/2)\langle n_e \rangle^2} \int_0^\infty \frac{J_0\left[(\vec{\rho}_d \cdot \vec{L}_\perp \cdot \vec{\rho}_d)^{1/2} u\right]}{(1+u^2)^n} u\, du$$

$$= \frac{\sqrt{\pi}\, q\delta L_0 (n-1) \langle \Delta n_e^2 \rangle}{2^{n-3}\Gamma(n-3/2)\langle n_e \rangle^2} (\vec{\rho}_d \cdot \vec{L}_\perp \cdot \vec{\rho}_d)^{(n-1)/2} K_{n-1}\left[(\vec{\rho}_d \cdot \vec{L}_\perp \cdot \vec{\rho}_d)^{1/2}\right] \qquad (B\text{-}3)$$

where J_0 is the Bessel function of order 0, K_{n-1} is the modified Bessel function of order n-1, $\vec{L}_\perp$ is a 2×2 matrix containing the x-y components of $\vec{L}$, and δ is defined in Equation 2-69.

For all values of n except n = 2, $A(\vec{\rho}_d)$ can be expanded in a power series of the form

$$A(\vec{\rho}_d) = A_0\{(1-A_2[(x/L_x)^2 + (y/L_y)^2]^{m/2}\} \qquad (B\text{-}4)$$

122

where $m = min(2,2n-2)$. For $n = 2$, A_2 does not exist unless an inner scale l_i is imposed. This is accomplished by truncating the integral over u in Equation B-3 at a cutoff $u = \varepsilon^{-1}$ where ε is chosen to be l_i/L_0. For values of n greater than 2, the J_0 Bessell function in the integrand of Equation B-3 can be expanded and the resulting series can be integrated term-by-term. The first two terms of the expansion give

$$A_0 = \frac{2\sqrt{\pi} \ q\delta L_0 \Gamma(n) \langle \Delta n_e^2 \rangle}{\Gamma(n-3/2) \langle n_e \rangle^2} \ [1-1/(1+\varepsilon^{-2})^{n-1}] \tag{B-5}$$

and

$$A_2 = \frac{(1+\varepsilon^{-2})^{n-1} - [1+(n-1)\varepsilon^{-2}]}{4(n-2)[(1+\varepsilon^{-2})^{n-1}-1]} \ . \tag{B-6}$$

In the limit that $n = 2$, the A_2 coefficient becomes

$$A_2 = \frac{(1+\varepsilon^{-2})\ln(1+\varepsilon^{-2}) - \varepsilon^{-2}}{4\varepsilon^{-2}} \ . \tag{B-7}$$

This expression can be further reduced in the limit that $l_i \ll L_0$ to

$$A_2 \approx \ln(L_0/l_i)/2 \ . \tag{B-8}$$

Now the phase variance, the decorrelation distance, and the coherence bandwidth can be written in terms of geometrical parameters and electron density fluctuation parameters. Using Equation 2-52, the phase variance due to the structured ionization is

$$\sigma_\phi^2 = 2q\delta L_0 L_\delta (r_e \lambda)^2 \langle \Delta n_e^2 \rangle \tag{B-9}$$

where L_δ is the thickness of the delta layer. The decorrelation distance and the coherence bandwidth are defined in Equations 2-78 and 2-79 respectively. Using these definitions,

123

$$\ell_0^2 = \frac{2(z_t + z_r)^2 L_0^2}{z_t^2 \ln(L_0/l_i)\sigma_\phi^2} \tag{B-10}$$

and

$$\omega_{coh} = \frac{2\pi\omega_0 \Lambda(z_t + z_r)L_0^2}{\lambda z_t z_r \ln(L_0/l_i)\sigma_\phi^2} . \tag{B-11}$$

These equations are only valid for the delta layer approximation, for the quadratic phase structure approximation and for a K^{-4} three dimensional electron density fluctuation PSD. It can be seen from the equations that the values of ℓ_0 and ω_{coh} are only weakly dependent on the inner scale l_i.

124

DISTRIBUTION LIST

DEPARTMENT OF DEFENSE

DEFENSE COMMUNICATIONS AGENCY
    ATTN: A200 R CRAWFORD
    ATTN: A320 P BIRD
    ATTN: A730 G JONES

DEFENSE COMMUNICATIONS ENGINEER CENTER
    ATTN: CODE R123 TECH LIB

DEFENSE INTELLIGENCE AGENCY
    ATTN: RTS-2B

DEFENSE NUCLEAR AGENCY
    ATTN: NATF
    ATTN: NAWE
3 CYS ATTN: RAAE
    ATTN: RAAE P LUNN
    ATTN: RAAE T WALSH
    ATTN: RAEE
    ATTN: SPAS
    ATTN: STNA
    ATTN: STSP
4 CYS ATTN: STTI-CA

DEFENSE TECHNICAL INFORMATION CENTER
12 CYS ATTN: DD

STRATEGIC DEFENSE INITIATIVE ORGANIZATION
    ATTN: KE
    ATTN: SLKT
    ATTN: SN
    ATTN: SY

DEPARTMENT OF THE ARMY

U S ARMY COMMUNICATIONS R&D COMMAND
    ATTN: DRDCO-COM-RY W KESSELMAN

U S ARMY NUCLEAR & CHEMICAL AGENCY
    ATTN: LIBRARY

U S ARMY SATELLITE COMM AGENCY
    ATTN: AMCPM-SC-3

U S ARMY STRATEGIC DEFENSE CMD
    ATTN: DACS-BM/TECH DIV

U S ARMY STRATEGIC DEFENSE CMD
    ATTN: DASD-H-SAV

U S ARMY STRATEGIC DEFENSE COMMAND
    ATTN: ATC-D WATTS
    ATTN: ATC-R ANDREWS
    ATTN: ATC-R D RUSS
    ATTN: ATC-R W DICKSON

DEPARTMENT OF THE NAVY

NAVAL RESEARCH LABORATORY
    ATTN: CODE 2627 TECH LIB
    ATTN: CODE 4040 D BOOK
    ATTN: CODE 4180 J GOODMAN
    ATTN: CODE 4720 J DAVIS
    ATTN: CODE 4732 B RIPIN
    ATTN: CODE 4750 P RODRIGUEZ
    ATTN: CODE 4780 J HUBA

DEPARTMENT OF THE AIR FORCE

AIR FORCE GEOPHYSICS LABORATORY
    ATTN: CA A STAIR
    ATTN: LID J RAMUSSEN
    ATTN: LIS J BUCHAU
    ATTN: LS
    ATTN: LS R O'NIEL
    ATTN: LYD K CHAMPION

AIR FORCE SPACE DIVISION
    ATTN: YA
    ATTN: YG
    ATTN: YK
2 CYS ATTN: YN

AIR FORCE SPACE TECHNOLOGY CENTER
    ATTN: XP

AIR FORCE WEAPONS LABORATORY, AFSC
    ATTN: NTED J RENICK
    ATTN: NTED LT KITCH
    ATTN: NTED R HENNY
    ATTN: NTEDA
    ATTN: NTES
    ATTN: NTN
    ATTN: SUL

DEPARTMENT OF ENERGY

LOS ALAMOS NATIONAL LABORATORY
    ATTN: R SELDEN
    ATTN: D SAPPENFIELD
    ATTN: M T SANDFORD
    ATTN: R WHITAKER

SANDIA NATIONAL LABORATORIES
    ATTN: A D THORNBROUGH
    ATTN: D DAHLGREN
    ATTN: D J RIGALI
    ATTN: ORG 314 W D BROWN
    ATTN: ORG 332 R C BACKSTROM
    ATTN: ORG 7112 A CHABAI
    ATTN: R G CLEM

DEPARTMENT OF ENERGY (CONTINUED)

SANDIA NATIONAL LABORATORIES (CONTINUED)
    ATTN: SPACE PROJECT DIV
    ATTN: TECH LIB 3141 RPTS RCVG CLRK

DEPARTMENT OF DEFENSE CONTRACTORS

AEROSPACE CORP
    ATTN: D OLSEN
    ATTN: H MIRELS
    ATTN: I GARFUNKEL
    ATTN: J KLUCK
    ATTN: J STRAUS
    ATTN: K S CHO
    ATTN: R SLAUGHTER
    ATTN: T SALMI

AUSTIN RESEARCH ASSOCIATES
    ATTN: J THOMPSON

BERKELEY RSCH ASSOCIATES, INC
    ATTN: J WORKMAN
    ATTN: S BRECHT

CHARLES STARK DRAPER LAB, INC
    ATTN: A TETEWSKI

EOS TECHNOLOGIES, INC
    ATTN: B GABBARD
    ATTN: W LELEVIER

JAYCOR
    ATTN: J SPERLING

KAMAN TEMPO
    ATTN: B GAMBILL
    ATTN: DASIAC
    ATTN: R RUTHERFORD

KAMAN TEMPO
    ATTN: DASIAC

M I T LINCOLN LAB
    ATTN: D TOWLE L-230
    ATTN: I KUPIEC L-100

MAXIM TECHNOLOGIES, INC
    ATTN: J LEHMAN
    ATTN: J MARSHALL
    ATTN: J SO
    ATTN: R MORGANSTERN

MISSION RESEARCH CORP
    ATTN: B R MILNER
    ATTN: C LAUER
    ATTN: D ARCHER
    ATTN: D KNEPP
    ATTN: F FAJEN
    ATTN: F GUIGLIANO
    ATTN: G MCCARTOR

    ATTN: R BIGONI
    ATTN: R BOGUSCH
2 CYS ATTN: R DANA
    ATTN: R HENDRICK
    ATTN: S GUTSCHE
    ATTN: TECH LIBRARY

MITRE CORPORATION
    ATTN: A KYMMEL
    ATTN: C CALLAHAN
    ATTN: D RAMPTON PH D
    ATTN: DR D RAMPTON

PACIFIC-SIERRA RESEARCH CORP
    ATTN: E FIELD JR
    ATTN: F THOMAS
    ATTN: H BRODE, CHAIRMAN SAGE

PHOTOMETRICS, INC
    ATTN: I L KOFSKY

PHYSICAL DYNAMICS, INC
    ATTN: E FREMOUW

PHYSICAL RESEARCH, INC
    ATTN: R DELIBERIS
    ATTN: T STEPHENS

PHYSICAL RESEARCH, INC
    ATTN: J DEVORE
    ATTN: J THOMPSON
    ATTN: W SCHLUETER

R & D ASSOCIATES
    ATTN: A KUHL
    ATTN: B LAMB
    ATTN: B MOLLER
    ATTN: C GREIFINGER
    ATTN: C K B LEE
    ATTN: F GILMORE
    ATTN: H ORY
    ATTN: J LEWIS
    ATTN: M GANTSWEG
    ATTN: M GROVER
    ATTN: P RAUSCH
    ATTN: R TURCO
    ATTN: W KARZAS

RAND CORP
    ATTN: C CRAIN
    ATTN: E BEDROZIAN
    ATTN: P DAVIS

SCIENCE APPLICATIONS INTL CORP
    ATTN: J COCKAYNE
    ATTN: W LAYSON

SRI INTERNATIONAL
    ATTN: W CHESNUT
    ATTN: W JAYE

DEPT OF DEFENSE CONTRACTORS (CONTINUED)

VISIDYNE, INC
    ATTN: J CARPENTER

TOYON RESEARCH CORP
    ATTN: J GARBARINO
    ATTN: J ISE